"CUMULUS CONVECTION"

by

Alan Keith Betts
July 1970

Citation: Betts, A. K. (1970): *Cumulus Convection.* Ph.D. Thesis, Dept. of Meteorology, Imperial College, Univ. of London. 151pp. Available from http://alanbetts.com/research/paper/cumulus-convection/#abstract

"CUMULUS CONVECTION"

by

Alan Keith Betts.

Department of Meteorology,

Imperial College of Science and Technology.

A Thesis submitted for the
Degree of Doctor of Philosophy
in the University of London,
July, 1970.

Frontispiece

Cumulus convection over Anaco, Venezuela at 1600 hrs (local time) on 17th August 1969. The cloud dominating the picture has nearly reached its maximum height, and later completely evaporates. Cloud base is at 855mb (1250m above the ground), and cloud top is at 650mb (3600m).

ABSTRACT

This thesis discusses the transports of sensible heat and water vapour by ordinary convection in a field of non-precipitating cumulus clouds. The stratification and time development of the convective boundary layer during dry and moist convection are investigated theoretically. A model is proposed which distinguishes for budget purposes 3 layers: the sub-cloud layer, and an upper and lower part of the cumulus layer. The model relates the cumulus convection to the surface boundary conditions, the 'free' atmosphere above the cumulus layer, and the large scale vertical motion.

The significant aspects of the thesis are as follows:

(1) Formulae for the dilution of clouds by their environment show the essential irreversibility of the vertical transports in non-precipitating cumulus convection. One significant consequence is that the convection destabilises the layer it occupies.

(2) A new conservative variable, θ_L, related to potential temperature and liquid water mixing ratio, greatly simplifies the understanding of cloud parcel thermodynamics and cloud heat transports. With this variable dry and wet convection become closely analogous.

(3) A mass transport model is used to clarify the mechanism of modification of the mean atmosphere by the convection.

(4) A model for the sub-cloud layer predicts from the surface fluxes and the large scale vertical motion the convective mass flux into the cumulus layer (a measure of the amount of active cloud).

(5) A lapse-rate model is developed by relating the mechanics and thermodynamics of a typical cloud to the mean stratification, so as to predict the lapse rate characteristic of the cumulus layer.

(6) The control of cloud-base variations and large-scale vertical motion on cumulus convection is made quantitative. For example rise of cloud-base and large-scale subsidence are found to have some closely similar quantitative effects: both tend to suppress clouds.

LIST OF CONTENTS

		Page No.
	Frontispiece	2
	Abstract	3
	List of Contents	4
	Acknowledgements	6
	Symbol List	7
Chapter 1	Introduction	
1.1	Description of the problem	10
1.2	Outline of the thesis	12
1.3	Discussion of time scales	13
Chapter 2	Existing Cumulus Models	
2.1	Introduction	15
2.2	Numerical Models	16
2.3	A linearised perturbation model : Kuo (1965)	17
2.4	A steady state cellular model : Asai (1967, 1968)	18
2.5	Constraints on ratio of horizontal to vertical scales	20
2.6	Warming of the Environment : slice theory Ratio of ascending to descending areas	21
2.7	Conclusion	24
Chapter 3	Modification of the Atmosphere by Convection	25
3.1	Introduction	25
3.2	Conservative variables in convection : Dry convection Wet convection	26
3.3	The transport equations for heat and water	29
3.4	Parcel lapse rates for ascent and descent with entrainment	32
3.5	Irreversibility of : Total heat transport Liquid water transport	38
3.6	Destabilising nature of cumulus convection	41
3.7	Mechanism for modifying the mean atmosphere: A mass transport model	42

3.8	Lapse rate control : Dry convection	45
	Wet convection	51
	Lapse rate structure : Diagram	53
3.9	Discussion of earlier work on mass flux models	55
	Fraser (1968), Pearce (1968), Haman (1969)	
3.10	Graphical Description of non-precipitating Cumulus convection	57
	Diagram	59
3.11	Conclusion	60
Chapter 4	The Dry convective layer	
4.1	Introduction	61
4.2	Dry convection : outline of problem	62
4.3	The dry layer : sensible heat balance and time development	63
4.4	The dry layer : water vapour balance	71
4.5	Surface boundary conditions	72
	Closure	73
4.6	The sub-cloud layer	75
	Cloud-base height; transition layer; heat balance	
4.7	Solution of equations for the sub-cloud layer	81
	I Sensible heat balance	
	Cloud mass flux	
4.8	II Water vapour balance	85
4.9	Relation between the heights of cloud-base and the transition layer	88
4.10	Summary of Chapter 4	92
Chapter 5	The Cumulus Layer	
5.1	Introduction	94
5.2	Lapse Rate Model	95
5.3	Time Development of the Cumulus layer	105
	Pt. I Temperature structure	
5.4	Pt. II Water vapour structure	113
5.5	Summary	116

Chapter 6	Observational Evidence	
6.1	Introduction	118
6.2	Analysis of the data, smoothing	119
6.3	Temperature stratification in the cumulus layer	125
	Cumulus convection beneath an inversion	129
6.4	Surface boundary conditions	134
6.5	Estimation of W_{Db}	139
	Conclusion	145
Chapter 7	Summary	148
	References	150
Reprint:	The Energy Formula in a Moving Reference Frame Quart. J.R. Met. Soc. (1969) 95, p.639	

ACKNOWLEDGEMENTS

The work in this thesis was supported by a grant from the Natural Environment Research Council.

The author is grateful to Professor F.H. Ludlam, his supervisor, for advice and encouragement (and for Fig. 6.3.2), and to Dr J.S.A. Green and Dr R.P. Pearce for their helpful comments.

SYMBOL LIST

Basic Variables and symbols.

T	temperature
T_v	virtual temperature
T_w	wet-bulb temperature
θ	potential temperature
θ_v	virtual potential temperature
θ_w	wet-bulb potential temperature
θ_s	saturation potential temperature
θ_E	equivalent potential temperature
θ_L	'liquid-water' potential temperature : see text 3.2
r	water vapour mixing ratio
r_s	saturation mixing ratio
r_L	liquid water mixing ratio
ρ	air density
V	scalar wind velocity
$\underset{\sim}{V}$	vector wind velocity
W	vertical air velocity
W_D	compensating vertical velocity in environment : see text 3.7
Z	height above surface
p	pressure
t	time
Γ	'lapse rate' : $\partial\theta/\partial Z$ NOT $-\partial T/\partial Z$
Γ_D	dry adiabatic lapse rate
Γ_w	wet adiabatic lapse rate
F_θ	flux of $\rho c_p \theta$: potential heat flux
$F_{\theta L}$	flux of $\rho c_p \theta_L$: total heat flux : see text 3.5
F_r	flux of $\rho L r$: L (water vapour flux)
F_{rT}	flux of $\rho L(r+r_L)$: L (total water flux)
α	areal cover of convective elements : see text 3.7
S	scale length for dilution or entrainment
E	dilution or entrainment parameter
D	kinetic energy dissipation parameter : see 5.2

k	kinetic energy dissipation parameter : see 3.8	
C_θ	surface θ transport coefficient	
C_r	surface r " "	
C_D	surface drag coefficient for neutral conditions	
M	parcel mass	
m_f	mass flux	
N	net radiative flux at surface	
G	ground storage of heat/unit area/unit time	
V_R	vegetative resistance to evaporation	
γ	virtual mass coefficient	see 2.2
K_2	entrainment constant	see 2.2
a	cloud radius	in model A
b	convective cell radius	in model A
d	depth of convective cell	see 2.4

Constants

L	latent heat of vaporisation of water
c_p	specific heat of air at constant pressure
g	acceleration due to gravity

Operators

$\sim$	denotes horizontal areal average : e.g.
$-$	denotes (vertical average
	(other defined average
$'$	denotes deviation from horizontal areal average

Subscripts and suffixes

c or (c)	cloud variable e.g. θ_c, r_c, T_c, Γ_c, w_c
e or (e)	environment variable
p or (p)	parcel variable
d	dry convective element variable e.g. Γ_d
o	surface variable e.g. θ_o, r_o
s or t	variables at levels s in dry layer : see 4.2 (t)
b	cloud-base variable
1 or 2	variables at levels (1) or (2) in cumulus layer : see overleaf

Diagram indicating layers and derived variables for cumulus model.

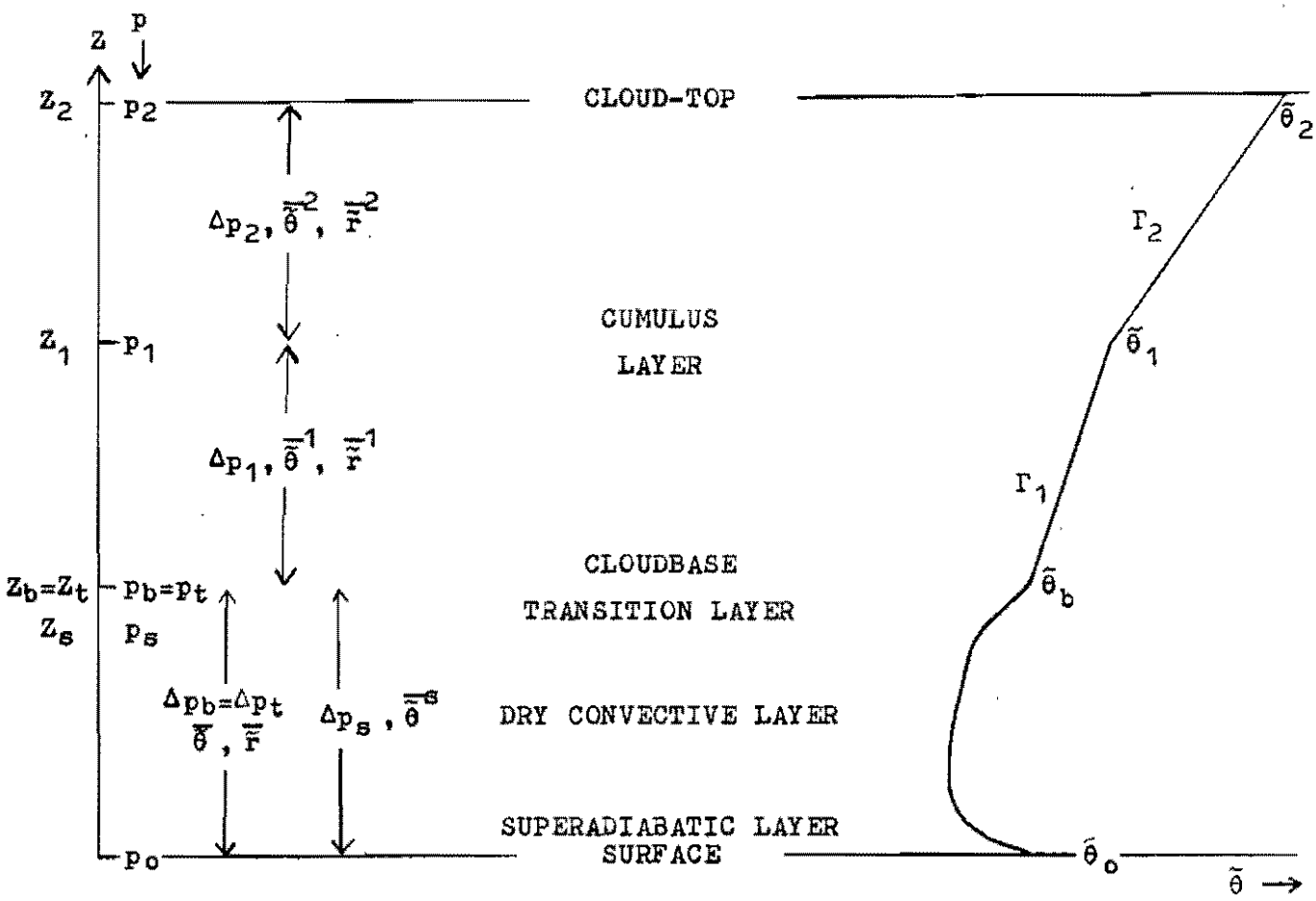

Further derived variables

$\phi = \theta_c - \theta_e$

$\Delta\theta$, $\delta\theta$ see 4.3 and 4.6

Δr , δr see 4.4

Γ_{c1}, Γ_{c2} respective parcel lapse rates for saturated ascent, and descent with dilution

Γ_{d1}, Γ_{d2} " " " " " dry " " " " "

CUMULUS CONVECTION

Chapter 1

1.1. Description of the problem

Convection in the atmosphere occurs on a variety of interacting scales. Ludlam (1966) suggested a classification into 4 scales: small scale including cumulus convection, intermediate scale, large scale and cumulonimbus convection. This thesis is concerned with the first: small scale convection, and particularly with non-precipitating cumulus convection.

Cumulus convection transfers sensible and latent heat from the earth's surface into the lower troposphere. Thus this study of cumulus convection is also a study of the heat transfers in the earth's boundary layer (which is here defined as the layer extending from the earth's surface to the top of the convective layer). Typically one sees scattered clouds of a range of sizes, but those which reach the top of the layer have horizontal dimensions comparable with its depth (a few km: see frontispiece). The influence of circulations of larger scale is very apparent, whether on an intermediate scale (for example over hills, or along a sea breeze front), or on a synoptic scale. Large-scale ascent, which implies horizontal convergence at low levels, promotes rapid deepening of the convection layer and the development of cumulonimbus, while large-scale subsidence, and low level divergence, inhibits growth of the convection layer (and in the extreme may prevent the formation of clouds).

Standing in this way between the very small scale motions effecting transports from the earth's surface (in the so-called constant flux layer), and the intermediate or synoptic-scale motion field, cumulus convection presents many problems of the 'feed-back' of one scale or another. In this thesis four important questions will be considered.

(1) How to relate the convection to the surface boundary conditions.

(2) How to relate the convection to the synoptic-scale field of motion, particularly its mean vertical component.

(3) How to handle the water transports (of liquid and vapour), and their role in cumulus convection.

(4) How to interrelate lapse-rate structure, and the mechanics

and thermodynamics of a typical cloud.

The calculation of the surface heat fluxes is involved in question (1), as these depend upon the transports in the convective layer.

The feed-back of the convective transports on the synoptic scale motion field is a matter not considered here. This thesis is concerned with developing a simple closed model of cumulus convection, which will predict the convective heat transports, given the synoptic-scale (or any larger scale) fields, and suitable surface boundary conditions (e.g. ocean surface temperature over the sea; and over land net radiative flux, ground heat storage, and some parameter defining evaporation from the surface.

A number of simplifications will be made, of which the most important are:

(a) Radiative transfers, except at the surface over land, are omitted from the model. These are important for time-scales longer than a day, but it is considered that they can be added when the convective transports, particularly of water vapour, are understood.

(b) There is no general consideration of momentum transfer. Only a simple model of the mechanics of a convective element subject to mixing is used; one which neglects the effects of wind shear.

(c) The model is applicable only to the development of the boundary layer in the absence of showers: it is assumed that condensed water moves with the air. Some of the concepts developed however are equally relevant to cumulo-nimbus convection.

Further , in the model it is assumed that individual clouds are transient: they are agents for the transport of water but finally totally evaporate. The model is thus not suited without further extension to the description of the development of layer cloud.

1.2 Outline of the thesis

The model proposed distinguishes three layers: the dry convective layer below cloud-base, and an upper and lower part of the layer occupied by cumulus. The shallow 'superadiabatic layer' above the surface and the 'transition layer' (see Ludlam, 1966) just below cloud-base will also be discussed, but in considering heat and water budgets, they will be regarded as part of the sub-cloud ('dry') layer.

The boundaries of the layers (apart from that at the surface) are specified by height or pressure and vary with time. Accordingly the equations expressing their heat and water economy are complicated, but it is convenient and physically realistic to distinguish the convective transports in the dry and the cumulus layers, rather than to refer to fixed levels.

In chaper 2, some existing models of cumulus convection will be surveyed in relation to the four questions posed in 1.1, and to the model studied in later chapters. The exposition has then been divided into three chapters.

In chapter 3 certain general questions are investigated concerning the way in which cumulus convection modifies the mean condition of the atmosphere. Equations are established for the transports of sensible heat, water vapour and liquid water in the cumulus layer. The significance of 'entrainment' (see 1.3) is considered, and a schematic model for the convective transport of heat in the cumulus layer, as a function of the input to the layer at cloud-base, is proposed.

In chapter 4 two similar models are developed which link the dry layer (in the presence and absence of cumulus clouds) to the surface boundary conditions, the large scale vertical motion, $\widetilde{w}$, and the stratification above the dry layer. These three sets of boundary conditions determine the convective mass, sensible heat and water vapour fluxes into the cumulus layer. The feed-back of the clouds on the dry convective layer, and the control on the clouds exerted by cloud-base variation, and $\widetilde{w}$ will become clear.

In chapter 5, this model of the boundary layer is closed by developing a two-layer model for the cumulus layer. This incorporates the model of chapter 3 and, taking as input the fluxes from the sub-cloud layer, predicts the time development of the cumulus layer as a function of $\widetilde{w}$, and the

stratification above the cumulus layer. Most of the physics of the convection process is incorporated into a lapse-rate model (5.2), while the remainder of the chapter considers simply a budget for heat and water vapour.

In chapter 6 some observational evidence, mainly from one day of convection over land, is analysed in the light of the model. The problems presented by available data are apparent, but the agreement between the evidence and the implications of the model is considered encouraging.

1.3 Discussion of time-scales

There are many interacting processes with various time-and-space scales involved in cumulus convection, as mentioned earlier. In the conceptual division of the whole range into a few distinct scales, a number of concepts such as 'cloud', 'environment', and 'entrainment' arise, which require some definition.

A visible cloud marks those parts of the cumulus circulation where water has condensed in moist, initially ascending, air. This circulation extends below cloud-base, and into the clear spaces between the clouds. It is useful to distinguish between the clouds (the saturated regions containing liquid water) and what is often called the environment (the unsaturated regions between the clouds). This is useful because transformations between latent and sensible heat, associated with the phase changes of water, occur only in the saturated regions. In the environment, apart from radiative cooling, potential temperature is conserved and the motion is dry adiabatic. Horizontal temperature gradients are produced largely by the latent heat release in the clouds and generate the kinetic energy of both the cumulus circulation and of the motions on a smaller scale, which mix or dilute the cloudy region with the surrounding unsaturated air of the environment. This process of mixing of unsaturated air into the clouds has been called entrainment, and has long been known to be important (Stommel, 1947). With entrainment, the potential temperature of a rising element of cloud departs from the wet adiabatic lapse rate, and this has far-reaching consequences, which are discussed in sections 3.4 to 3.7. In order to quantify entrainment, it has proved useful to define horizontally averaged variables in the two regions: cloud and environment (for which we shall use the subscripts c and e). The relation of the environmental

averages to the synoptic scale horizontal mean, including both cloud and environment (here denoted by the symbol $\sim$ e.g. $\tilde{\theta}$) will be considered in 3.7.

This distinction between cloud and environment is useful because the life-cycle of each transient cloud depends directly on the stratification at that time. This life-cycle modifies the stratification a little, but on a timescale long compared with the life-time of an individual cloud (see Table 1.3.1). This link between stratification and the life-cycle of a typical cumulus cloud is discussed in 5.2 .

Some important timescales in cumulus convection are summarised in Table 1.3.1. In the descending branch of a large scale circulation (see Ludlam 1966), the timescale for the modification of the layer by the cumulus clouds and the synoptic scale may be longer still: days rather than hours.

Table 1.3.1

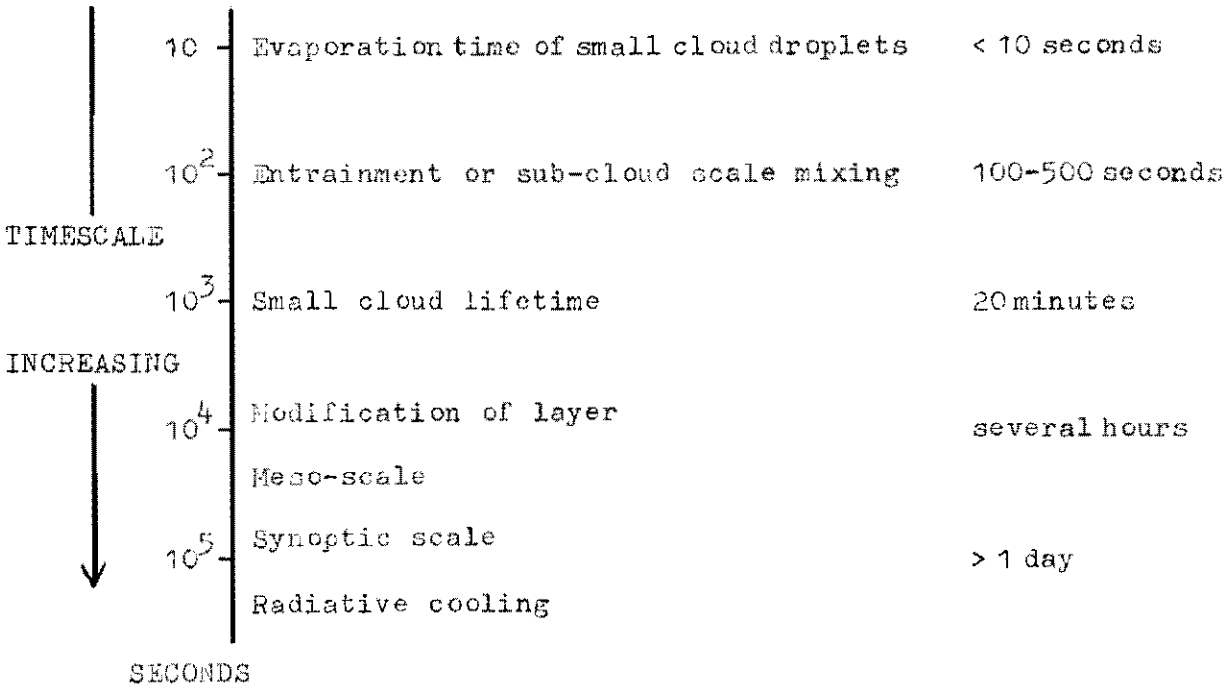

The term 'convective element' will be used both to describe a single cloud or cloud tower and its motion field; and, in our brief discussion of the dry convective layer, a single thermal or plume and its circulation.

Chapter 2 Existing Cumulus Models

2.1 Introduction

Existing approaches to the cumulus problem may be grouped into four categories:

(1) 1, 2 or 3D numerical models, including parcel models

(2) Linear perturbation models

(3) Steady-state cellular models

(4) Mass transport models.

The first category are models of a convective element which relate the internal properties of the element to the mean atmosphere. We shall take as an example Simpson et al (1965, 1969; model S): a 1-D model designed to relate the internal properties of a cloud tower to the diameter at cloud base, and a nearby sounding. This model is informative in describing the role of mixing and the water phase change in the life of a single convective element.

As an example of a perturbation model, we shall consider briefly that of Kuo (1965; model K), which investigated the marginal stability problem for a 2-D linearised formulation of moist convection. This related horizontal and vertical scales of motion, and determined a preferred ratio for the areas of ascending and descending regions.

Asai (1967, 1968) has developed a steady-state cellular model which attempts to interrelate a space-filling field of most efficient heat-transporting convective cells, the surface sensible heat flux, and the lapse rate in the cumulus layer. This model undertakes two of the questions posed in 1.1: namely, to relate the convection to the surface heat fluxes, and to connect lapse rate structure to the physics of a convective element. Hence we shall examine this model in a little detail. It fails in its main purpose, because it oversimplifies the heat transports and the role of water in cumulus convection, but it does indicate a relationship between horizontal and vertical scales of motion. In the same context we shall comment on the warming of the environment and 'slice theory'.

The mass transport models, which are most germane to this thesis, will be considered in chapter 3.

2.2. Numerical Models

The value of a numerical model of a single buoyant element is that one can parameterise in some detail motions on a smaller scale than the mean motion of the element (motions which may be regarded as turbulent mixing or entrainment). Stommel (1947) first pointed out that the evaporation of cloud water, during dilution with unsaturated air from the environment, greatly reduces cloud buoyancy. Further consequences of this dilution are discussed in sections 3.4 and 3.5.

The 1-D model S is a development of Levine's spherical vortex model (1959), and parameterises dilution of a rising cloud parcel, mass M, in the form

2.2.1 $$\frac{1}{M}\frac{dM}{dZ} = \frac{9}{32}\frac{K_2}{a}$$

where a is the radius of the rising cloud. The parameter K_2 has been chosen so that

$$\frac{9}{32} K_2 = 0.2$$

which is the value for the dilution obtained in laboratory experiments on starting plumes. In the latest model (1969) K_2 is used in conjunction with a virtual mass coefficient ($\gamma = 0.5$, see 2.2.2), which replaced a drag coefficient used in earlier models.

Eq. 2.2.1 is used with an environmental sounding, assumed to be representative of the air entrained into the cloud, to deduce $\phi(Z)$ ($= \theta_c - \theta_c$) from the temperature at cloud-base, and a value of a. This radius a is usually measured at the level where a tower emerges from a parent cloud, and is assumed to be the same at all heights. This is a conventional entrainment calculation (Stommel: 1947).

The vertical velocity of a cloud tower W_c (Z) is determined by

2.2.2 $$W_c \frac{dW_c}{dZ} = \frac{1}{\delta}\frac{g\phi}{1+\gamma} - \left(\frac{9}{32} K_2\right)\frac{W_c^2}{a}$$

Given $\phi(Z)$, this equation is integrated from cloud-base to give the height which the cloud tower reaches. The calculation is not sensitive to the assumed vertical velocity at cloud-base. $(1 + \gamma)$ is a virtual mass term included to represent the effect of the vertical gradient of the perturbation

pressure field which has been omitted from 2.2.2. This perturbation pressure field exists to provide the horizontal accelerations of the circulation. The last term is the drag on the cloud tower due to entrainment of mass from the environment, which is assumed stationary.

With the values given above for the two parameters K_2, γ, the model predicts cloud top height and cloud internal properties quite well.

In 2-D or 3-D numerical models, the set of quasi-Boussinesq equations can be integrated to explore the time development of the structure of an element, but at present it remains vital to include sub-grid-scale motions to obtain realistic cloud internal properties. Our present computer capacity is sufficient to handle a grid length of about 50m for a cumulus model, but this is still too large to develop the small scale 'turbulent' motion field, which mixes cloud and environment. Thus how to parameterise these turbulent motions remains an important problem; their intensity must be determined by comparing the results of a numerical experiment with observations. 3-D primitive equation models will be needed to investigate the structure of convection in shear, and these are being developed in this department (by M.J. Miller).

Nonetheless, the simple 1-D formulation of the mechanics and thermodynamics of an element, which has been observationally tested by Simpson and Wiggert (1969), will prove useful in modified form in later chapters (3 and 5). As it stands, this model is designed to predict the properties of a cloud, given the stratification, but (in 5.2) we shall use a model of this kind in the reverse sense; to relate lapse rate structure to the properties of a typical individual cumulus cloud.

2.3 Model K (Kuo: Tellus 1965 17, 413)

This is a 2-D linearised model: including turbulent transfers of heat and momentum modelled by constant eddy coefficients. Kuo derives eigen functions for ascending and descending regions, and deduces scales for the motion.

2.3.1 $$1 \leqslant \frac{2a}{d} \leqslant 1.4$$

2.3.2 $$\frac{a}{b-a} \approx \frac{r_w - r_e}{2r_e} \quad \text{for } R_2 \geqslant 100$$

where d is the depth of the layer

a horizontal scale of ascending region

b-a horizontal scale of descending region

R_2 is a Rayleigh no in the descending region.

He obtained similar results both for the marginal stability problem and by using a principle of maximum available potential energy production.

If we define

$$\alpha = \frac{a}{b} = \frac{\text{ascending area}}{\text{total area}}$$

we obtain from 2.3.2

2.3.3 $$\alpha \leq \frac{\Gamma_w - \Gamma_e}{\Gamma_w + \Gamma_e}$$

with the limit of approximate equality being when $R_2 > 100$

Equation 2.3.1 implies that the diameter of a model 'cloud' is comparable with the depth of the layer, a very reasonable and useful result, which we shall see is a characteristic of Asai's model also. We shall comment on this in 2.5.

The relationship between fractional area coverage, and wet and environmental lapse rates is open to more criticism. We shall examine it in 2.6 and 2.7, but find it not useful.

2.4 Model A (Asai: J. Meteor. Soc. Jap. 45, 251 and 46, 301)

The reader may refer to the original papers for the details of the mathematics. We wish to discuss the nature of the solution. Asai envisages a spacefilling array of simple cells each consisting of an ascending region, surrounded by a descending region.

Fig. 2.4.1

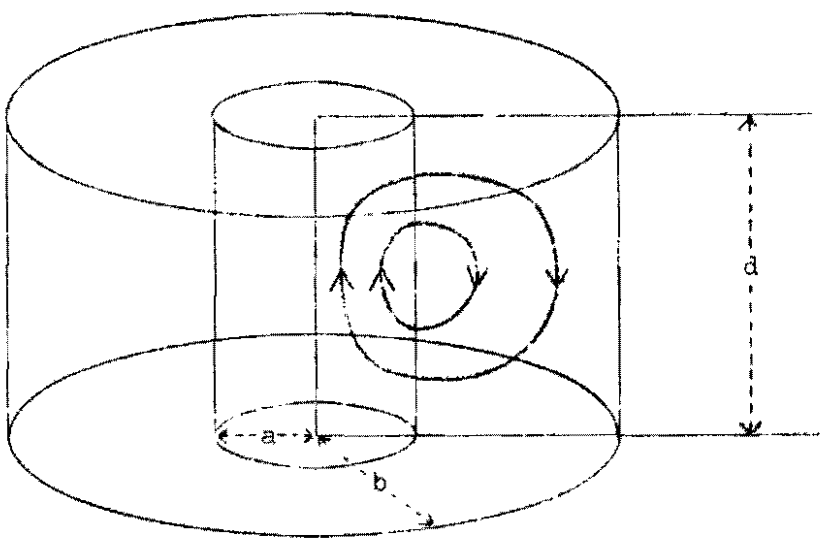

Symbols

Ascending region radius	a
Descending annulus radius	b-a
Depth of layer	d
Surface Sensible heat flux	F_θ
Mean lapse rate in layer	Γ $(= \partial\theta/\partial Z$ not $-\partial T/\partial Z)$
Average vertical velocity in ascending region	$\langle W \rangle$
Average potential temp. difference between ascending and descending regions	$\langle \Delta\theta \rangle$

The model includes entrainment or mixing in both the horizontal and vertical directions, and Asai obtains steady state solutions for $\langle W \rangle$, $\langle \Delta\theta \rangle$ and Γ as functions of the upward sensible heat flux carried by his model cell. He envisages this heat flux being supplied at the bottom, as a surface sensible heat flux, and removed at the top. This immediately raises difficulties, as the potential temperature excess $\langle \Delta\theta \rangle$ is supplied in the model by the condensation of water (which is immediately removed) in the ascending region. Of the released heat of condensation, part is advected upwards in the model to be removed at the top, while the remainder warms the whole cell steadily. There is no evaporation in his model, both because the liquid water is immediately removed, and the environment, the descending region, is mathematically treated as if it were always saturated.

These are major inadequacies in the handling of the heat and water transports, which are equally true of model K, and which invalidate many of the conclusions of the two papers. We shall return to this question in 2.6, and indeed the whole of chapter 3 will be concerned with the profound consequences of the correct modelling of the heat and water transports in non-precipitating cumulus convection.

However we shall examine model A more closely, to bring out its useful aspects, as well as those where it differs markedly from the model to be developed in later chapters.

We may envisage starting model A with a stably stratified atmosphere, and turning on a surface sensible heat flux, F_θ The horizontal and vertical scales of motion which are established, are selected by requiring that the upward sensible heat transport shall be a maximum. If this maximum, determined by the given starting mean lapse rate, is less than F_θ, then the layer destabilises until the heat flux carried by the cell (which increases as Γ decreases) is equal to F_θ.

Thus a steady state results, when F_θ determines all the other variables d, a, b and Γ.

The model is mathematically fully consistent, and manifestly relates a, b, d, Γ, Γ_w, and an optimum value of $\alpha\langle W\rangle\langle\Delta\theta\rangle$, the sensible heat flux carried by the clouds. As such it is a useful steady state model relating these variables, provided one accepts the assumptions of saturated environment, and immediate fallout of water. (These alone make it inadequate as a model of non-precipitating cumulus convection.). The model, like model K, is useful in clarifying the constraints on the scales of motion.

2.5 Constraint on ratio of horizontal to vertical scale $^a/_d$

Like model K, model A also concludes

$$2.5.1 \qquad \frac{2a}{d} \approx 1$$

As A is a steady state model, the occurrence of the scales of motion in the inertia term, is not involved in this solution. It is mixing which determines the optimum $^a/_d$, and not surprisingly this optimum is when horizontal and vertical scales are comparable. We may summarise the result:

Large $^a/_d$ is inhibited by vertical exchange of horizontal momentum
Small $^a/_d$ is inhibited by horizontal exchange of vertical momentum
and by horizontal exchange of potential temperature

Asai has extended the mixing-length formulation of entrainment to both horizontal and vertical motion. We may criticise this model, because it makes no distinction between turbulent mixing in the cloud region, which is known to be large, and in the subsiding air, where turbulent mixing may be small. However in cloud the vertical exchange

coefficient may be larger than the horizontal one, which is another asymmetry working in the opposite direction. We conclude that though the quantitative accuracy of model A, and model K (which had isotropic diffusion) is open to doubt, we should still expect clouds to have diameters comparable with the depth of some layer, not necessarily the whole layer occupied by the convection.

This is in accord with observation (Plank 1967). Ludlam (1966) notes that cumulus and cumulonimbus towers tend to have diameters between 0.4 and 0.5 of the heights of their tops, which would indicate that their diameter is perhaps more comparable with the depth over which they gain upward momentum.

The validity of the steady-state model as an approximation to the life-cycle of a typical cumulus cloud is uncertain. However model K did consider the amplifying problem, and concluded that the preferred horizontal and vertical scales satisfied 2.3.1, closely similar to 2.5.1.

2.6 Warming of the 'Environment' - Slice Theory.

Ratio of Ascending to descending areas:

The well-known 'slice theory' (Bjerknes 1938) deals with the warming of the environment by the subsidence of the stably stratified air between the clouds. This is a characteristic of all models which include both ascending and descending regions, and thus is an aspect of models K, and A.

A simple derivation of this theory for a wet adiabatic model (i.e. one without mixing) is as follows:

Define

$$\phi = \theta_c - \theta_e$$

$$\frac{d}{dt} = \frac{\partial}{\partial t} + W\frac{\partial}{\partial Z}$$

where $\frac{d}{dt}$ is an operator following an ascending element of cloud.

Let the area coverage of cloud be α

of environment be $1-\alpha$

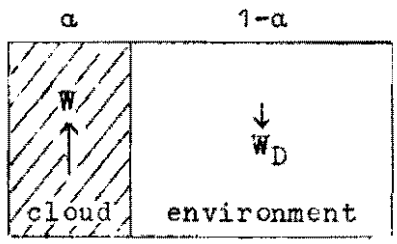

Fig. 2.6.1

$$\frac{d\phi}{dt} = \frac{d\theta_c}{dt} - \frac{d\theta_e}{dt}$$

$$= W_c\Gamma_w - \frac{\partial\theta_e}{\partial t} - W_c\Gamma_e$$

$$= W_c\Gamma_w + W_D\Gamma_e - W_c\Gamma_e$$

If $\overline{w}^{xy} = 0$

$$\alpha W_c + (1-\alpha)W_D = 0$$

$$\therefore \quad \frac{d\phi}{dt} = W_c\left(\Gamma_w - \frac{\Gamma_e}{1-\alpha}\right)$$

This is what has come to be known as the result of the 'slice theory'. The warming of the environment $\partial\theta_e/\partial t$ produced by subsidence is a stabilising influence: the cloud parcel will gain buoyancy only if

$$\Gamma_w > \frac{\Gamma_e}{1-\alpha}$$

Attention has always been focussed in the past on this aspect of the warming of the environment - that it reduces the buoyancy of an ascending cloud. However we shall show later in chapter 6 that the area fraction of active cloud may be only 1-2%. Nonetheless the warming of the environment, and therefore of the mean cumulus layer, by this subsidence, remains of vital importance (even though α may be negligible in 2.6.1).

This aspect of the problem has been ignored by Asai. As mentioned in 2.4; only part of the latent heat released in model A by condensation in the updraft is removed from the top of layer: the rest warms the whole layer steadily. Now if the cumulus layer is warming steadily, then the continuation of the convection depends on whether the sub-cloud layer is also warming at least as fast. It is in this way that the cumulus convection is linked to the surface sensible heat fluxes, not in the manner suggested by Asai. Asai relates the surface heat flux to the upward sensible heat flux in the cumulus clouds. However it is precisely that part of the latent heat flux, liberated as sensible heat in the cumulus layer, which is <u>not</u> advected upwards, but is associated with the warming of the cumulus layer, which relates the cumulus layer to the surface sensible heat flux, which warms the sub-cloud

layer. This is not a simple connection, and is the subject of chapter 4.

Moreover as already mentioned, the latent heat reabsorption which occurs when liquid water is evaporated (as clouds decay), further complicates the problem, and will be discussed in chapters 3 and 5. We shall find that non-precipitating cumulus convection is a destabilising process. In the absence of subsidence, the cumulus layer grows steadily in depth. Thus the conclusion of Asai (1968) that deep cumulus convection requires low level convergence will also prove invalid. It will also be necessary to replace the model of lapse rate control in terms of a sensible heat flux (as suggested by model A). by one in terms of a sensible heat and liquid water transport (see 5.2)

Ratio of ascending to descending areas : α

It will become clear in chapters 3 to 5 that the constraints on cumulus convection are more complex than maximising heat flux, growth rate of elements, or available potential energy production. The convection must be linked to the sub-cloud layer and the surface heat fluxes, and to large scale circulations. We shall find that the area of active cloud is determined by these factors in an intricate manner, rather than simply by the environmental lapse rate as predicted by model K (Eq. 2.3.3) or model A (from which a similar relationship may be extracted).

2.7. Conclusion:

It will be clear from this chapter that we consider none of the cumulus models A, K or S adequately answers the four questions posed in 1.1.

However, in later chapters, we shall use

(a) a 1-D formulation of the effects of mixing, similar to that of model A.

(b) the concept of a dominant cloud size related to the depth of the layer. Models A and K suggest that there is an optimum cloud size for which $a/d \sim 1/2$ . . In reality we observe a wide spectrum of cloud-sizes, but we shall be able to make considerable progress in modelling the cumulus layer with only a single cloud size.

This thesis will not require a very detailed model of a convective element. We shall be concerned first with developing equations and concepts to understand the role of water in cumulus convection (chapter 3), and then with the constraints on the structure of the cumulus layer, and the convective transports. A simple 1-D model will enable us to determine convective fluxes, lapse rates, layer depths, and area coverage of active cloud (in fact all the questions posed by the models of this chapter) in terms of the surface and synoptic-scale boundary conditions.

Chapter 3 Modification of the Atmosphere by Convection

3.1 Introduction

In this chapter we shall discuss the modification of the atmosphere by cumulus convection. It is necessary to examine the role played by the condensation and evaporation of water in some detail: and to this end, we shall first develop the continuity and thermodynamic equations involving potential temperature and water substance. Then we shall consider how entrainment leads to a net downward total heat flux. An alternative description of the modification of the environment in terms of a mass flux model is followed by a discussion of lapse rate control, and the mass flux models of Fraser (1968), Pearce (1968) and Haman (1969). Finally we present a graphical description of cumulus convection for the special case of zero mean vertical motion ($\tilde{W} = 0$). It will be found that the cumulus convection is primarily related to the sub-cloud layer by a heat and mass flux through cloud base. The discussion of this link, and the water vapour flux through cloud-base, which connect the convection to the surface fluxes, is the subject of chapter 4. The development of a more detailed model of the cumulus layer, in which the variation of cloud base and cloud top are determined as functions, not only of the surface variables, but also of a large scale vertical motion field and the stratification above the cumulus layer, will be left to chapter 5.

3.2 Conservative Variables in Convection

Dry Convection

Dry potential temperature θ is conserved if an unsaturated parcel of air is displaced to a different pressure. The corresponding extensive quantity (proportional to total enthalpy)

$$\sum_{i=1,2} M_i c_p \theta_i = M_1 c_p \theta_1 + M_2 c_p \theta_2$$

is also conserved if two unsaturated parcels (mass M_1, M_2) of different θ are mixed isobarically. If radiative and conductive transfers, and the variation of c_p with temperature, are neglected, we may use θ as an exact conservative variable for dry convection. (Ball, 1956).

3.2.1
$$\frac{D\theta}{Dt} = 0$$

Expanding the substantial derivative

3.2.2
$$\frac{\partial\theta}{\partial t} + \underset{\sim}{V}.\underset{\sim}{\nabla}\theta = 0$$

We shall take deviations from a horizontal mean,

$$\theta = \tilde{\theta} + \theta'$$
$$V = \tilde{\underset{\sim}{V}} + V'$$

multiply by a mean density $\tilde{\rho}$ (all triple correlations with ρ' will be neglected), and assume $\mathrm{div}\,\tilde{\rho}\underset{\sim}{V}' = 0$

to obtain

$$\tilde{\rho}\frac{\partial\tilde{\theta}}{\partial t} + \tilde{\rho}\tilde{\underset{\sim}{V}}.\nabla\tilde{\theta} = -\mathrm{div}(\tilde{\rho}\widetilde{\underset{\sim}{V}'\theta'})$$

All horizontal fluxes of heat (and later water) will be neglected, (though by suitable choice of co-ordinate system, the mean horizontal advection could be combined with $\partial\tilde{\theta}/\partial t$)

3.2.3
$$\tilde{\rho}\frac{\partial\tilde{\theta}}{\partial t} + \tilde{\rho}\tilde{W}\frac{\partial}{\partial Z}\tilde{\theta} = -\mathrm{div}(\tilde{\rho}\widetilde{W'\theta'})$$

Wet Convection

In wet convection the phase changes of water are very important sources and sinks of potential temperature. Only the water vapour phase change will be considered in this thesis. Applying the first law of thermodynamics to corresponding changes in a fixed mass of saturated air

3.2 Conservative Variables in Convection

Dry Convection

Dry potential temperature θ is conserved if an unsaturated parcel of air is displaced to a different pressure. The corresponding extensive quantity (proportional to total enthalpy)

$$\sum_{i=1,2} M_i c_p \theta_i = M_1 c_p \theta_1 + M_2 c_p \theta_2$$

is also conserved if two unsaturated parcels (mass M_1, M_2) of different θ are mixed isobarically. If radiative and conductive transfers, and the variation of c_p with temperature, are neglected, we may use θ as an exact conservative variable for dry convection. (Ball, 1956).

3.2.1
$$\frac{D\theta}{Dt} = 0$$

Expanding the substantial derivative

3.2.2
$$\frac{\partial\theta}{\partial t} + \underset{\sim}{V}.\underset{\sim}{\nabla}\theta = 0$$

We shall take deviations from a horizontal mean,

$$\theta = \tilde{\theta} + \theta'$$
$$V = \underset{\sim}{\tilde{V}} + V'$$

multiply by a mean density $\tilde{\rho}$ (all triple correlations with ρ' will be neglected), and assume $\mathrm{div}\,\tilde{\rho}\underset{\sim}{V}' = 0$

to obtain

$$\tilde{\rho}\frac{\partial\tilde{\theta}}{\partial t} + \tilde{\rho}\underset{\sim}{\tilde{V}}.\nabla\tilde{\theta} = -\mathrm{div}(\tilde{\rho}\,\widetilde{\underset{\sim}{V}'\theta'})$$

All horizontal fluxes of heat (and later water) will be neglected, (though by suitable choice of co-ordinate system, the mean horizontal advection could be combined with $\partial\tilde{\theta}/\partial t$)

3.2.3
$$\tilde{\rho}\frac{\partial\tilde{\theta}}{\partial t} + \tilde{\rho}\tilde{W}\frac{\partial}{\partial Z}\tilde{\theta} = -\mathrm{div}(\tilde{\rho}\,\widetilde{W'\theta'})$$

Wet Convection

In wet convection the phase changes of water are very important sources and sinks of potential temperature. Only the water vapour phase change will be considered in this thesis. Applying the first law of thermodynamics to corresponding changes in a fixed mass of saturated air

$$c_p \delta T + L \delta r - \frac{\delta p}{\rho} = 0$$

(r stands for water vapour mixing ratio)

By definition $$c_p \frac{\delta \theta}{\theta} = c_p \frac{\delta T}{T} - \frac{\delta p}{\rho T}$$

$$\therefore \quad c_p \delta \theta + \frac{\theta}{T} L \delta r = 0$$

As substantial derivatives, we obtain

3.2.4 $$c_p \frac{D\theta}{Dt} + \frac{\theta}{T} L \frac{Dr}{Dt} = 0$$

For the conservation of water substance

3.2.5 $$\frac{Dr}{Dt} + \frac{Dr_L}{Dt} = 0$$

Hence from 3.2.4 and 3.2.5

3.2.6 $$c_p \frac{D\theta}{Dt} - \frac{\theta}{T} L \frac{Dr_L}{Dt} = 0$$

Equivalent Potential Temperature: θ_E

It has been customary to extend 3.2.4 to define a new variable, the equivalent potential temperature, θ_E :

3.2.7 $$c_p \frac{D\theta}{Dt} + \frac{\theta}{T} L \frac{Dr}{Dt} = c_p \frac{\theta}{\theta_E} \frac{D\theta_E}{Dt} \qquad \theta_E \approx \theta \exp\left(\frac{Lr}{c_p T}\right)$$

θ_E is conserved for a wet adiabatic change, but $\sum_i M_i c_p \theta_{Ei}$ only approximately under isobaric mixing. This is clear from 3.2.7: if 2 parcels of different θ_E are mixed, the equivalent potential temperature of the mixture is not the arithmetic mean unless both have initially the same θ/θ_E . (In contrast isobaric mixing always conserves θ , because the ratio T/θ is a function of pressure only).

A second derived potential temperature θ_L

An analogous variable, conservative to the same degree of approximation as θ_E, can be defined from 3.2.6

3.2.8 $$c_p \frac{D\theta}{Dt} - \frac{\theta}{T} L \frac{Dr_L}{Dt} = c_p \frac{\theta}{\theta_L} \frac{D\theta_L}{Dt} \qquad \theta_L \approx \theta \exp\left(\frac{-Lr_L}{c_p T}\right)$$

This new variable, θ_L, as yet unnamed, is also conserved under a wet adiabatic change, provided the liquid water is carried along with the air.

We shall use both the separate variables θ, r, r_L; which may be handled without approximation, and θ_L. It is important to realise that the single variable θ_E (or θ_L), or the variable pairs (θ, θ_E) or (θ, θ_L), are inadequate to describe cumulus convection. Of the 3 equations 3.2.4, 3.2.5, 3.2.6 only 2 are independent. Thus we have the choice of using any 2 of the variable pairs (θ, r), (θ, r_L), (r, r_L), or in approximate form any two of θ_E, θ_L, $(r + r_L)$.

It will become clear in succeeding sections that the most useful equations are those in θ_L (or θ, r_L) and (r, r_L) and not equation 3.2.4 or 3.2.7. Thus I fear that the concentration on the use of θ_E (or θ, r) as the variable for handling the water in cumulus convection has obscured our understanding of the process.

Expansion of equations 3.2.4, 3.2.5, 3.2.6

If equations 3.2.4, 3.2.5, 3.2.6 are expanded in terms of horizontal mean values, and deviations, and simplified by neglecting horizontal fluxes and the variation of $\frac{\theta + \theta'}{T + T'}$, we obtain (analogous to the derivation of 3.2.3 from 3.2.1)

3.2.9 $$\tilde{\rho} c_p \left(\frac{\partial \tilde{\theta}}{\partial t} + \tilde{W}\frac{\partial \tilde{\theta}}{\partial Z}\right) + \frac{\theta}{T}\tilde{\rho} L \left(\frac{\partial \tilde{r}}{\partial t} + \tilde{W}\frac{\partial \tilde{r}}{\partial Z}\right) = -\frac{\partial}{\partial Z}\left(\tilde{\rho} c_p \widetilde{W'\theta'}\right) - \frac{\theta}{T}\frac{\partial}{\partial Z}\left(\tilde{\rho} L \widetilde{W'r'}\right)$$

3.2.10 $$\tilde{\rho} c_p \left(\frac{\partial \tilde{\theta}}{\partial t} + \tilde{W}\frac{\partial \tilde{\theta}}{\partial Z}\right) - \frac{\theta}{T}\tilde{\rho} L \left(\frac{\partial \tilde{r}_L}{\partial t} + \tilde{W}\frac{\partial \tilde{r}_L}{\partial Z}\right) = -\frac{\partial}{\partial Z}\left(\tilde{\rho} c_p \widetilde{W'\theta'}\right) + \frac{\theta}{T}\frac{\partial}{\partial Z}\left(\tilde{\rho} L \widetilde{W'r_L'}\right)$$

3.2.11 $$\tilde{\rho}\frac{\partial}{\partial t}(\tilde{r} + \tilde{r}_L) + \tilde{\rho}\tilde{W}\frac{\partial}{\partial Z}(\tilde{r} + \tilde{r}_L) = -\frac{\partial}{\partial Z}\left(\tilde{\rho}\widetilde{W'r'} + \tilde{\rho}\widetilde{W'r_L'}\right)$$

The variations of L and c_p with T have been neglected, and $\bar{\rho}$ is a horizontal mean density: triple correlations with a perturbation density have been neglected

In the next section we shall consider what can be learned from these equations.

3.3 The transport equations

The situations in which some of the terms in equations 3.2.9, 3.2 10, and 3.2.11 are small, greatly further our understanding of cumulus convection.

Sensible heat and liquid water transport equation: 3.2.10

The condensation of liquid water in the cumulus layer releases latent heat. If the water is dropped out, or the layer steadily fills with cloud, then the layer will also warm up. If however all the liquid water evaporates again, then the latent heat is removed again, and the layer is only modified if the regions of condensation and evaporation do not coincide. In this thesis we wish to consider non-precipitating, fully-evaporating clouds, so the question of liquid water transport becomes important. In a wide range of convective situations, the accumulation of liquid water in the cumulus layer, (as the area coverage and depth of typical clouds increases) has a longer time-scale than the processing of water through the system by the individual clouds. We shall find that because there is an upward liquid water transport (3.5), the clouds though transient, modify the mean atmospheric temperature, $\tilde{\theta}$. Yet the mean liquid water in the cumulus layer may be constant, or changing only slowly. Specifically, there are a wide range of circumstances, when

$$\frac{\theta}{T}\frac{L}{c_p}\frac{\partial \tilde{r}_L}{\partial t} \ll \frac{\partial \tilde{\theta}}{\partial t}$$

An example of a system in which $\tilde{r}_L$ may be essentially constant, while $\tilde{\theta}$ is being continuously modified by the convection, is the trade cumulus layer. The timescale comparison is essentially one between cloud life-time, and the doubling time for total cloud liquid water in the layer, so that even for diurnal convection, the neglect of $\frac{\partial \tilde{r}_L}{\partial t}$ is a good first approximation.

A second widely valid simplification to 3.2.10 is to neglect

$$\frac{\theta}{T}\frac{L}{c_p}\frac{\partial \tilde{r}_L}{\partial Z} \ll \frac{\partial \tilde{\theta}}{\partial Z}$$

This is a good approximation when the clouds cover a small fractional horizontal area.

It will be possible in principle to use the model retrospectively to test the validity of these approximations. This neglect of mean liquid water variations in the cumulus layer, (but not liquid water transports) is not essential to this cumulus model, merely a helpful simplication with a wide range of validity.

With these 2 approximations, 3.2.10 becomes

3.3.1 $$\tilde{\rho} c_p \frac{\partial \tilde{\theta}}{\partial t} + \tilde{\rho} c_p \tilde{W} \frac{\partial \tilde{\theta}}{\partial Z} = -\frac{\partial}{\partial Z}(\tilde{\rho} c_p \widetilde{W'\theta'}) + \frac{\theta}{T}\frac{\partial}{\partial Z}(\tilde{\rho} L \widetilde{W'r_L'})$$

This is closely analogous to 3.2.3 for dry convection, but contains an extra term, the divergence of the vertical liquid water flux as well as that of the sensible heat flux.

The analogy with dry convection becomes closer if we use the variable θ_L . The neglect of

$$\frac{L\theta}{c_p T}\tilde{r}_L \ll \tilde{\theta}$$

is also the approximation

$$\tilde{\theta} = \tilde{\theta}_L$$

Eq. 3.2.8 may be used to replace the R H S. of 3.3.1 by a transport of θ_L

3.3.2 $$\tilde{\rho} c_p \frac{\partial \tilde{\theta}}{\partial t} + \tilde{\rho} c_p \tilde{W} \frac{\partial \tilde{\theta}}{\partial Z} = -\left(\frac{\overline{\theta}}{\overline{\theta}_L}\right)\frac{\partial}{\partial Z}(\tilde{\rho} c_p \widetilde{W'\theta_L'})$$

As mentioned in 3.2, this can only be an approximate relationship as the ratio θ/θ_L differs for cloud and environment, so that θ_L is not strictly conserved. An average factor ($\overline{\theta/\theta_L}$), which is not well defined, has been included to indicate this. Fortunately however, the inaccuracy of the approximation is only a few percent, even if the factor ($\overline{\theta/\theta_L}$) is omitted altogether

The cloud-environment circulation is the agent for these transports, and we know both from simple dynamical models, and from observation, that in the clouds

$$\overline{w'\theta'} \ll \frac{L\overline{r_L'w'}}{c_p}$$

(typically 0.2°C and 2.5°C respectively in small cumulus). However θ and r_L are also closely correlated in small cumulus (see for example: Telford and Warner, 1962), so it follows that there exist situations when

$$\overline{w'\theta'} \ll \frac{L}{c_p}\overline{w'r_L'}$$

In general the last term in 3.3.1 is always dominant.

It represents the source of sensible heat from the net liquid water condensation in a horizontal slice of the atmosphere. Only part of this released latent heat is advected upwards as a sensible heat flux $\overline{w'\theta'}$, while the warming of the mean layer $\tilde{\theta}$ completes the heat balance. The full mechanism of this process will be examined in the next few sections (3.4 to 3.7). However, it seems clear from these figures that, unlike dry convection (eq. 3 2.3) where the warming of the layer is related to the divergence of sensible heat flux· in cumulus convection, the warming of the layer has the sign of the divergence of the liquid water flux. This is important, as the upward advection of liquid water by the clouds (see 3.5) is a truly latent (i.e. hidden) heat flux. This redistribution of heat by the liquid water dominates over the sensible heat transfer, while only the latter is associated with the kinetic energy generation.

Only at cloud-base where $\overline{w'r_L'} = 0$, is the sensible heat flux of major significance, but the discussion of its magnitude will be left to chapter 4.

Total Water transport equation

It will also be a useful approximation to simplify 3.2.11 by neglecting the variations in the mean liquid water content of the layer: assuming

$$\frac{\partial}{\partial t}\tilde{r}_L \ll \frac{\partial}{\partial t}\tilde{r}$$

$$\frac{\partial}{\partial Z}\tilde{r}_L \ll \frac{\partial}{\partial Z}\tilde{r}$$

if cloud cover is small.

Then

3.3.3 $$\tilde{\rho}\frac{\partial \tilde{r}}{\partial t} + \tilde{\rho}\tilde{W}\frac{\partial}{\partial Z}\tilde{r} = -\frac{\partial}{\partial Z}\left(\tilde{\rho}\overline{W'r'} + \tilde{\rho}\overline{W'r_L'}\right)$$

This simplification is useful, because again, although the cumulus are continually putting water vapour into the layer they occupy, this process has typically a shorter time-scale than the time-scale of total liquid water increase.

In 3.3.1 (or 3.3.2), and 3.3.3 we have 2 equations for the change in mean potential temperature, and water vapour mixing ratio of the cumulus layer in terms of the transports by the clouds. Both these changes are comparable, so it follows that eq. 3.2.9 cannot usefully be simplified.

3.4 Parcel Lapse Rates for wet ascent and descent

Before the vertical liquid water transport in the cumulus layer can be discussed it is necessary to consider parcel lapse rates for saturated motion.

The wet adiabatic lapse rate for the ascent or descent of an isolated saturated air mass in pressure equilibrium with its surroundings is well known. The non-precipitating cumulus layer is only a few km. deep, so the distinction between strictly reversible and pseudo-wet adiabatic processes is not important.

It is also well known that dilution ("mixing") with an unsaturated environment evaporates cloud water, and that this process is important in ordinary cumulus convection. One major, and perhaps poorly appreciated, factor is that dilution introduces an asymmetry between saturated ascent and descent. Dilution or entrainment can be parameterised, in a manner similar to that of Stommel (1947), in terms of the rate of dilution (dM/dZ) of a saturated cloud parcel (of mass M, temperature T_c, and saturation mixing ratio $r_s(T_c)$) by the unsaturated environment (T_e, r_e). Γ_c (equals $\partial\theta_c/\partial Z$) is the resultant cloud parcel lapse rate.

The extensive quantity corresponding to eq. 3.2.4, which is conserved in isobaric mixing, as well as vertical displacement, is $\sum_i (M_i c_p \theta_i) + \frac{\theta}{T} \sum_i (M_i L r_i)$ In differential form, dilution may therefore be expressed

3.4.1 $$\frac{d}{dZ}(M\theta_c) + \frac{L\theta}{c_p T}\frac{d}{dZ}(M r_c) = \frac{dM}{dZ}\left(\theta_e + \frac{L\theta}{c_p T} r_e\right)$$

where $r_c \left(= r_s(T_c)\right)$ and r_e are water vapour mixing ratios for cloud and environment respectively.

$$\therefore \qquad \frac{d\theta_c}{dZ} + \frac{L\theta}{c_p T}\frac{dr_c}{dZ} = -\frac{1}{M}\frac{dM}{dZ}\left((\theta_c - \theta_e) + \frac{L\theta}{c_p T}(r_c - r_e)\right)$$

Now it follows from the definition of Γ_w, that

$$\frac{d\theta_c}{dZ} + \frac{L\theta}{c_p T}\frac{dr_c}{dZ} = -K(\Gamma_w - \Gamma_c)$$

where

$$K = 1 + \frac{L^2 r_s(T_c)}{c_p R_v (T_c)^2}$$

and R_v is the gas constant for water vapour.

3.4.2 $$\therefore \qquad \Gamma_w - \Gamma_c = \frac{1}{K}\frac{1}{M}\frac{dM}{dZ}\left((\theta_c - \theta_e) + \frac{L\theta}{c_p T}(r_c - r_e)\right)$$

This is the familiar entrainment relationship (see Hess, 1959). The factor θ/T arises from our definition of Γ_c, Γ_w as $d\theta/dZ$. The numerical factor K is the ratio of the so-called saturation specific heat of air to the dry specific heat at constant pressure: c_p. These specific heats differ, because to change the temperature of a saturated air mass it is also necessary to evaporate or condense water, as $r_s(T)$ changes.

The cloud parcel lapse rate differs from the wet adiabatic lapse rate, if both

(a) $\theta_c \neq \theta_c$, or the environment is unsaturated

(b) there is dilution, or entrainment, here parameterised by dM/dZ.

Simplification of 3.4.2

It is possible to make an approximation to 3.4.2 which contains only the properties of the environment. Typically

$$\theta_c - \theta_e < 1^\circ$$

when $K(T_c) = K(T_e)$

Further $$r_c = r_s(T_c) = r_s(T_e) + (K-1)\frac{T}{\theta}(\theta_c - \theta_e)$$

$$\therefore \quad \frac{\frac{L\theta}{c_pT}(r_c - r_e) + (\theta_c - \theta_e)}{K} = \frac{\frac{L\theta}{c_pT}(r_s(T_e) - r_e)}{K} + (\theta_c - \theta_e)$$

In most circumstances it is a good first approximation to neglect

3.4.3 $$\theta_c - \theta_e << \frac{\frac{L\theta}{c_pT}(r_s(T_e) - r_e)}{K}$$

($< 1^\circ$ $\sim 4^\circ$)

That is, the subsaturation of the environment matters more than the temperature difference between cloud and clear air represented by $\theta_c - \theta_e$ in 3.4.2.

A scale length for dilution: S

It is convenient to write the fractional rate of dilution of cloud mass in terms of a scale length for the entrainment. Ascent and descent are distinguished in 3.4.2, because with Z positive upwards, $\frac{1}{M}\frac{dM}{dZ}$ changes sign.

3.4.4 ASCENT $$\frac{1}{M}\frac{dM}{dZ} = \frac{1}{S}$$

3.4.5 DESCENT $$\frac{1}{M}\frac{dM}{dZ} = -\frac{1}{S}$$

S is some characteristic of cumulus convection, a length (numerically positive) about which we know little. It may differ for ascent or descent, but only some gross average value will be used here. We shall further express S

in terms of the depth of the convective layer in 5.2, when it will become possible to determine values for S (~few km). $\frac{1}{M}\frac{dM}{dZ}$ or $\frac{1}{S}$ is intended to symbolise a rate of dilution, or entrainment. It is this that determines the internal temperature of the cloud. It does not necessarily follow that the ascending cloud mass increases at this same rate: there may be a 2-way mixing process involving the loss of cloudy air to the environment. The tacit assumption, that has always been made in entrainment calculations, is that the environmental air, with which the cloud is diluted, has not been modified significantly by the cloud now ascending through it. This is not obvious, but more detailed study of the sub-cloud scale transports are necessary before a better model can be suggested. It will be necessary in this thesis to use the simple formulation above (3.4.4 and 3.4.5), and obtain suitable values for S in terms of the layer depth by comparison with observation. (see 5.2 and 6.3).

Parcel Lapse rates for saturated ascent and descent with entrainment

Using approximation 3.4.3 and equations 3.4.4 and 3.4.5, one obtains the pair of equations

3.4.6 ASCENT $\qquad \Gamma_{c_1} = \Gamma_w - \frac{\theta}{T}\frac{R}{KS}$

3.4.7 DESCENT $\qquad \Gamma_{c_2} = \Gamma_w + \frac{\theta}{T}\frac{R}{KS}$

where $R = \frac{L}{c_p}(r_s(T_e) - r_e)$ is a measure of the unsaturation of the environment

S is a scale length for dilution or entrainment

The asymmetry is clear. On ascent water is condensed at a rate proportional to Γ_w, but some is evaporated again while on descent both the entrainment and the descent are working in the same sense, to evaporate liquid water, and reduce θ.

One may express 3.4.2 in terms of θ_E by noting the exact relation

3.4.8 $$\frac{1}{\theta_E}\left(\frac{\partial\theta_E}{\partial Z}\right)_c = -\frac{K}{\theta}(\Gamma_w - \Gamma_c)$$

where $\left(\frac{\partial\theta_E}{\partial Z}\right)_c$ is the change of θ_E with Z following a saturated cloud parcel which is being diluted.

Using an approximate average value of (θ_E/T) (see 3.2), one can write:

3.4.9 $$\left(\frac{\overline{\theta_E}}{\overline{T}}\right)\left[\frac{L}{c_p}(r_s(T_c) - r_e) + (T_c - T_e)\right] = \theta_E(\text{cloud}) - \theta_E(\text{environment})$$

Then, from 3.4.2, 3.4.4, 3.4.5, 3.4.6,

3.4.10 $$\left(\frac{\partial\theta_E}{\partial Z}\right)_c \simeq \mp \frac{\theta_E(c) - \theta_E(e)}{S}$$

for ascent and descent respectively. The approximation is the neglect of the difference between θ_E/T in the cloud and in the environment. This is a simple dilution relationship for an (approximately) conserved variable.

The θ_L analogue of 3.4.10 may be derived by considering the dilution of a cloud parcel by the environment, in the light of conservation relation 3.2.6

$$\frac{d}{dZ}(M\theta_c) - \frac{L\theta}{c_pT}\frac{d}{dZ}(M r_L) = \frac{dM}{dZ}\theta_e$$

3.4.11 $$\therefore \quad \frac{d\theta_c}{dZ} - \frac{L\theta}{c_pT}\frac{dr_L}{dZ} = -\frac{1}{M}\frac{dM}{dZ}\left\{(\theta_c - \theta_e) - \frac{L\theta}{c_pT}r_L\right\}$$

Once again, if we neglect horizontal variations of θ_L/T, we obtain

3.4.12 $$\left(\frac{\partial\theta_L}{\partial Z}\right)_c = -\frac{1}{M}\frac{dM}{dZ}\left(\theta_L(c) - \theta_L(e)\right)$$

a dilution relation for an (approximately) conserved variable. The suffix L on $\theta_L(e)$ is redundant as

$$\theta_L(e) = \theta_e$$

$$\simeq \tilde{\theta} \qquad \text{(see 3.7)}$$

It is the absence of liquid water in the environment that makes θ_L such a useful variable. The use of θ_E involves the passive transport of water vapour, and the water vapour stratification. If we use θ_L, we consider only the water vapour that condenses, and thereby significantly affects the motion, and the modification of the temperature structure of the cumulus layer.

Substituting from 3.4.4 and 3.4.5, one obtains

3.4.13 $$\left(\frac{\partial \theta_L}{\partial Z}\right)_c = \mp \frac{\theta_L(c) - \theta_L(e)}{S}$$

for ascent and descent respectively. This is a very useful relationship as it enables one to show that the flux of θ_L, and therefore the total heat flux, is downwards (see 3.5). We shall also use it in 3.8 and 5.2 to discuss lapse rate structure.

If we drop the suffix L from 3.4.13 we obtain

3.4.14 $$\left(\frac{\partial \theta}{\partial Z}\right)_d = \mp \frac{\theta(d) - \theta(e)}{S}$$

This is the dilution relation for dry convection, where (d) indicates a dry parcel.

Thus our treatment of wet convection in terms of θ_L transport (Eqs. 3.3.2 and 3.4.13), is equally applicable to dry convection, where $\theta = \theta_L$ (Eqs 3.2 3 and 3.4.14). Only the boundary conditions at the top and bottom of the convective layers are different. The similarities in lapse rate structure between dry and cumulus layers will become apparent in 3.8.

In the next section we shall show that the consequence of 3.4.13 is a downward total heat transport in the cumulus layer.

3.5 Irreversibility of (total heat transport in the cumulus layer (liquid water transport

It has been shown in 3.4 that dilution, or entrainment, leads to an asymmetry between the thermodynamics of upward and downward motion. One consequence is that the parcel lapse rate $\left(\frac{\partial\theta}{\partial Z}\right)_c$ for saturated descent is greater than that for saturated ascent when entrainment of unsaturated air is taking place. There are further general consequences of dilution, which determine the direction of the total heat transport, and the liquid water transport, in the cumulus layer.

The general solution is most easily found in terms of θ_L . Putting $\theta_L(e) = \theta_e$ in 3.4.13, and subtracting $\partial\theta_e/\partial Z$

3.5.1
$$\left(\frac{\partial\theta_L}{\partial Z}\right)_c - \left(\frac{\partial\theta_e}{\partial Z}\right) = - \frac{\partial\theta_e}{\partial Z} \mp \frac{\theta_L(c) - \theta_e}{S}$$

for ascent and descent respectively.

The solution of these linear differential equations is straightforward. For constant S , $\partial\theta_e/\partial Z$, we obtain

ASCENT $\quad Z_b < Z < Z_2$

$$\left(\theta_L(c) - \theta_e\right)_Z = \left(\theta_L(c) - \theta_e\right)_{Z_b} e^{-(Z-Z_b)/S} - S\frac{\partial\theta_e}{\partial Z}\left(1 - e^{-(Z-Z_b)/S}\right)$$

DESCENT

$$Z < Z_2$$

$$\left(\theta_L(c) - \theta_e\right)_Z = \left(\theta_L(c) - \theta_e\right)_{Z_1} e^{-(Z_1-Z)/S} + S\frac{\partial\theta_e}{\partial Z}\left(1 - e^{-(Z_1-Z)/S}\right)$$

The detailed solutions are not important. We need only to sketch $\theta'_L = \theta_L(c) - \theta_e$ (which is essentially $\frac{L\theta}{c_pT}r_L$) against Z , to see that at any height, θ'_L has a larger negative value on the way up than on the way down (see Figure 3.5.1).

The total heat flux ($\propto \overline{W'\theta'_L}$) through any level depends also on the specification of the total cloud mass flux through that level. This we do not yet know. However the rate of dilution sets an upper bound to the rate of increase of mass flux. If one assumes there is no loss of cloudy air from a cloud, only entrainment into it, one may rewrite 3.5.1 as

3.5.2
$$\frac{d}{dZ}\left(m_f\,\theta'_L\right) = - m_f \frac{\partial\theta_e}{\partial Z}$$

where m_f is the cloud mass flux through any level.

$$\pm \frac{1}{S} = \frac{1}{m_f} \frac{dm_f}{dZ}$$ for ascent and descent respectively.

Since m_f is steadily increasing with dilution, it is clear that on descent $-m_f \partial\theta_e/\partial Z$ is greater negative, than on ascent through the same level. We can thus sketch the curve of the flux of θ_L' (see Fig. 3.5.1). Even in this limiting case, the net flux of θ_L' which is the total heat flux, (sensible plus liquid water flux) is downwards. This is true for every cloud, and therefore must be true for the whole population.

If cloudy air is left behind (i.e. 'detrained'), so that the cloud mass flux increases less quickly than the dilution, this can only decrease the mass flux descending through any level, which does not affect our conclusion.

We conclude that the total net heat transport ($\rho c_p \overline{W'\theta_L'}$) by the clouds is downwards at all levels, provided only that the liquid water is carried along with the air.

Fig. 3.5.1

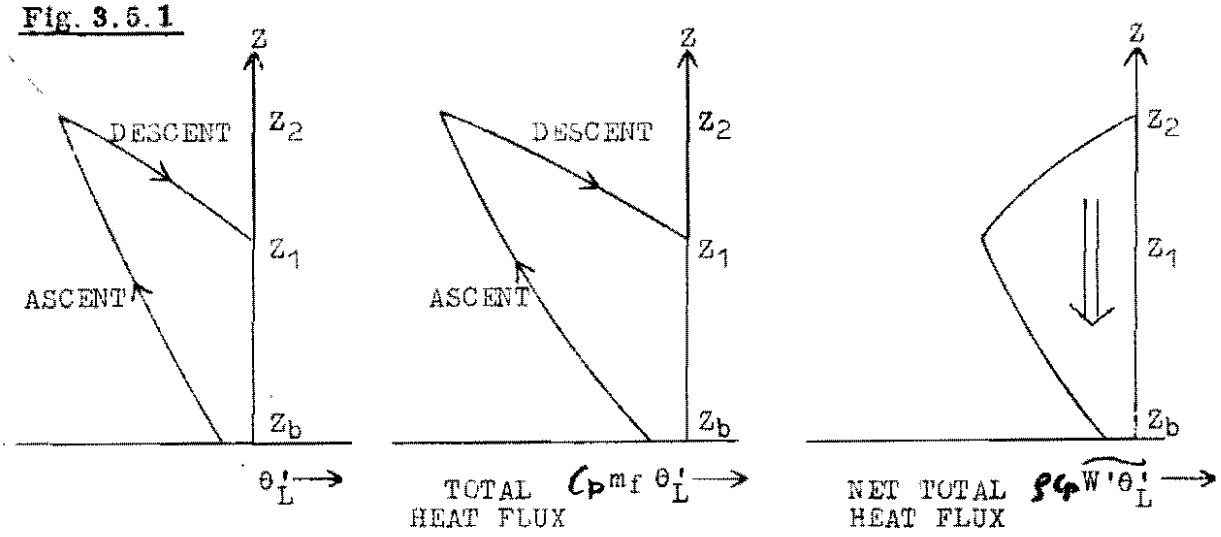

At cloud base θ_L' ($= \theta'$) is negative (see 3.8 and chapter 4). The diagrams then follow immediately because the slope of $d\theta_L'/dZ$, $d(m_f\theta_L')/dZ$ are greater negative on descent than ascent, because of dilution.

As mentioned earlier the diagrams for liquid water transport are schematically identical, but with sign reversed. Substituting 3.4.4, 3.4.5 [34] in 3.4.11, we obtain

$$\frac{L\theta}{c_pT} \frac{dr_L}{dZ} = \Gamma_{c_{1,2}} \mp \frac{1}{S}\left((\theta_c - \theta_e) - \frac{L\theta}{c_pT} r_L\right)$$

Fw

for ascent and descent respectively. This is no more than 3.5.1 re-expanded, and shows even greater asymmetry in $\frac{dr_L}{dZ}$ for ascent and descent, than in $d\theta'_L/dZ$; since Γ_{c1} , Γ_{c2} differ (see 3.4.6, 3.4.7) if the environment is nowhere saturated. Thus in the absence of shelf-cloud ($\overset{sc}{cu}_{gen}$), which we shall not consider in this thesis, all the liquid water is evaporated on descent before θ'_L reaches zero. The last part of the descent in Fig. 3.5.1 is therefore dry, ending in potential temperature equilibrium with the environment.

We shall integrate 3.5.1 for a simple 2-layer structure in 5.2, as a way of incorporating the dilution of a parcel during ascent and descent into a lapse rate model.

Dry Convection

The dry convection problem is essentially similar, except that the surface boundary condition is a positive heat flux. This varies with height as specified by 3.5.2 and is sketched in Fig.3.5.2.

Fig. 3.5.2

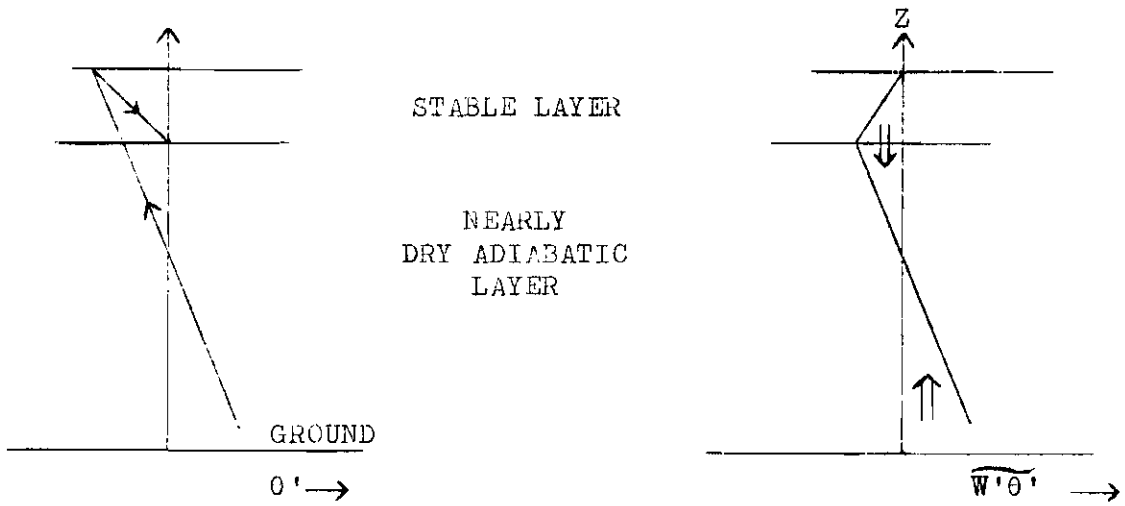

We shall return to these diagrams in 3.8.

3.6 Destabilising Nature of Cumulus Convection

It was shown in the last section that the essential consequence of entrainment into individual clouds is a net downward total heat flux, and a net upward liquid water flux. Averaging over the lifecycle of many clouds, water is condensed in the lower part of the cumulus layer, advected upwards, and evaporated in the upper part of the layer. Latent heat is released in the lower part and reabsorbed at a higher level. This is a destabilising process of great importance, as it is the mechanism by which the cumulus layer can grow in depth in the absence of subsidence.

Putting the large scale vertical motion field $\tilde{W} = 0$ in 3.3.2

3.6.1
$$\tilde{\rho}\, c_p \frac{\partial \tilde{\theta}}{\partial t} = -\left(\frac{\bar{\theta}}{\theta_L}\right) \frac{\partial}{\partial Z}\left(\tilde{\rho}\, c_p \widetilde{W'\theta_L'}\right)$$

We have sketched the form of $\widetilde{W'\theta_L'}$ in Fig. 3.5.1. It is clear that

$Z_1 < Z < Z_2$ $\quad \frac{\partial \tilde{\theta}}{\partial t}$ NEGATIVE

$Z_b < Z < Z_1$ $\quad \frac{\partial \tilde{\theta}}{\partial t}$ POSITIVE

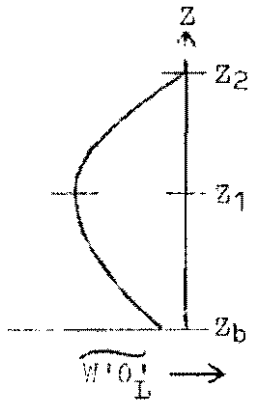

Fig. 3.6

Non-precipitating cumulus convection is a destabilising process (as of course is dry convection; see Fig.3.5.2). Even without large scale vertical motion, the cumulus layer will modify the vertical structure of the mean atmosphere, and deepen until the onset of precipitation introduces further factors (which accelerate the process). It will be remembered that Asai (1968) did not come to this conclusion, simply because his model did not evaporate any liquid water in the upper part of the layer (see 2.4 and 2.6).

The influence of large scale vertical motion ($\tilde{W}$) is complicated, and will be discussed in chapters 4 and 5.

We have established from the continuity equation for heat in the cumulus layer, and a semiquantitative discussion of the cloud heat fluxes, how the mean potential temperature in the cumulus layer is modified. However the mechanism has not been discussed, although 3.5.2 indicates a connection

with the environmental stratification. In the next section, we shall show that it is the mean vertical motion of the stably stratified environment, which alters the local potential temperature of the cumulus layer.

3.7 Mechanism for modifying the mean atmosphere: a mass flux model

In this section we shall discuss how the potential temperature structure of the cumulus layer is modified by compensating motions in the environment. The frequently used concept of cloud and environment was introduced in 1.3. It is a useful concept, as the timescale of modification of the mean stratification is longer than the lifetime of an individual cloud. Hence to good approximation one can calculate the life-cycle of a single transient cumulus cloud, assuming the stratification to be constant. Nonetheless each cloud slightly changes the stratification or environment for the next cloud. As far as the potential temperature distribution is concerned this is not a process which requires thorough mixing of cloud and environment.

This model can be made precise by isolating a single cloud's life-cycle. The idealised starting condition is a finite isolated region of atmosphere, enclosed by rigid vertical boundaries, at rest, and with a given stratification. A single cloud is allowed to pass through its entire life-cycle. In the cloud, which shall occupy only part of this isolated region, the potential temperature of air parcels is modified, by condensation and evaporation processes, from the horizontal mean $\tilde{\theta}$. This modified cloudy air rises, and then sinks, while in the rest of the layer, the environment, there are compensating vertical motions. After the cloud has completely evaporated, and the entire system come to hydrostatic equilibrium again, one can measure the vertical displacement of environment away from the cloud, where parcels of air have conserved potential temperature.

For an environmental parcel:

$$0 = \delta\theta = \left(\frac{\partial\theta_e}{\partial Z}\right)_t \delta Z + \left(\frac{\partial\theta_e}{\partial t}\right)_Z \delta t$$

If $\delta t >> \tau$, the lifetime of the cloud, then δZ is the final displacement of the environment produced by the cloud. It is now simple to calculate an average vertical velocity of the environment, appropriate to the area density of clouds in the real atmosphere. Suppose there are N such clouds in time

Relation between environment and mean atmosphere

$$\tilde{\theta} = (1 - \alpha)\theta_e + \alpha\theta_c$$

where α is the mean area coverage of cloud at a level.

3.7.4 $$\therefore \quad \tilde{\theta} = \theta_e + \alpha\phi$$

where $\phi = \theta_c - \theta_e$

$$\therefore \quad \frac{\partial\tilde{\theta}}{\partial t} = \frac{\partial\theta_e}{\partial t} + \frac{\partial}{\partial t}(\alpha\phi)$$

From 3.7.3, 3.7.4

$$\frac{\partial\tilde{\theta}}{\partial t} - \frac{\partial}{\partial t}(\alpha\phi) = -(\tilde{W} + W_D)\left(\frac{\partial\tilde{\theta}}{\partial Z} - \frac{\partial}{\partial Z}(\alpha\phi)\right)$$

If the area coverage of cloud is small, then both of the terms in $(\alpha\phi)$ are negligible. The second term on the left hand side represents an increased storage of heat in the clouds; we have already neglected a similar (but larger) term for the increase of liquid water storage (in 3.3), so we shall neglect $\frac{\partial}{\partial t}(\alpha\phi)$ here. Equally, in the absence of extensive layer cloud there will be no regions where $\frac{\partial}{\partial Z}(\alpha\phi)$ is significant.

Hence one obtains to good approximation:

3.7.5 $$\frac{\partial\tilde{\theta}}{\partial t} = -(\tilde{W} + W_D)\frac{\partial\tilde{\theta}}{\partial Z}$$

Thus if the area coverage of clouds is small, one may use the stratification and time rate of change of environment and mean atmosphere interchangeably. It is the mean vertical velocity of the environment, however, that is responsible for changing the potential temperature structure of the layer.

[Missing discussion of 'detrainment' of cloud water]

3.8 Lapse Rate Control and Structure

Before synthesising sections 3.4 to 3.7, we shall consider the problem of the lapse rates in the convective layer. This is a natural development from the model of 3.7. There it was shown that the life-cycle of a convective element modifies the stratification. Conversely this life-cycle is determined by the stratification. As the convection proceeds, it seems logical to expect the development of a stratification characteristic of either dry or cumulus convection. This is observed (Ludlam, 1966). The idea that there is a close connection between the life-cycle of an individual cloud and the stratification will be used in 5.2 to develop a closed model for the lapse rate structure of the cumulus layer. In this section, a few general topics will be discussed, and the structure of the dry and cumulus convective layers will be compared.

It would have been more logical to develop a complete model for dry convection before considering cumulus convection, as it is necessary to model the dry layer, in order to link the cumulus convection to the ground. However, as the author has chosen to investigate cumulus convection, the dry layer will be dealt with more briefly. We shall first examine the structure of the dry convective layer, and then contrast it with that of the cumulus layer. The similarities will be apparent (indeed the lapse rate model of 5.2 could be adapted to determine a 2-layer structure for the dry convective layer above the superadiabatic layer), but only the model for the cumulus layer will be fully justified in this thesis.

Dry Convective Layer

There has been little work on the problem of the characteristic stratification of this layer. In the so-called constant flux layer close to the surface, there is a down gradient heat transfer by turbulence, locally generated by shear and horizontal temperature gradients. Above this surface superadiabatic layer, there is a largely buoyant transfer of heat upwards against a stable potential temperature gradient ($\partial\tilde{\theta}/\partial z$ positive). This dry convective layer warms and its stratification is maintained.

The mass flux model of 3.7 is useful in understanding this process. Because of the difference in timescale between the lifetime of a convective element and the modification of the stratification, one can again consider the

isolated ascent of a single buoyant element through an environment initially uniform and at rest. The buoyant element rises; the environment sinks in compensation conserving potential temperature. Again one can describe the process by an equation

3.8.1 $$\frac{\partial \tilde{\theta}}{\partial t} = -W_D \frac{\partial \tilde{\theta}}{\partial Z} \qquad (\tilde{W} = 0)$$

as the same approximations are valid ($\alpha \sim 0.1$: see later).

As the stratification is stable, the mean temperature of the layer rises, while the rising element loses buoyancy, and comes to rest. The warming of the layer does not require thorough mixing of the convective element and the environment.

The precise details of the process are now included in the computation of W_D , but we shall estimate a consistent set of numerical values for the relevant variables based on the surface heat flux, and the potential temperature excess of an element displaced upwards from the superadiabatic layer.

Turbulent mixing occurs in the subcloud layer as well as in the cumulus layer, but as there is no evaporation of water, its effects are numerically smaller, and initially it will be omitted.

Two simple equations relate the surface heat flux to the parameters of a typical convective element, at a height of say 100m above the surface:

3.8.2 $$F_{o\theta} \sim \rho c_p \alpha W'\theta'$$

where $F_{o\theta}$ is the surface heat flux

α " " fractional area coverage of rising convective elements

W' " " a typical vertical velocity of a rising convective element

θ' " " " " potential temp. excess of a rising convective element

3.8.3 $$W'^2 \sim g \frac{\theta'}{\bar{\theta}} Z$$

Numerical constants have been omitted. Hence one obtains a set of numbers, in accord with observation for a height of 100m .

From $F_{o\theta}/\rho c_p = 10 \quad ^\circ C \text{ cm } s^{-1}$

$\theta' = 1 \quad ^\circ C$

we deduce $W' = 100 \quad \text{cm } s^{-1}$

$\alpha = 1/10$

3.8.4 Since $\alpha W' = -(1-\alpha) W_D$

$W_D \approx -10 \quad \text{cm. } s^{-1}$

This representative set of numbers can be completed by supposing: that the dry convective layer has depth

$$Z_s = 1 \text{ km} \quad ;$$

that all the surface heat flux goes to warming this layer; that there is no other heat flux into this layer; and that $\frac{\partial\tilde{\theta}}{\partial t}$, $\frac{\partial\tilde{\theta}}{\partial Z}$ are independent of height.

Then

3.8.5
$$\frac{F_{\odot\theta}}{\rho c_p} = \frac{\partial\tilde{\theta}}{\partial t} Z_s$$

$$\therefore \quad \frac{\partial\tilde{\theta}}{\partial t} = 10^{-4} \text{ °C s}^{-1} \approx 10\text{°C day}^{-1}$$

From 3.8.1
$$\frac{\partial\tilde{\theta}}{\partial Z} = -\frac{1}{W_D}\frac{\partial\tilde{\theta}}{\partial t}$$

$$\approx 10^{-5} \text{ °C cm}^{-1} = 1\text{°C km}^{-1}$$

Thus the typical stratification in the dry convective layer, deduced from this simple consideration is $+1\text{°C km}^{-1}$: in agreement with observation (e.g. Grant, 1965; Warner and Telford, 1967).

Combining 3.8.1, 3.8.2, 3.8.4, 3.8.5, one obtains

3.8.6
$$\frac{\partial\tilde{\theta}}{\partial Z} = (1-a)\frac{\theta'}{Z_s}$$

We see the temperature difference between top and bottom of the layer is not quite θ'. The region is warming up as the buoyant elements rise, so that, with the stratification given by 3.8.6, the rising elements have just lost their buoyancy on reaching the height Z_s. This is a model without mixing (see later), but it clearly illustrates, how air is cycled through the system, and the stratification is maintained as the layer warms up. (Fig. 3.8.1).

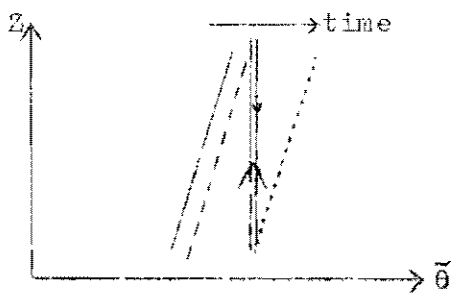

Fig. 3.8.1

The firm line is the stratification when a convective element starts its ascent, the dashed line the stratification when it reaches the top of the layer, and the dotted line the stratification when the same air, after a much

longer time, has subsided with the environment back to near ground level.

One further point about 3.8.6 is that it is really

3.8.7 $$\frac{\partial \tilde{\theta}}{\partial z} = (1 - \alpha)\left[\Gamma_p + \frac{\theta'}{Z_s}\right]$$

but Γ_p, the dry parcel lapse rate is zero in the absence of mixing.

The model presented above is oversimplified in two important respects

(a) There is no dilution or mixing of ascending buoyant elements

(b) The heat flux everywhere in the layer is upwards. This means a kinetic energy generation at all levels, the dissipation of which we have not considered. Ball (1960) showed that there will be a downward sensible heat flux at the top of the layer, where most of the kinetic energy, generated in the lower part of the layer, is reconverted to potential energy. In other terms, the convective elements overshoot their first level of no buoyancy.

By considering these factors and the observed temperature structure we can qualitatively extend the model.

Graphical Description of Dry Convection

The observed temperature structure of the dry convective layer (see for example Grant (1965); Warner and Telford (1967), and chapter 6) is shown in Fig. 3.8.2, together with the path of a typical parcel rising with mixing from the superadiabatic layer. Figs. 3.8.2, and 3.8.3 for the heat flux, together give a self-consistent picture of dry convection. (see Fig.3.5.2).

The surface superadiabatic layer is dominated by mechanical stirring, and there is a down gradient transfer of heat. Convective elements rise from this layer, and being buoyant gain kinetic energy. These elements are diluted by mixing (eq.3.4.14) as they ascend through the nearly dry adiabatic layer, which subsides between the rising elements, as modelled earlier in this section. At the top of this layer there is a more stable layer, which we shall call a transition layer if there is cumulus convection above. The convective elements overshoot their first level of zero buoyancy (e.g. see Grant 1965), and fall back finally to the base of the stable layer.

The heat flux curve plotted against height is shown in Fig.3.8.3. It has a turning point at the base of the stable layer.

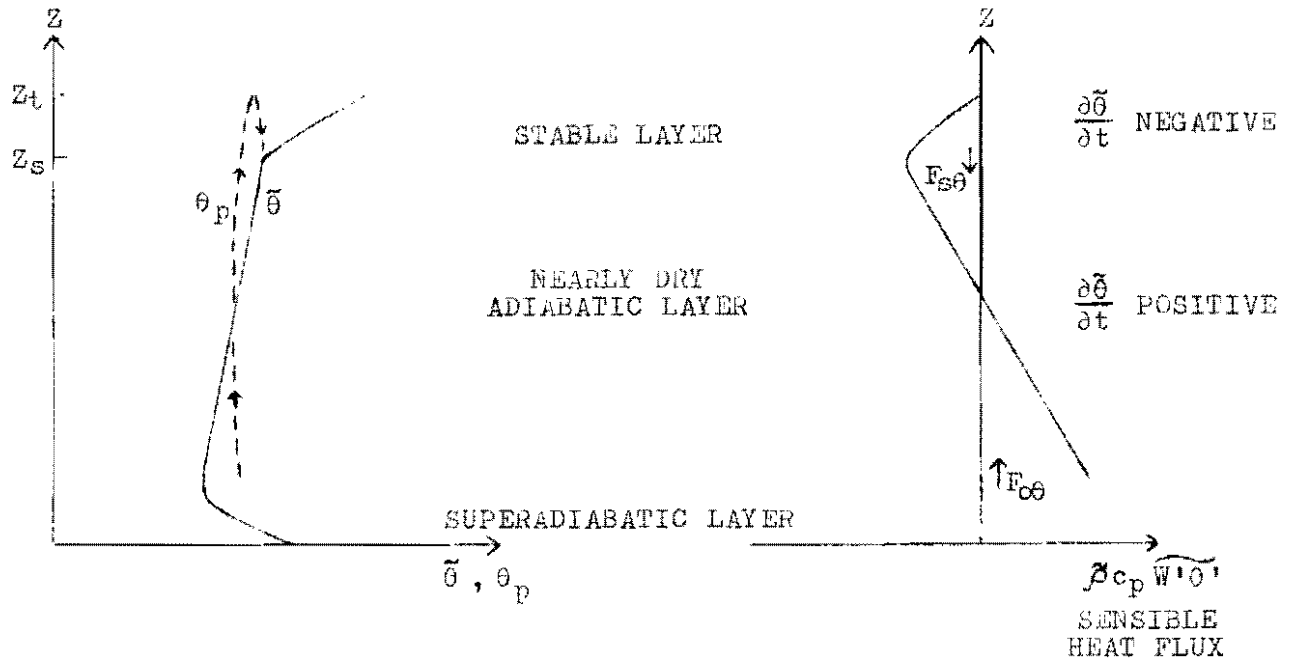

Fig. 3.8.2 Fig. 3.8.3

LEGEND The dashed line is the path of a typical parcel potential temperature: θ_p. The firm lines are the mean lapse rate, and the upward sensible heat flux. $\tilde{W} = 0$.

Recalling 3.2.3 for $\tilde{W} = 0$

3.8.8 $$\rho \frac{\partial\tilde{\theta}}{\partial t} = - \frac{\partial}{\partial Z}(\tilde{\rho}\widetilde{W'\theta'})$$

it is clear that the nearly dry adiabatic layer is being warmed, while the stable layer is being cooled. There is a downward heat transfer (maximum $F_{s\theta}$) the upper part of the layer associated with this cooling, in fact lifting, of the stable layer. (This has often been called 'erosion', but in fact the stable layer is cooled largely by compensating ascent as described by 3.8.1).

The positive area under the curve of Fig. 3.8.3 is related to the net kinetic energy generation in the layer. If two simplifications are made, in which

(a) one assumes no kinetic energy dissipation (as opposed to transformation back into potential energy), and no <u>net</u> kinetic energy

generation;

(b) one replaces the stable layer of finite depth by an idealised inversion of zero depth. (This requires very rapid mixing when the elements reach Z_S), and assumes that the lapse rate in the nearly adiabatic layer does not change with time ,

then one obtains the limiting case deduced by Ball (1960), in which the downward heat flux from the inversion equals the surface heat flux.

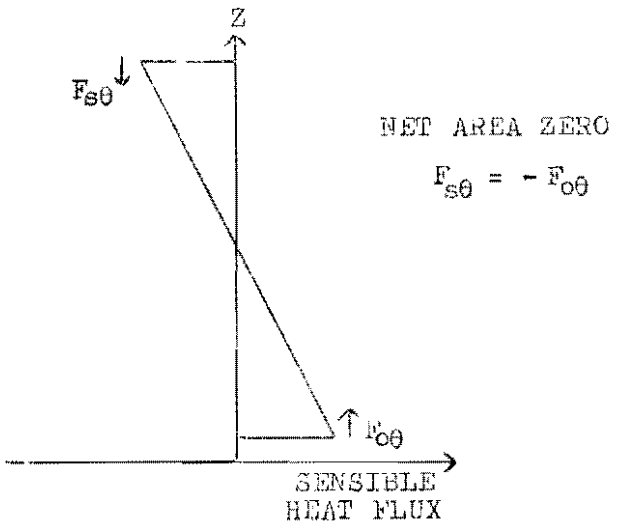

Fig. 3.8.4

In general one might expect

3.8.9 $$F_{s\theta} = -k F_{o\theta} \qquad \text{where} \qquad 0 < k < 1$$

A detailed model of the lapse rate structure of the dry convective layer similar to that of 5.2, would yield a value for k as a function of the dilution of a typical convective element. Preliminary calculations, and comparison with observations, indicate that k is about 0.5, rather than 0.1 or less.

In chapter 4, we too shall idealise the problem by considering only a sharp inversion of zero depth, but kinetic energy dissipation will be allowed for through the use of 3.8.9.

The Cumulus Layer

The lapse-rate structure of the cumulus layer presents some different problems, but once their nature is understood, it can be seen that the structure in the two layers is essentially similar. The simplest workable model has a 2 layer structure and a typical convective element. Such a model will be developed in detail in 5.2.

In this section we shall outline the similarities and differences between the lapse rate problem in the cumulus and dry convective layers, for $\bar{w} = 0$

(a) Parcel lapse rates for ascent and descent, with entrainment, are different in both layers. The analogues of 3.4.5, 3.4.6 in the dry layer were 3.4.14

$$\Gamma_{d1} = -\delta\theta/S ; \qquad \Gamma_{d2} = +\delta\theta/S$$

where $\delta\theta$ is an excess temperature of an element over its surroundings, S is a scale length for mixing.
However these are centred on Γ_D which is zero, while in the cumulus layer Γ_{c1}, Γ_{c2} are centred on Γ_w.

(b) The presence of the water phase change in the cumulus layer produces complications. As shown in 3.3.1, the total heat flux is no longer simply the sensible heat flux, so that the kinetic energy generation is no longer related to the total heat flux.
Nonetheless if the approximate variable θ_L is used to replace θ then the heat flux diagrams for dry and wet convection become closely analogous, and so too do parcel paths on a θ_L-Z diagram. (see Figs. 3.5.1 and 3.5.2).

(c) However the boundary conditions at the bottom of the layers are significantly different, and this accounts for the difference between Figs. 3.5.1 and 3.5.2. There is a positive sensible heat flux into the dry layer at the ground, but, because of the stable layer at the top of this dry layer, there is a negative sensible heat flux into the cumulus layer through cloud-base (see also chapter 4). Hence whereas $\frac{\partial\tilde{\theta}}{\partial Z} - (1-\alpha)\Gamma_p$ is positive in the dry layer, in the cumulus layer it must be negative if the clouds are to regain

buoyancy, and accelerate upwards.

$$\therefore \quad \Gamma_1 < \Gamma_{c1}$$

where Γ_1 is the lapse rate in the lower part of the cumulus layer. This must be generally true for cumulus convection: that Γ_{c1} sets an upper bound for the lapse rate in the lower part of the cumulus layer. How much smaller than Γ_{c1} is Γ_1 will be resolved in 5.2. (We shall also find that α is very small in the cumulus layer: only a few percent).

(d) In the upper part of the cumulus layer there is a more stable layer where

$$\Gamma_2 > \Gamma_{c1}$$

This brings the ascending cloudy air to rest. It then descends, evaporating its liquid water and comes into potential temperature equilibrium with the environment at the level z_1, which divides the 2 characteristic lapse rates Γ_1, Γ_2 and is also the level of maximum downward total heat flux. This is the simple structure modelled in 5.2. Real soundings may not show such a sharp division between Γ_1 and Γ_2, but this is a discontinuous two layer approximation to reality.

The essential difference here from the dry layer is that the dry convective elements are losing kinetic energy over the whole region where the (sensible) heat flux is downwards, whereas the clouds lose kinetic energy only above z_1, although the total heat flux is downwards throughout the cumulus layer.

We can sum up the fluxes, parcel paths and stratifications in Fig.3.8.5.

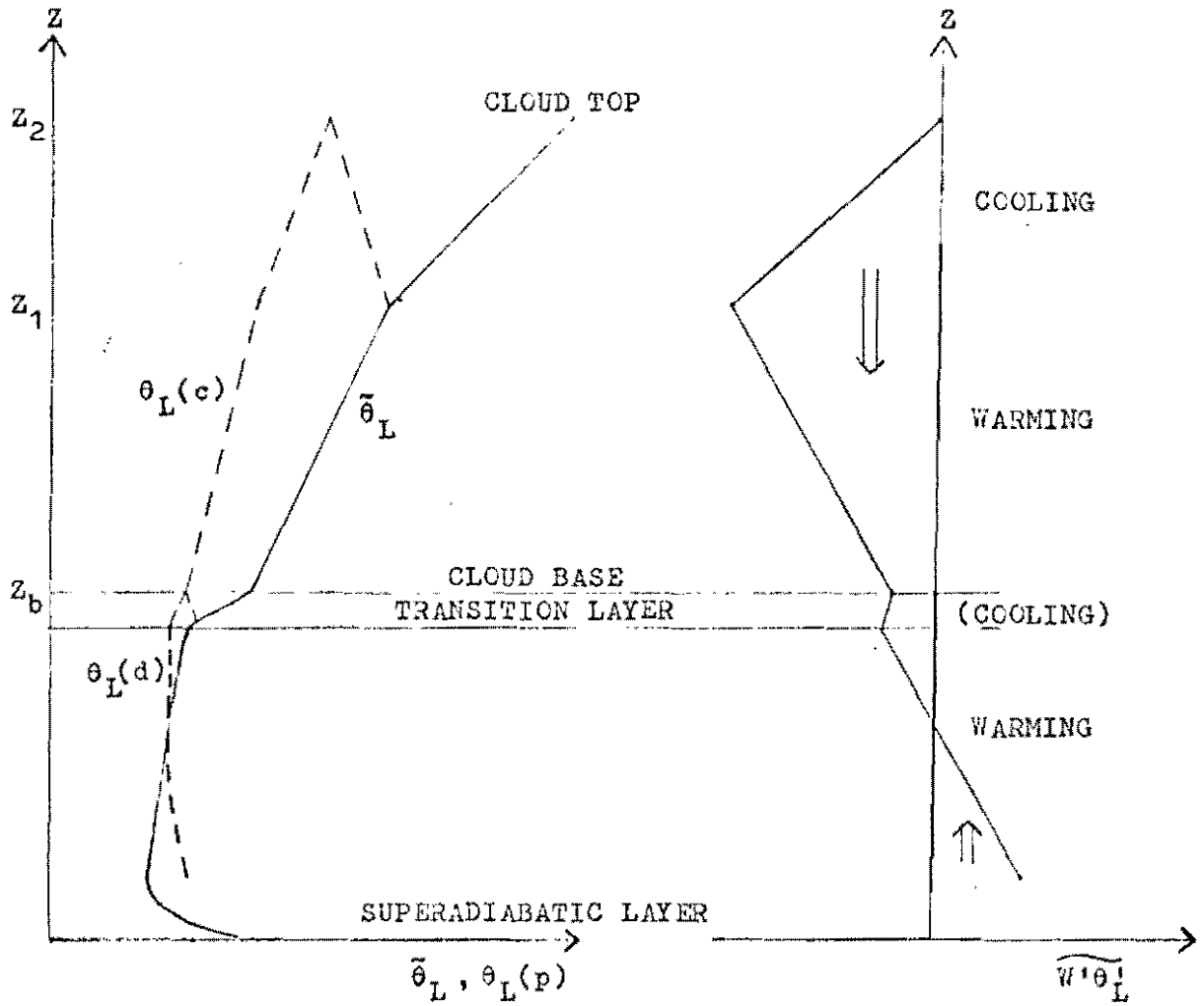

Fig. 3.8.5

Notes:

(i) $\tilde{w} = 0$

(ii) θ and θ_L are identical in the sub-cloud layer and $\bar{\theta} \simeq \theta_L$ in the cumulus layer.

(iii) The dashed lines are typical parcel paths. $\theta_L(c)$ is less than θ_c while the typical cloud parcel has a non-zero liquid water content. θ_c is in fact greater than $\tilde{\theta}$ over most of the range z_b to z_1.

Figure 3.8.5 requires some further comments

(i) Following Ludlam (1966), we have used the term transition layer for the more stable layer at the top of the dry convective layer, just below cloud base. Whether this layer is being cooled, that is lifted, will depend on whether cloud base is rising. This is discussed in chapter 4.

(ii) Though not easily apparent from this diagram, much of the dry convection from the ground does not rise through into the cumulus layer. This is because the lapse rate $\partial\tilde{\theta}/\partial Z$ in the cumulus layer is several times that in the sub-cloud layer. It follows from

$$\frac{\partial\tilde{\theta}}{\partial t} = -W_D \frac{\partial\tilde{\theta}}{\partial Z}$$

that W_D, or the convective mass flux, in the cumulus layer need only be a fraction of W_D in the sub-cloud layer to maintain equal $\partial\tilde{\theta}/\partial t$ in the two layers. If the two layers warm at equal rates, then the transition layer, which determines the fraction of the convective mass flux in the sub-cloud layer, which regains buoyancy, and rises to form clouds in the cumulus layer, is also maintained. It should be clear that this is a delicate control mechanism; as too large a W_D in the cumulus layer produces a more stable transition layer, which correspondingly reduces this W_D . This is made quantitative in chapter 4.

(iii) In Fig. 3.8.4, we are approximating a spectrum of sizes of convective element by just two: those that are trapped in the sub-cloud layer, the majority; and a second group which rise to the top of the cumulus layer. We shall regard all the little clouds which mark the top of dry convection from the ground, but which never regain buoyancy in the cumulus layer, as in the first category.

(e) The detailed structure of the cumulus layer is considered diagramatically in 3.10, and more quantitatively in chapter 5. We shall compare our deductions with some observations in chapter 6.

3.9 Discussion of earlier work on mass flux models

The fourth category of models, referred to in 2.1 as mass transport models, were not discussed in that section. We shall here consider three such models of convection, in the light of earlier sections of this chapter, particularly 3.7.

1) Fraser (1968) discussed cumulus convection in terms of a net cloud mass flux, and attempted to distinguish cloud and environment in a manner similar to the discussion in 3.7.

2) Pearce (1968) used a mass flux model to discuss the modification of the environment by cumulonimbus towers. This author used synoptic data, in a budget study of the synoptic scale fields, to deduce the environmental vertical velocity $W_e = \bar{\tilde{W}} + W_D$ (see eq. 3.7.5). He found that $W_e << \bar{\tilde{W}}$

3) Haman (1969) discussed the modification of the atmosphere by cumulus convection. He presented his work in a different, though essentially equivalent, manner in terms of what he called 'net entrainment or detrainment' from the environment at any level. (This is the Z derivative of our net cloud mass flux, averaged over the life-cycle of a cloud.

The present author is indebted to all these.

Haman presented his results in a graphical form, which we shall use, and extend here. He considered only $\bar{\tilde{W}} = 0$.

Using the symbols of 3.7.2, net cloud flux is $\alpha W_c = -(1 - \alpha)W_D$ He used the term 'net entrainment' (E) from the environment if $\partial/\partial Z\,(\alpha W_c)$ was positive at a height Z (that is, if over its life-cycle a cloud removed mass from the environment at that height), and 'net detrainment' (D) for the reverse situation where $\partial/\partial Z\,(\alpha W_c)$ was negative at a height. Haman's typical non-precipitating cumulus, averaged over its life-cycle, may be expressed equivalently in 2 diagrams.

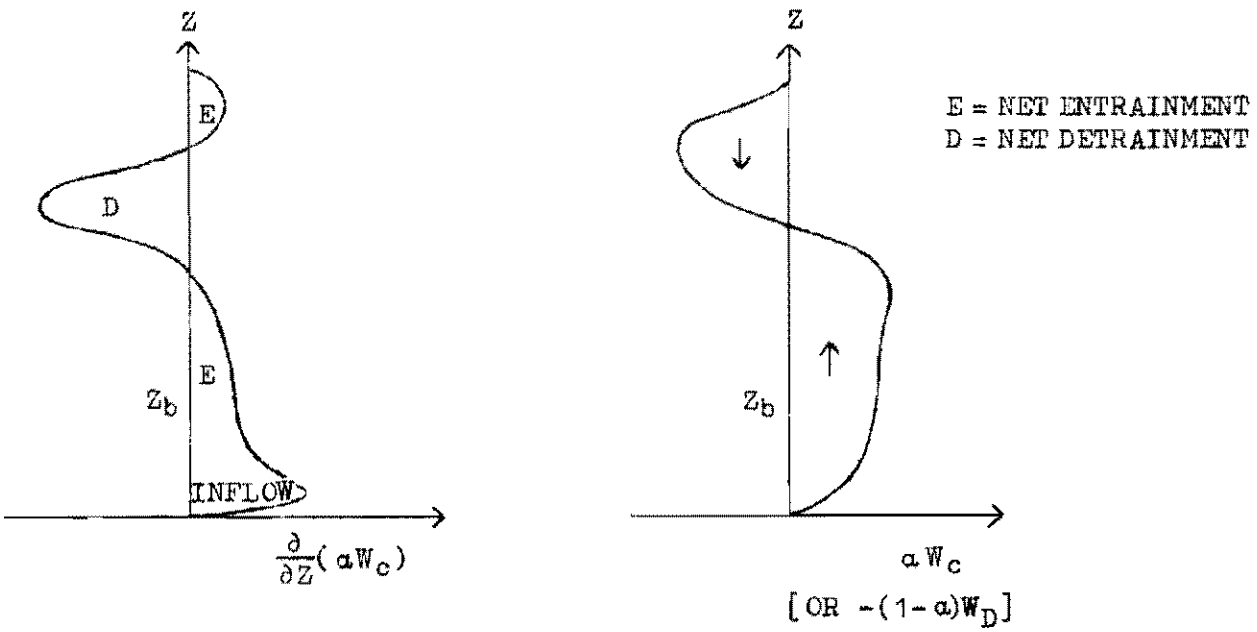

Fig. 3.9.1

The left-hand curve is the height derivative of the curve on the right. Haman showed that the changes in stratification follow from the net entrainment or detrainment. This is entirely equivalent to specifying W_D, and using 3.7.5

$$\frac{\partial \tilde{\theta}}{\partial t} = - W_D \frac{\partial \tilde{\theta}}{\partial Z} \qquad \text{(for } \tilde{W} = 0\text{)}$$

Fraser showed with reasonable assumptions that there must be a region of net downward cloud mass flux near the top of a layer of non-precipitating cumulus. This is important as it excludes the possibility shown in **Fig. 3.9.2**

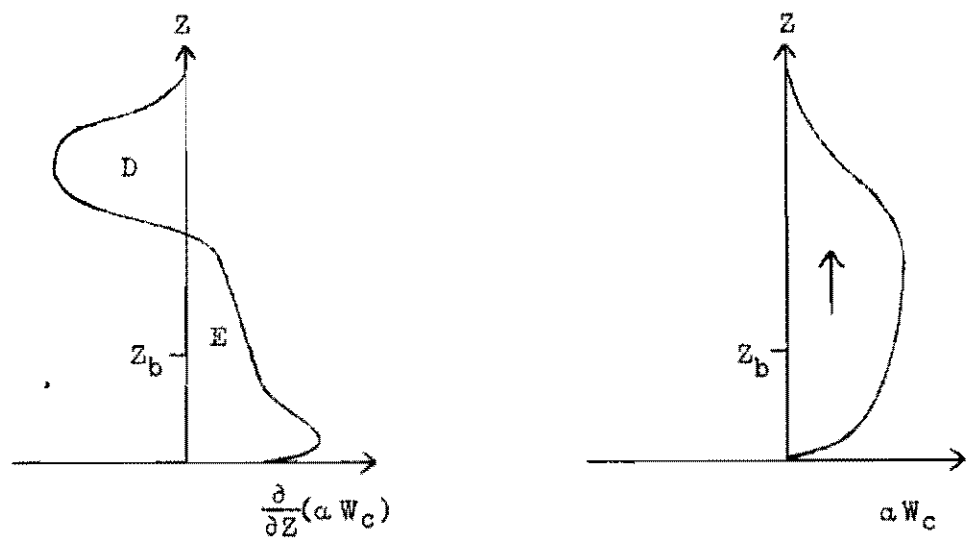

Although both these authors were aware that cumulus convection can destabilise the atmosphere, both papers are largely qualitative. In 3.10 we shall draw together the work of this chapter, and establish Fig. 3.9.1 on a firm quantitative basis using equations 3.6.1 and 3.7.5.

3.10 Graphical Description of non-precipitating cumulus convection

The ideas developed in this chapter will now be interrelated to give a quantitative picture of non-precipitating cumulus convection for $\tilde{W} = 0$. It will become clear which unknowns remain to be investigated. We shall indicate how the model will be extended in later chapters.

The two important equations are, after putting $\tilde{W} = 0$

3.6.1 $$\tilde{\rho}\, c_p \frac{\partial \tilde{\theta}}{\partial t} = - \left(\frac{\overline{\theta}}{\theta_L}\right) \frac{\partial}{\partial Z} \left(\tilde{\rho}\, c_p \widetilde{W'\theta_L'}\right)$$

3.7.5 $$\frac{\partial \tilde{\theta}}{\partial t} = - W_D \frac{\partial \overline{\theta}}{\partial Z}$$

The form of the total heat transport function in 3.6.1 has been sketched in Fig.3.6. The general form of the lapse rate $\frac{\partial \overline{\theta}}{\partial Z}$ in the cumulus layer will be considered in 5.2; but we know from observation that the stratification of $\tilde{\theta}$ is stable for dry air. We can therefore draw consistent graphs of total heat flux, $\partial\tilde{\theta}/\partial t$, W_D, $\partial\tilde{\theta}/\partial Z$.

Integral constraint

Integrating 3.6.1 from cloud-base to the top of the cumulus layer, and neglecting the variation of (θ/θ_L)

3.10.1 $$\int_{Z_b}^{Z_2} \tilde{\rho}\, c_p \frac{\partial \tilde{\theta}}{\partial t}\, dZ = \left(\tilde{\rho}\, c_p \widetilde{W'\theta'}\right)_{Z_b}$$

since the liquid water flux is zero at both limits, and the sensible heat flux may be assumed zero above the cumulus layer.

The sensible heat flux into the cumulus layer through cloud-base is an unknown we require

3.10.2 $$F_{b\theta} = \tilde{\rho}_b\, c_p \left(\widetilde{W'\theta'}\right)_{Z_b}$$

It will be determined in chapter 4. $F_{b\theta}$ will typically be rather smaller than the maximum value of the upward total heat flux in the cumulus layer. In the two layer model of the cumulus layer which will be developed in

chapter 5, the mid level, Z_1, will be at this level of maximum total (downward) heat flux.

3.10.3 $$F_{1\theta L} = \left(\frac{\tilde{\theta}}{\theta_L}\right)(\tilde{\rho}\, c_p \widetilde{W'\theta'_L})_{Z_1} = (\tilde{\rho}\, c_p \widetilde{W'\theta'} - \frac{\theta}{T}\tilde{\rho} L \widetilde{W'r'_L})_{Z_1}$$

Typically $F_{1\theta L}$ will be several times greater than $F_{b\theta}$, as indicated in Fig.3.6. However we shall not calculate $F_{1\theta L}$ from the above formula, but from

3.10.4 $$F_{1\theta L} - F_{b\theta} = -\int_{Z_b}^{Z_1} \tilde{\rho}\, c_p \frac{\partial \tilde{\theta}}{\partial t}\, dZ$$

The changing temperature in the cumulus layer will be determined from $d\tilde{\theta}_b/dt$, and a lapse rate model for the time development of the structure of the cumulus layer above (see chapter 5).

Using 3.7.5, 3.10.2; 3.10.1 and 3.10.4 may be re-expressed

3.10.5 $$\int_{Z_b}^{Z_2} \tilde{\rho}\, c_p\, W_D \frac{\partial \tilde{\theta}}{\partial Z}\, dZ = -F_{b\theta}$$

3.10.6 $$\int_{Z_b}^{Z_1} \tilde{\rho}\, c_p\, W_D \frac{\partial \tilde{\theta}}{\partial Z}\, dZ = F_{1\theta L} - F_{b\theta}$$

With $|F_{1\theta L}| > |F_{b\theta}|$ (both negative), and $\partial\tilde{\theta}/\partial Z$ positive everywhere in the cumulus layer, it follows that W_D is downwards between Z_b and Z_1 and upwards between Z_1 and Z_2 provided the total heat flux function has the uniform variation shown in Figs. 3.6 and 3.10.

In circumstances where the lapse rates in the cumulus layer are not changing rapidly (see chapter 5) one may to first approximation assume

$$F_{b\theta} << F_{1\theta L}$$

Recalling 3.7.2

3.7.2 $$\alpha W_c = -(1-\alpha) W_D$$

which for $\alpha << 1$ becomes

$$\alpha W_c = -W_D$$

we see that both 3.10.5 and 3.10.6 may be written in terms of a cloud mass flux.

The series of diagrams in Fig.3.10, summarise the description of the modification of the cumulus layer in terms of 3.6.1 and 3.7.5 (i.e. for $\tilde{W} = 0$) We have also added a curve for the net entrainment or detrainment (see 3.9 and Haman (1969)).

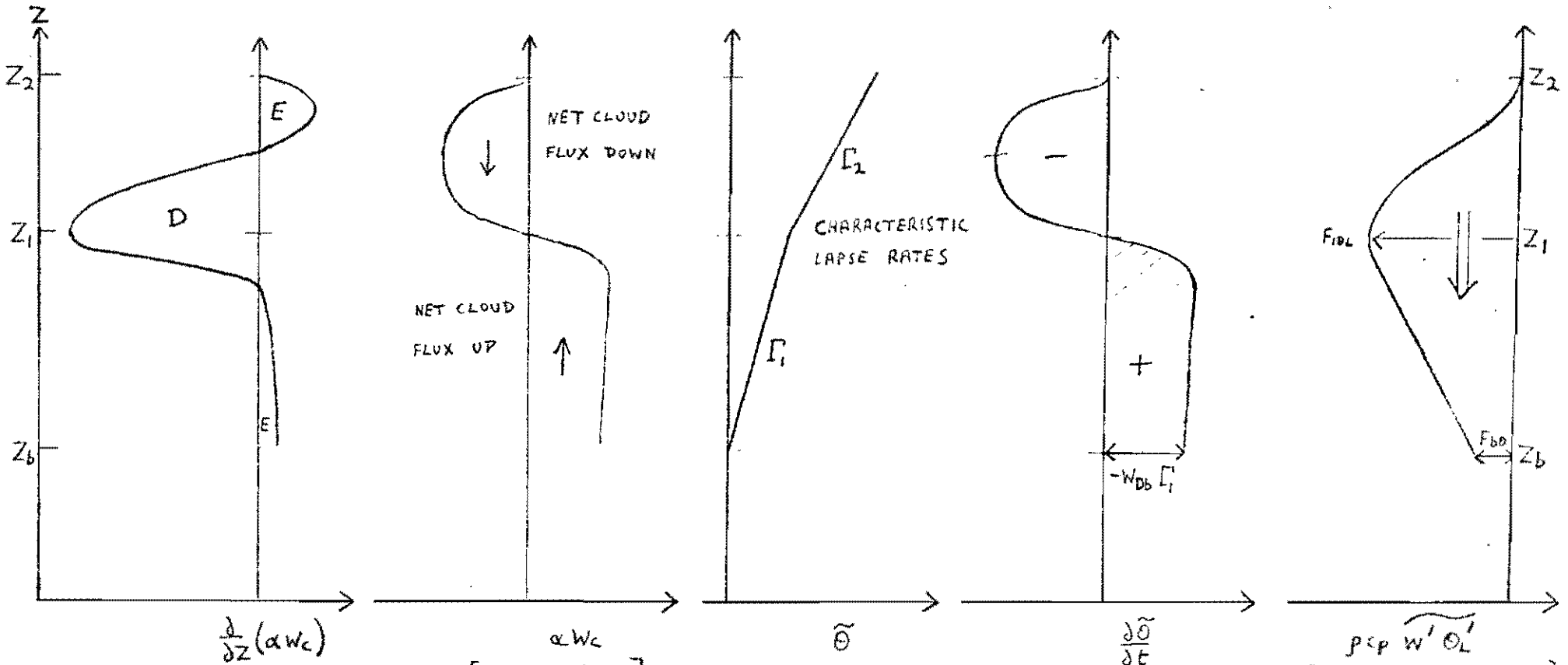

FIG. 3.10

$$\int_{z_b}^{z_2} \rho c_p \frac{\partial \tilde{\theta}}{\partial t}\, dz = F_{b\theta} \qquad \rho c_p \frac{\partial \tilde{\theta}}{\partial t} = -\left(\frac{\bar{\theta}}{\theta_L}\right)\frac{\partial}{\partial z}\left(\rho c_p \widetilde{w'\theta_L'}\right)$$

3.11 Conclusion:

The parameters we shall require in chapter 5 for the heat transports by the cumulus clouds in our 2-layer model are $F_{b\theta}, F_{1\theta L}$. The sensible heat flux through cloud base will be calculated in the next chapter. As mentioned above $F_{1\theta L}$ will be calculated indirectly from 3.10.4. $F_{1\theta L} - F_{b\theta}$ is the shaded area in Fig. 3.10. It is clear that this requires the specification of the lapse-rate Γ_1 in the cumulus layer, and the cloud mass flux into the cumulus layer. The lapse rate problem is considered in 5.2, and the cloud mass flux through cloud-base will be determined together with $F_{b\theta}$ in the next chapter. All these variables will be determined for the general case when the levels z_b, z_1, z_2 are varying, and there is a larger scale vertical motion field $\bar{w}$, so Fig. 3.10 must be regarded as valid only for a simple case.

Recalling chapter 2, and the model of Asai, it is now apparent that either cloud mass flux, or total heat transport $(\widetilde{w'\theta'_L})$ might be regarded as a measure of the intensity of the cumulus convection, rather than just $\widetilde{w'\theta'}$. It has not yet been shown how the cumulus convection is linked to the surface heat fluxes. This is the subject of chapter 4, in which we shall develop a model for the dry convective layer.

Water vapour transport in the cumulus layer has not yet been discussed other than to develop eq. 3.3.2. This will receive further consideration in later chapters, when water vapour budgets as well as heat budgets will be considered. It is thought that as a good first approximation the changes in the temperature structure of the cumulus layer may be calculated with the given water vapour distribution (as in the lapse-rate model of 5.2).

Chapter 4 The Dry Convective Layer

4.1 Introduction

In this chapter we shall examine how the convective mass flux into the cumulus layer (W_{Db}) depends on the boundary conditions at the surface and the large-scale vertical motion ($\bar{W}$). For this purpose the structure of the cumulus layer above cloud-base will be assumed.

In sections 4.2 to 4.5 a simple closed model is developed for a layer of dry convection when there are no cumulus clouds above. The sensible heat and water vapour balances are considered, and the time development of the layer predicted. The interrelation of the surface fluxes, surface parameters: $\bar{\theta}_o, \bar{r}_o$, and values of $\bar{\theta}$, $\bar{r}$ in the dry layer are discussed for the different cases of convection over land and sea.

In 4.6 to 4.9, this model is extended to describe the sub-cloud layer, when the fluxes of sensible heat and water vapour into the cumulus layer require additional parameterisation. The height of cloud-base and its relation to the height of the transition layer are examined. The control exerted on cumulus convection (through W_{Db}) by cloud base variation and large-scale subsidence is made quantitative.

It will become clear that over land the nature of the surface boundary conditions is such that no aspect of the problem can be determined without a closed model of the whole convective boundary layer. Such a model is necessary to calculate $\bar{\theta}_o$, $\bar{r}_o$ at the surface. Over the sea where $\bar{\theta}_o$, $\bar{r}_o$ follow from the surface temperature and pressure, the heat and water vapour budgets can be considered separately (but only if the virtual temperature correction is neglected).

4.2 Dry Convection

The general structure of the dry convective layer was outlined in the last chapter (Figs. 3.5.2, 3.8.5) and is repeated below in Fig.4.2. As mentioned in 3.8, we shall discuss the time development of the dry convective layer in only a simplified manner, but it is essential to have some simple model of this layer in order to link the cumulus layer to the surface fluxes. The basic assumption we shall make is that the lapse rate structure of the dry layer can be approximated by 2 layers: a lower nearly dry adiabatic layer, beneath a much shallower very stable layer. Some budget equations will be developed for this simple 2-layer model, which will then be further idealised to a dry adiabatic layer, beneath an idealised inversion of zero depth.

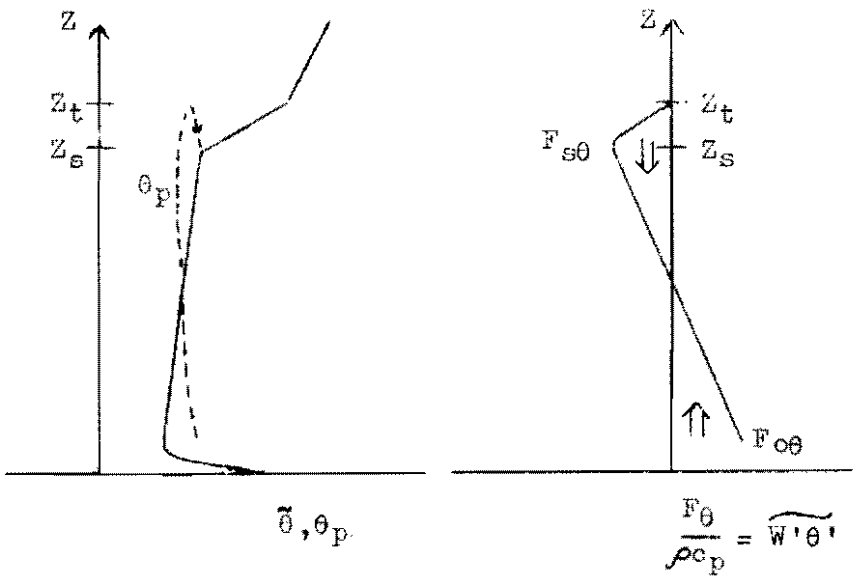

The structure of the superadiabatic layer will not be considered in this thesis. 'Surface' variables should be taken to mean values in the superadiabatic layer at screen level, not the earth's surface.

The first feature to be considered in modelling the convective layer is whether or not there are cumulus clouds, as these will require additional parameterisation even in the dry layer (see 4.6). A suitable simple criterion is to assume no clouds if the lifting condensation level (L.C.L.) of surface air is more than a few hundred metres above Z_s. If there are cumulus clouds, it appears that cloud-base closely coincides with Z_t (the top of

the more stable transition layer), so we must examine in some detail the connection between the heights of cloud-base and the stable layer (see 4.6 and 4.9). The first few sections of this chapter will be concerned with the development of the dry convective layer when there are no cumulus clouds.

It is clear from Fig. 4.2, that the dry layer will deepen as the stable top is cooled, that is, lifted. This problem was discussed by Ball (1960) (see Fig. 3.8.4), though only in terms of the erosion of an idealised inversion at the top of a dry adiabatic layer. His model involved some approximations which we shall mention, but it remains useful; it will be extended to form a closed model for the dry convective layer, including large scale subsidence.

We shall first discuss a model of Fig. 4.2, before simplifying the lapse rate structure.

4.3 The dry layer: sensible heat balance, and time development

The following simplifications will be made

(i) Radiative transfers are neglected (away from the surface)

(ii) Horizontal derivatives of $\tilde{\theta}, \tilde{r}$ are assumed zero.

(iii) The initial condition is a constant stable stratification, Γ, and constant lapse of mixing ratio ($\partial\tilde{r}/\partial Z$), above the convective layer.

(iv) $\tilde{\rho}\tilde{W}$ will be taken to increase linearly with ρ from zero at the ground to a constant value $\tilde{\rho}_t\tilde{W}_t$ at the top of the stable layer.

Both (iii) and (iv) are only algebraic simplifications.

The basic equation which we established for dry convection was:

3.2.3
$$\tilde{\rho}\frac{\partial\tilde{\theta}}{\partial t} + \tilde{\rho}\tilde{W}\frac{\partial\tilde{\theta}}{\partial Z} = -\frac{\partial}{\partial Z}(\tilde{\rho}\widetilde{W'\theta'})$$

The form of $\widetilde{W'\theta'}$ is sketched in Fig. 4.2. We shall be concerned with the two layers:

$$0 < Z < Z_s$$
$$Z_s < Z < Z_t$$

We note that Z_t, the top of the stable layer is also taken to be where $F_{t\theta} = 0$.

The surface heat flux $F_{o\theta}$, is the value in the so-called "constant flux" layer. The stable layer, Z_s to Z_t, is being cooled by a downward heat flux $(-F_{s0})$.

We shall define an average variable for

4.3.1 $$\frac{\Delta p_s}{g}\,\overline{\tilde{\theta}}^{s} = \int_0^{Z_s} \tilde{\theta}\,\tilde{\rho}\,dZ$$

where $\Delta p_s = p_o - p_s$ (p_o will be assumed constant).

There are several algebraic steps in the derivation of the time-rate of change of this vertically averaged variable, since the height Z_s of the base of the stable layer is in general changing. However the end result (eq. 432 below) has a simple physical interpretation. First we obtain, from the definition of $\overline{\tilde{\theta}}^{s}$, that

$$\frac{d}{dt}\,\overline{\tilde{\theta}}^{s} = g\,\frac{d}{dt}\,\frac{1}{\Delta p_s}\int_0^{Z_s} \tilde{\theta}\,\tilde{\rho}\,dZ$$

$$= -\frac{1}{\Delta p_s}\,\frac{dp_s}{dt}\,(\tilde{\theta}_s - \overline{\tilde{\theta}}^{s}) + \frac{g}{\Delta p_s}\int_0^{Z_s} \frac{\partial\tilde{\theta}}{\partial t}\,\tilde{\rho}\,dZ$$

The first term represents the increase in $\overline{\tilde{\theta}}^{s}$ through the incorporation of air with potential temperature $\tilde{\theta}_s$. The second term is easily computed by substituting from 3.2.3, and then making simplification (iv) to give

$$\int_0^{Z_s} \frac{\partial\tilde{\theta}}{\partial t}\,\tilde{\rho}\,dZ = \frac{F_{o\theta}}{c_p} - \frac{F_{s\theta}}{c_p} - \tilde{\rho}_s\,\tilde{W}_s\,(\tilde{\theta}_s - \overline{\tilde{\theta}}^{s})$$

The physical interpretation of the last term is that, with mass divergence uniform with respect to pressure (iv), subsidence removes air from the layer $0 < Z < Z_s$ with the mean potential temperature of that layer ($\overline{\tilde{\theta}}^{s}$) and replaces it with air from above ($\tilde{\theta}_s$).

Combining the above equations, we obtain

4.3.2 $$\frac{\Delta p_s}{g}\,\frac{d}{dt}\,\overline{\tilde{\theta}}^{s} = \frac{F_{o\theta}}{c_p} - \frac{F_{s\theta}}{c_p} + \tilde{\rho}_s\left(\frac{dZ_s}{dt} - \tilde{W}_s\right)(\tilde{\theta}_s - \overline{\tilde{\theta}}^{s})$$

There is a similar equation for the whole layer $0 < Z < Z_t$

4.3.3 $$\frac{\Delta p_t}{g}\,\frac{d}{dt}\,\overline{\tilde{\theta}}^{t} = \frac{F_{o\theta}}{c_p} + \hat{\rho}_t\left(\frac{dZ_t}{dt} - \hat{W}_t\right)(\hat{\theta}_t - \overline{\tilde{\theta}}^{t})$$

since $F_{t\theta} = 0$.

The complete solution of the problem involves the calculation of the time-development of the separate layers from the boundary conditions, and either a model for the transports by the dry convective elements, or a model for the lapse rate structure in terms of those elements. We have developed a model of the latter kind in chapter 5 for the cumulus layer, and this could be adapted to the dry layer (although at present we probably know less about the behaviour of dry convective elements than about cumulus clouds). This task will not be attempted in this thesis, so we shall simplify 4.3.2 and 4.3.3 by idealising the lapse rate structure to a dry adiabatic layer, beneath an inversion of zero depth. Fig. 4.2 becomes Fig. 4.3, but we can no longer plot a meaningful parcel path.

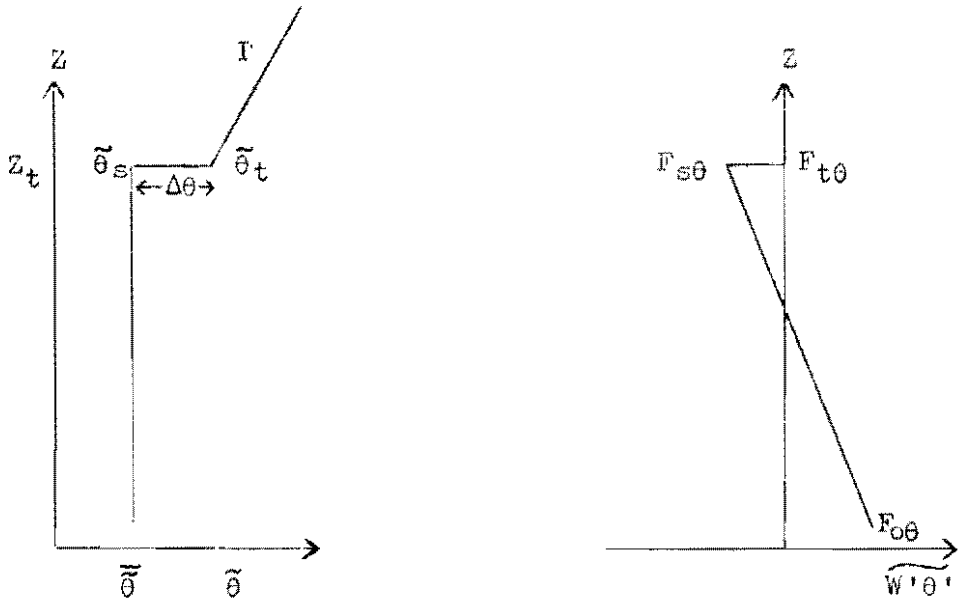

Fig. 4.3

In letting $Z_s \longrightarrow Z_t$, we lose all information about the depth of the more stable layer (or transitionlayer if there is a cumulus layer above), but it enables one to make a simple budget for the layer $0 < Z < Z_t$. In treating the layer $0 < Z < Z_s$ as dry adiabatic , we lose sight of the mechanism by which this layer gets warmer, and we can no longer present a physical picture for the heat flux curve. However without a complete lapse rate model for the dry layer, we cannot determine $(\theta_s - \overline{\tilde{\theta}}^{\theta})$: by approximating to Fig. 4.3, we neglect it.

The justification for this simplification is that we know from observation (see for example Chapter 6), that

$z_t - z_s$ is small compared with z_s

$\tilde{\theta}_s - \overline{\tilde{\theta}}^s$ is small compared with $\tilde{\theta}_t - \tilde{\theta}_s$

With this simplification, 4.3.2, 4.3.3 reduce to

4.3.4 $$\frac{\Delta p_t}{g} \frac{d}{dt} \overline{\tilde{\theta}} = \frac{F_{o\theta}}{c_p} - \frac{F_{s\theta}}{c_p}$$

4.3.5 $$\frac{\Delta p_t}{g} \frac{d}{dt} \overline{\tilde{\theta}} = \frac{F_{o\theta}}{c_p} + \bar{\rho}_t \left(\frac{dz_t}{dt} - \tilde{w}_t \right) (\theta_t - \overline{\tilde{\theta}})$$

We have dropped the superfix on $\overline{\tilde{\theta}}$; and $\tilde{\theta}_s = \overline{\tilde{\theta}}$.

It follows that

4.3.6 $$F_{s\theta} = - \rho_t \, c_p \, \Delta\theta \left(\frac{dz_t}{dt} - \tilde{w}_t \right)$$

where $\Delta\theta = \tilde{\theta}_t - \overline{\tilde{\theta}}$ is the strength of the inversion.

The interpretation of 4.3.4 to 4.3.6 is straightforward. If

$$\frac{dz_t}{dt} - \tilde{w}_t = 0$$

the inversion is moving with the mean vertical motion of the air at that level, and there is no incorporation of air from above the inversion into the dry adiabatic layer. But in so far as

$$\frac{dz_t}{dt} - \tilde{w}_t > 0$$

(e.g. if $\tilde{w}_t = 0$ and z_t rises), and $\Delta\theta$ is non-zero, there is incorporation of air from above the inversion, with excess temperature $\Delta\theta$, into the dry adiabatic layer which increases $\overline{\tilde{\theta}}$. The mechanism of this process can be understood satisfactorily only by returning to Fig. 4.2.

The essential purpose in expressing the heat flux, $F_{s\theta}$, through the base of the inversion in this manner, is to relate the surface heat flux to $\Delta\theta$ and the rise of the inversion relative to the mean vertical air motion, using equation 3.8.9:

3.8.9 $$F_{s\theta} = - k \, F_{o\theta} \qquad \text{where } 0 < k < 1$$

If we put $\tilde{w} = 0$
$k = 1$
all our results reduce to those of Ball (1960).

However this model can be extended, and indeed closed, by adding an equation for $\Delta\theta$.

Equation for Inversion strength: $\Delta\theta$

$$\frac{d}{dt}\tilde{\theta}_t = \left(\frac{\partial\tilde{\theta}}{\partial t}\right)_t + \frac{dZ_t}{dt}\Gamma$$

$$\frac{d}{dt}\tilde{\theta}_t = \left(\frac{dZ_t}{dt} - \tilde{W}_t\right)\Gamma$$

That is $\tilde{\theta}_t$ changes if the inversion does not move with the mean vertical air motion. By definition

$$\Delta\theta = \tilde{\theta}_t - \bar{\tilde{\theta}}$$

4.3.7 $$\therefore \quad \frac{d}{dt}(\Delta\theta) = \Gamma\left(\frac{dZ_t}{dt} - \tilde{W}_t\right) - \frac{d\bar{\tilde{\theta}}}{dt}$$

The warming of the dry adiabatic layer reduces $\Delta\theta$, and the lifting of the inversion relative to the mean air motion, increases $\Delta\theta$.

Solution:

The set of equations 4.3.4, 4.3.6, 4.3.7, and 3.8.9 can be solved for the four variables Z_t, $\bar{\tilde{\theta}}$, $\Delta\theta$, $F_{s\theta}$, given $F_{o\theta}$, $\tilde{W}_t$, Γ, $\tilde{\rho}$, k; and assuming the hydrostatic relation between p and Z.

4.3.4 $$c_p \frac{\Delta p_t}{g} \frac{d}{dt}\bar{\tilde{\theta}} = F_{o\theta} - F_{s\theta}$$

3.8.9 $$F_{s\theta} = -k F_{o\theta}$$

4.3.6 $$F_{s\theta} = -\rho_t c_p \Delta\theta \left(\frac{dZ_t}{dt} - \tilde{W}_t\right)$$

4.3.7 $$\frac{d}{dt}(\Delta\theta) = \Gamma\left(\frac{dZ_t}{dt} - \tilde{W}_t\right) - \frac{d\bar{\tilde{\theta}}}{dt}$$

3.8.9 relates $F_{s\theta}$ to $F_{o\theta}$ in terms of a dissipation parameter k whose value has to be determined, either theoretically or from observations. The author would suggest a likely value to be in the range 0.2 to 0.7, based on some very provisional calculations.

$\frac{d\bar{\tilde{\theta}}}{dt}$ as a function of Δp_t, $F_{o\theta}$ follows immediately from 4.3.4 and 3.8.9

4.3.8 $$\frac{d\bar{\tilde{\theta}}}{dt} = \frac{g(1+k)F_{o\theta}}{c_p \Delta p_t}$$

This can be integrated from an initial state, given p_t (or Z_t) as a function of time (see below).

$\frac{d}{dt}(\Delta\theta)$ is found by eliminating $F_{o\theta}$, $F_{s\theta}$ from 4.3.4 using 3.8.9 and 4.3.6, and then substituting for $d\bar{\tilde{\theta}}/dt$ in 4.3.7, to give

4.3.9 $$\frac{\Delta p_t}{g}\frac{d}{dt}(\Delta\theta) = \frac{\Delta p_t}{g}\Gamma\left(\frac{dZ_t}{dt} - \tilde{W}_t\right) - \frac{1+k}{k}\Delta\theta\,\tilde{\rho}_t\left(\frac{dZ_t}{dt} - \tilde{W}_t\right)$$

Given p_t and $\tilde{W}_t$ as functions of time, one may solve for $\Delta\theta$. An alternative equation for $\Delta\theta$ in terms of the surface flux is found by eliminating $\left(\frac{dZ_t}{dt} - \tilde{W}_t\right)$ from 4.3.7 using 4.3.6, and the eliminating $F_{s\theta}$, $\frac{d\bar{\theta}}{dt}$ by 3.8.9, 4.3.8, to give

4.3.10 $$\frac{d}{dt}(\Delta\theta) = \frac{k\,\Gamma\,F_{o\theta}}{\bar{\rho}_t c_p \Delta\tilde{\theta}} - \frac{g(1+k)F_{o\theta}}{c_p\,\Delta p_t}$$

In general, one may solve 4.3.9, and 4.3.10 for $\Delta\theta$ and p_t as functions of time, from given initial conditions.

Some simple solutions

General solutions will not be obtained for these equations, but simple cases are illustrative. It is clear from 4.3.8 that the total heat flux into the layer $0 < Z < Z_s$ is between one and two times the surface heat flux depending on the value of k. This is true in general, and was first suggested by Ball (1960). For simple cases, it is easy to calculate both $\Delta\theta$ in terms of the depth of the dry layer, and the rate of deepening of this same layer.

(a) $\tilde{W} = 0$

If the mean vertical velocity is zero everywhere, then 4.3.9 simplifies. Thus, changing to pressure co-ordinates and keeping p_o constant, we obtain

4.3.11 $$\frac{\Delta p_t}{g}\frac{d}{dt}(\Delta\theta) = \frac{\Delta p_t}{g}\left(\frac{\partial\tilde{\theta}}{\partial p}\right)\frac{d}{dt}(\Delta p_t) - \frac{1+k}{k}\Delta\theta\frac{d}{dt}(\Delta p_t)$$

With $(\partial\tilde{\theta}/\partial p)$ and k constants, this is a homogeneous ordinary differential equation with constant coefficients: the solution is

4.3.12 $$\Delta\theta = \frac{k}{2k+1}\left(\frac{\partial\tilde{\theta}}{\partial p}\right)\Delta p_t$$

$$\Delta\theta \simeq \frac{k}{2k+1}\,\Gamma\,Z_t \quad \text{if variations of } \tilde{\rho} \text{ are neglected.}$$

Thus the strength of the inversion is directly related to the depth of the layer and to the lapse rate Γ above in the free atmosphere (which has been taken as constant). If 4.3.12 is substituted in 4.3.6 and 3.8.9, an equation is obtained for the rate at which the dry layer deepens:

4.3.13 $$\frac{d}{dt}(\Delta p_t)^2 = \frac{g(4k+2)F_{o\theta}}{c_p(\partial\tilde{\theta}/\partial p)}$$

(b) $\tilde{W}$ non-zero: a steady state solution for Z_t, $\Delta\theta$.

If the mean vertical velocity is non-zero, and we start the model with a small Δp_t and $\Delta\theta$, then the inversion lifts rapidly, as given by substituting 3.8.9 in 4.3.6, and rearranging

4.3.14 $$\frac{dZ_t}{dt} = \frac{k\ F_{o\theta}}{c_p \tilde{\rho}_t \Delta\theta} + \tilde{W}_t$$

But if $\tilde{W}$ is negative (large scale subsidence), then as $\Delta\theta$ increases, dZ_t/dt decreases, and there exists a solution with Z_t, $\Delta\theta$ constant when

4.3.15 $$-\ kF_{o\theta} = \tilde{\rho}_t\, c_p\, \Delta\theta\, \tilde{W}_t$$

and, from 4.3.10, for constant $\Delta\theta$

4.3.16 $$\Delta\theta = \frac{k}{k+1}\,\Gamma\,\frac{\Delta p_t}{\tilde{\rho}_t g}$$

$$\Delta\theta \doteq \frac{k}{k+1}\,\Gamma\,Z_t \qquad \text{neglecting } \tilde{\rho} \text{ variations}$$

Eliminating $\Delta\theta$ gives a third relation:

4.3.17 $$(k+1)\,F_{o\theta} = -\,c_p\,\tilde{W}_t\,\Gamma\frac{\Delta p_t}{\tilde{\rho}_t g}$$

Conclusions

These equations indicate useful relations between the approximate structure of a dry convective layer, the large scale motion field, and the sensible heat flux at the surface.

(i) Eqs. 4.3.12 and 4.3.16 suggest that the dissipation parameter k, itself related to the physics of an individual dry convective element, may be estimated from the strength, $\Delta\theta$, and the height of an inversion.

(ii) Eq. 4.3.13 gives the rate of lifting of an inversion, for example, the inversion produced by nocturnal cooling. In diurnal convection the dry convective layer will deepen until Z_t reaches the lifting condensation level of elements rising (with mixing) from the surface superadiabatic layer. The cumulus must then be parameterised (see 4.6).

(iii) If there is subsidence, then the maximum height of the inversion is given by 4.3.17. We see that the greater the subsidence, the lower the inversion height. Thus it is clear that sufficient subsidence will suppress clouds altogether, by depressing the steady state inversion height to below the L.C.L. of surface air. However no amount of subsidence will depress the inversion to the ground in this model, since the shallower the dry adiabatic layer, the greater $d\bar{\bar{\theta}}/dt$. This keeps $\Delta\theta$ small, constant, and satisfying the above equations. (The influence of radiation is considered below).

(iv) Eq. 4.3.15 relates the inversion strength to the surface heat flux and the large scale subsidence. This could be of great use in synoptic scale studies as a means of estimating $\tilde{w}_t$ from $F_{o\theta}$ and vice-versa, once we have a good value for k.

The approximation of the lapse rate structure, and the convective transports, is less serious than the omission of radiation.

Radiation:

On timescales longer than a day, radiative cooling of a dry convective layer beneath an inversion is important. Typically the dry adiabatic layer is moist and the subsiding air above the inversion very dry, so the radiative cooling of the dry layer may represent a rate of heat loss comparable with the surface heat flux. This adds an additional term to 4.3.4, reducing $d\bar{\bar{\theta}}/dt$. The steady state inversion strength $\Delta\theta$ will be increased, to a value bigger than that given by 4.3.16. However 4.3.15 will still be satisfied (see (iv)).

Most subsidence inversions are long lived, and for these, radiative fluxes cannot be neglected, as in this simple treatment.

4.4 Water Vapour Balance

In dry convection, the transports of heat and water vapour may be treated independently, except for the virtual temperature correction in estimating density and buoyancy. When the Bowen ratio is small, this correction becomes important, as the virtual potential temperature flux $\widetilde{w'\theta'_v}$, and the potential temperature flux $\widetilde{w'\theta'}$, then differ markedly. For example when the

$$\text{Bowen ratio} \sim 1/15$$
$$\widetilde{w'\theta'_v} \sim 2\,\widetilde{w'\theta'}$$

Even smaller Bowen ratios are common in the Trades. The set of equations in 4.3 are however valid with θ replaced by θ_v (defined by $\frac{\theta}{\theta}v = \frac{T}{T}v$)

Nonetheless, an independent set of equations is required for the water vapour balance. Our approach is fundamentally the same as in 4.3, but as we neither need, nor have, a direct relationship between F_{sr} and F_{or} , we shall not idealise the vertical water vapour structure. It is necessary only to define

$$\frac{\Delta p_t}{g}\,\overline{\tilde{r}}^t = \int_0^{Z_t} \tilde{r}\,\tilde{\rho}\,dZ$$
$$\Delta r = r_t - \overline{\tilde{r}}^t$$

when the analogues of 4.3.3 and 4.3.7 are

4.4.1 $$\frac{\Delta p_t}{g}\,\frac{d}{dt}\,\overline{\tilde{r}}^t = \frac{F_{or}}{L} + \tilde{\rho}_t\,\Delta r\left(\frac{dZ_t}{dt} - \tilde{w}_t\right)$$

4.4.2 $$\frac{d}{dt}\,\Delta r = \left(\frac{\partial \tilde{r}}{\partial Z}\right)\left(\frac{dZ_t}{dt} - \tilde{w}_t\right) - \frac{d}{dt}\,\overline{\tilde{r}}$$

With F_{or}, $(\partial\tilde{r}/\partial Z)$, (above the inversion) and $\tilde{w}_t$ given, and Δp_t , dZ_t/dt determined in 4.3 from the $\tilde{\theta}$ balance, this pair of equations can be integrated from an initial condition to give $\overline{\tilde{r}}^t$, Δr .

4.5 Surface Boundary Conditions: closure

These are a common problem to both dry and cumulus convection and have received much attention. We shall only indicate very briefly how the surface fluxes $F_{o\theta}$, F_{or} are constrained. If these can be related to $\overline{\theta}$ and $\overline{r}$, the dry convective problem becomes closed.

Land and sea surface boundaries can conveniently be distinguished.

Sea

The sea surface variables $\tilde{\theta}_o$, $\tilde{r}_o$ are determined once the sea surface temperature and pressure T_o, p_o are given $(r_o = r_s(T_o, p_o))$.

We shall suppose that the fluxes are adequately related to $\tilde{\theta}_o$, $\overline{\theta}$; $\tilde{r}_o$, $\overline{r}$ by bulk aerodynamic equations of the form

4.5.1 $$F_{o\theta} = C_\theta \tilde{\rho}_o c_p(\tilde{\theta}_o - \overline{\theta}) V_o$$

4.5.2 $$F_{or} = C_r \tilde{\rho}_o L(\tilde{r}_o - \overline{r}) V_o$$

where V_o is the magnitude of the wind at some level in the superadiabatic layer

C_θ, C_r are coefficients appropriate to that level, and to the finite differences $\tilde{\theta}_o - \overline{\theta}$, $\tilde{r}_o - \overline{r}$.

C_θ, C_r are essentially drag coefficients, but have some dependence on Richardson number in the superadiabatic layer. $(\tilde{\theta}_o - \overline{\theta})$, $(\tilde{r}_o - \overline{r})$ become finite differences from screen level to the top of the superadiabatic layer, if $\frac{\partial \tilde{\theta}}{\partial z}$, $\frac{\partial \tilde{r}}{\partial z}$ are small in the dry layer above. In this situation it is probable that

$$C_\theta = C_r$$

These are only approximate relations, and clearly depend critically on the coefficients C_θ, C_r. A more careful study of the structure of the superadiabatic layer is desirable.

Land

The land surface boundary conditions are more complicated. 4.5.1 and 4.5.2 may still be used, but θ_o, r_o are no longer given, but are functions of the solar heating, and evaporation from the surface.

Two further relations are required. One relates the heat fluxes to the net radiative flux at the ground, and the ground storage of heat:

4.5.3 $$F_{o\theta} + F_{or} = N - G$$

where

N is the net radiative flux at the ground

G is the downward heat flux into the ground.

Another relationship, which in some way describes the availability of water for evaporation, is necessary. One may write an equation of the form

4.5.4 $$V_R F_{or} = \left(r_s(T_o) - r_o\right)$$

where

V_R is a vegetative resistance to evaporation, dependent on type of vegetation, soil moisture etc. The easier it is to evaporate water from the surface, the smaller V_R. (An open water surface has $V_R = 0$). Strictly T_o, r_o should not be screen level values but those at the level of the vegetation.

With these 2 further relations, one can solve for the surface fluxes over land given V_R, N, G, $\tilde{\bar{\theta}}$, $\tilde{\bar{r}}$.

Closure: Summary of 4.2 to 4.5

In these sections we have established in outline a closed system of equations to describe the dry convective layer, when there are no cumulus clouds.

Over the Sea

The heat and water vapour problems are distinct, apart from the virtual temperature correction.

(a) Given θ_o, V_o and C_θ at the surface
$\bar{\bar{W}}_t$, Γ in the 'free' atmosphere
and k
one may calculate
$F_{o\theta}$, $F_{s\theta}$, $\tilde{\bar{\theta}}$, $\Delta\theta$, Z_{*t} as functions of time from a given initial condition of the atmosphere, using 4.3.4, 3.8.9, 4.3.6, 4.3.7, 4.5.1.

(b) Given r_o, V_o and C_r at the surface
$\bar{\bar{W}}_t$ $(\partial r/\partial Z)$ in the free atmosphere
and Z_{*t} from (a)
one may calculate

F_{or}, $\bar{\bar{r}}$, Δr as functions of time from a given initial condition, using 4.4.1, 4.4.2 and 4.5.2

Over land

The whole set of equations above can be solved simultaneously together with

4.5.3 and 4.5.4

as additional equations for $F_{o\theta}, F_{or}$. Instead of being given θ_o, r_o, we require N, G; V_R.

(Didn't understand radiative coupling over oceans at that time)

4.6 The Sub-cloud Layer

In the last 3 sections, a simple model has been developed relating the dry convective boundary layer to the surface fluxes, the mean vertical motion field and the 'free' atmosphere above. In this and succeeding sections, this model will be extended to the sub-cloud layer. There are three new factors to be considered:

(i) the height of cloud-base, which becomes the upper bound of the dry convective layer;

(ii) the parameterisation of the heat and vapour fluxes into the cumulus layer, as there are now convective fluxes through the top of the dry layer, whereas before $F_{t0} = F_{tr} = 0$;

(iii) above the dry layer, there is no longer the 'free' atmosphere, but the cumulus layer which has its own characteristic structure.

In this chapter the structure of the cumulus layer (iii) will be assumed, but we shall discuss (i) and (ii). In chapter 5 the structure of the cumulus layer will be related to the sub-cloud layer, $\tilde{W}$, and the 'free' atmosphere above the cumulus layer.

Control of cloud-base

Cloud-base is typically 100 to 200m above the lifting condensation level (L.C.L.) of air at screen level, because of dilution of 'surface air' rising through the sub-cloud layer, with air whose L.C.L. is higher. However as a first approximation, it is useful to assume that cloud-base is determined by the surface parameters $\tilde{\theta}_o, \tilde{r}_o$. Once $\bar{\tilde{\theta}}, \bar{\tilde{r}}$ have been determined on this assumption, further iteration is possible. We suppose

4.6.1 $$Z_b = f(\tilde{\theta}_o, \tilde{r}_o)$$

4.6.2 $$\therefore \quad \frac{dZ_b}{dt} = \left(\frac{\partial Z_b}{\partial \tilde{\theta}_o}\right)_{\tilde{r}_o} \frac{d\tilde{\theta}_o}{dt} + \left(\frac{\partial Z_b}{\partial \tilde{r}_o}\right)_{\tilde{\theta}_o} \frac{d\tilde{r}_o}{dt}$$

where the coefficients vary only slightly with height, and have values in the tropics ($T_o = 30°C$)

$$\left(\frac{\partial Z_b}{\partial \tilde{\theta}_o}\right)_{\tilde{r}_o} \sim 120 \text{ m/°C}$$

$$\left(\frac{\partial Z_b}{\partial \tilde{r}_o}\right)_{\tilde{\theta}_o} \sim -130 \text{ m/g/kg} .$$

To this approximation, the height of cloud-base varies only slowly over the sea, as the sea surface temperature changes. (There is also a small diurnal variation, which is not well understood, but may be important - see 4.7). Over land however the diurnal variation of $\tilde{\theta}_o, \tilde{r}_o$ is very large, and Z_b correspondingly may have a large diurnal variation (see for example· chapter 6).

While Z_t, the top of the dry convective layer is below the L.C.L. of surface air, the model of 4.2 $\longrightarrow$ 4.5 remains valid. However if Z_t rises to this L.C.L., then clouds form and the model must be modified.

Transition Layer:

It is observed that in cumulus convection there is a shallow (200m), more stable layer at the top of the dry convective layer, just below cloud-base (e.g. Grant, 1965; Warner & Telford, 1967). This has been called the transition layer. (Ludlam, 1966). The transition layer may be understood from opposite viewpoints, already briefly indicated in the discussion of Fig. 3.8.5. point (ii).

(a) The transition layer is the more stable layer at the top of the dry layer which stops most of the ascending elements of the dry convection.

(b) The potential temperature increase $\Delta\theta$ across the transition layer implies that parcels of air rising from the ground are negatively buoyant at cloud-base (if $Z_b > Z_s$). Thus $\Delta\theta$ ensures that only a fraction of the dry convective elements (the most buoyant - typically the largest) regain buoyancy in the cumulus layer, and continue to ascend.

The transition layer $\Delta\theta$ is maintained when

$$\frac{\partial\tilde{\theta}}{\partial t} = -W_D \frac{\partial\tilde{\theta}}{\partial Z} \qquad \tilde{W} = 0$$

is the same above and below. Since the lapse rate $\frac{\partial\tilde{\theta}}{\partial Z}$ is typically several times greater in the cumulus layer than in the nearly adiabatic dry layer, the transition layer is maintained, when the convective mass flux W_D is much smaller above Z_t than below Z_s. Thus we reach the important conclusion that a

difference in lapse rates in cumulus and dry convective layers, means that much of the dry convection from the ground is stopped at the transition layer. Indeed roughly speaking the larger $\Delta\theta$, the smaller the fraction of the convective elements which regain buoyancy in the cumulus layer. Conversely, only if the lapse rate is essentially unchanged as one goes from the dry to the cumulus layer (and $\Delta\theta$ is zero), does all the convection from the ground rise up into the cumulus layer. There is some evidence to support these ideas. The general question of lapse rates in the cumulus layer will be discussed theoretically in 5.2, and observationally in chapter 6.

Yet another aspect of the transition layer is that it must be 'tied' to cloud-base Z_b whether this varies in height or not. Taking Z_t as the top of the transition layer

4.6.3 $$\frac{dZ_t}{dt} \doteq \frac{dZ_b}{dt}$$

It does not immediately follow that $Z_t - Z_b$ is zero. The transition layer $\Delta\theta$ must satisfy a set of relations for the dry layer, similar to those of 4.3. However it must also control the convective mass flux into the cumulus layer, which is not the same dynamical problem. It is possible that small variations of $(Z_t - Z_b)$ of about 100m, that is in the relation of the height of the transition layer to the height of cloud-base, may be a further necessary degree of freedom in the problem (see section 4.9).

This is a complication which will be neglected in the first instance. We shall assume

4.6.4 $$Z_b = Z_t \ .$$

Then, as in 4.3, we shall idealise the transition layer to an inversion of zero depth, coincident with cloud-base.

$$Z_s \longrightarrow Z_t$$

Simple equations can now be written for $\Delta\theta$, and for the heat balance of the layer $0 < Z < Z_b$, with a specific parameterisation for the cumulus.

The heat flux through Z_t $(=Z_b)$ is no longer zero.

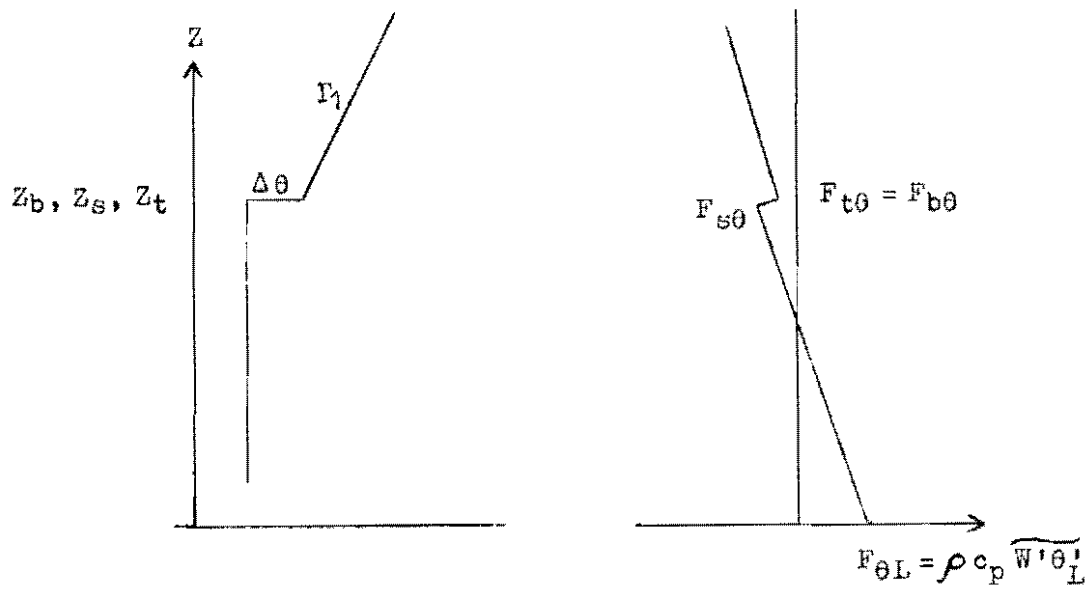

Fig. 4.3

Heat Balance of the Sub-cloud layer

The heat flux out of the sub-cloud layer due to cumuli can be parameterised (assuming 4.6.4) as

4.6.5 $$\frac{F_{t\theta}}{c_p} = \frac{F_{b\theta}}{c_p} = \tilde{\rho}_b (\alpha W_c)_b \left(\theta(p) - \tilde{\theta}_b\right)$$

where $\theta(p)$ is the potential temperature of parcels rising through cloud-base.

and $(\alpha W_c)_b$ is a cloud mass flux just above Z_b (more exactly Z_t, but we are assuming 4.6.4).

From 3.7.2

$$(\alpha W_c)_b = - W_{Db} \qquad \text{if } \alpha << 1$$

Writing

$$\left(\theta(p) - \theta_b\right) = (\delta\theta - \Delta\theta)$$

where

$$\Delta\theta = \tilde{\theta}_b - \bar{\tilde{\theta}}^b$$
$$\delta\theta = \theta(p) - \bar{\tilde{\theta}}^b$$

4.6.5 becomes

4.6.6 $$\frac{F_{b\theta}}{c_p} = \tilde{\rho}_b W_{Db} (\Delta\theta - \delta\theta)$$

The analogues of 4.3.4, 4.3.5 now become with $Z_t = Z_t$ and $\Delta p_b = p_o - p_b$

4.6.7 $$\frac{\Delta p_b}{g} \frac{d}{dt} \bar{\tilde{\theta}} = \frac{F_{o\theta}}{c_p} - \frac{F_{s\theta}}{c_p}$$

4.6.8 $$\frac{\Delta p_b}{g} \frac{d}{dt} \bar{\delta} = \frac{F_{o\theta}}{c_p} - \frac{F_{b\theta}}{c_p} + \tilde{\rho}_b \left(\frac{dZ_b}{dt} - W_b\right) \Delta\theta$$

where $\bar{\tilde{\theta}} = \bar{\theta}^b = \bar{\theta}^s$

$$\therefore \quad F_{s\theta} = -\tilde{\rho}_b \left(\frac{dZ_b}{dt} - \tilde{\bar{W}}_b - W_{Db} \right) \Delta\theta - \tilde{\rho}_b W_{Db} \delta\theta$$

This Eq. is written in this form because we shall, as a first approximation, neglect

$$\delta\theta << \Delta\theta$$

This is a comparable approximation to the neglect of

$$\tilde{\theta}_s - \bar{\tilde{\theta}}^s << \bar{\theta}_t - \tilde{\theta}_s$$

which is being made, when a dry adiabatic lapse rate is assumed in the sub-cloud layer. Both are necessary without a more detailed model of the sub-cloud layer, dealing with lapse rate structure and parcel paths.

4.6.9 $$\therefore \quad F_{s\theta} = -\rho_b c_p \left(\frac{dZ_b}{dt} - \tilde{\bar{W}}_b - W_{Db} \right) \Delta\theta$$

$F_{s\theta}$ will be again related to the surface sensible heat flux

3.8.3 $$F_{s\theta} = -k F_{o\theta}$$

so that most of the details of the processes in the sub-cloud layer are hidden in the computation of k, which we shall not attempt here.

The argument which led to 3.8.9 (see Ball, 1960 and 3.8) involved the generation and removal of kinetic energy by buoyancy forces, locally in the dry convective layer. The circulations of the cumulus clouds exchange energy between dry and cumulus layers, and the effect on 'k' is not clear.

3.8.3 parameterises the incorporation of the transition layer into the dry layer by the dry convection in the sub-cloud layer. Qualitatively it is likely that as the mass flux into the cumulus layer increases, $F_{s\theta}$ may become a smaller fraction of $F_{o\theta}$ (that is 'k' may fall), simply because the fraction of the convection from the surface trapped in the dry layer decreases.

3.8.3 is to be regarded only as a useful first approximation.

Equation for $\Delta\theta$

This follows immediately from the definition of $\Delta\theta$

$$\Delta\theta = \tilde{\theta}_b - \bar{\tilde{\theta}}$$

From 3.7.5

$$\left(\frac{\partial\tilde{\theta}}{\partial t} \right)_{Z_b} = -(\tilde{\bar{W}}_b + W_{Db})\Gamma_1$$

4.6.10 $$\therefore \quad \frac{d\tilde{\theta}_b}{dt} = \left(\frac{dZ_b}{dt} - \tilde{W}_b - W_{Db}\right)\Gamma_1$$

4.6.11 $$\therefore \quad \frac{d\,\Delta\theta}{dt} = \Gamma_1\left(\frac{dZ_b}{dt} - \tilde{W}_b - W_{Db}\right) - \frac{d\bar{\tilde{\theta}}}{dt}$$

The interpretation of this equation is essentially similar to 4.3.7. We have shown that the vertical motion ($\tilde{W} + W_D$) of the environment controls the local potential temperature in the cumulus layer (eq. 3.7.5). To the extent that cloud-base height does not subside with the environment $(\frac{dZ_b}{dt} - \tilde{W}_b - W_{Db})$ just above cloud-base, $\Delta\theta$ is increased; while the warming of the sub-cloud layer reduces $\Delta\theta$.

4.7 Solution of equations for the sub-cloud layer

I Heat balance and cloud mass flux

We have now a complete set of equations for the heat balance of the sub-cloud layer.

4.5.1 $$F_{o\theta} = C_\theta \tilde{\rho}_o c_p (\tilde{\theta}_o - \bar{\theta}) V_o$$

4.6.1 $$Z_b = f(\theta_o, r_o)$$

4.6.7 $$c_p \frac{\Delta p_b}{g} \frac{d\bar{\theta}}{dt} = F_{o\theta} - F_{s\theta}$$

3,8,9 $$F_{s\theta} = -k F_{o\theta}$$

4.6.9 $$F_{s\theta} = -\tilde{\rho}_b c_p \Delta\theta \left(\frac{dZ_b}{dt} - \tilde{w}_b - W_{Db} \right)$$

4.6.11 $$\frac{d}{dt}(\Delta\theta) = \Gamma_1 \left(\frac{dZ_b}{dt} - \tilde{w}_b - W_{Db} \right) - \frac{d\bar{\theta}}{dt}$$

The surface boundary problem remains as discussed in 4.5. Here we shall assume that θ_o , r_o are known. The six equations can then be solved for the variables $F_{o\theta}$, $F_{s\theta}$, Z_b , $\bar{\theta}$, $\Delta\theta$, W_D given Γ_1 , $\tilde{w}_b$, $\tilde{\rho}$ and k (and assuming the hydrostatic relation between p and Z).

The equation added to those of the problem of wholly dry convection discussed in 4.3 is 4.6.1 for cloud-base height. Since the height of cloud-base and of the transition layer are determined (see 4.9 also) we can solve for the convective mass flux (W_{Db}) into the cumulus layer. W_{Db} is not determined directly from the surface sensible heat flux, but indirectly from $F_{o\theta}$, $\tilde{w}_b$ and $\frac{dZ_b}{dt}$. This is clear if we substitute 3.8.9 in 4.6.9 and re-arrange, giving

4.7.1 $$-W_{Db} = \frac{k F_{o\theta}}{c_p \tilde{\rho}_b \Delta\theta} + \tilde{w}_b - \frac{dZ_b}{dt}$$

This equation is to be compared with 4.3.14, which is essentially the same, but with $W_{Db} = 0$. We have parameterised the cumulus in terms of a subsidence of the environment. The stable transition layer is lifted, relative to the environmental air, by the dry convection trapped in the sub-cloud layer, but subsides with $\tilde{w}_b$ and W_{Db} (which are respectively the mass flows out of the sub-cloud layer by subsidence and through the bases of the cumulus clouds); thus the transition layer rises and falls with cloud-base.

Some simple solutions will be considered.

Solutions

$\frac{d\bar{\tilde{\theta}}}{dt}$ as a function of Δp_b , $F_{o\theta}$ follows immediately from 4.6.7 and 3.3.9

4.7.2 $$\frac{d\bar{\tilde{\theta}}}{dt} = \frac{g(1+k)F_{o\theta}}{c_p \Delta p_b}$$

This is identical with 4.3.8 and can be integrated from an initial condition given $F_{o\theta}$, p_b (or Z_b) as a function of time. However an additional approximation has been made $\delta\theta << \Delta\theta$ (see 4.6.9), which does involve the neglect of a correction which would reduce k.

$F_{o\theta}$ follows from 4.5.1 given $\bar{\tilde{\theta}}$ and the surface $\tilde{\theta}_o$ so 4.5.1 and 4.7.2 can be solved simultaneously with the surface problem (see 4.5) to give $\bar{\tilde{\theta}}$, $F_{o\theta}$ given k and Δp_b .

$F_{s\theta}$ follows from k and $F_{o\theta}$.

$\frac{dZ_b}{dt}$ has been related to the surface variables (4.6.1) so Z_b , p_b follow from $\tilde{\theta}_o, \tilde{r}_o$.

Thus over the sea, where $\tilde{r}_o$ follows from $(\tilde{\theta}_o, \tilde{r}_o)$ the set of equations

4.5.1, 4.6.7, 3.3.9

can be solved simultaneously for

$$F_{o\theta} , \quad F_{s\theta} , \quad \bar{\tilde{\theta}}$$

given Z_b from 4.6.1 and k.

Over land the solution for Z_b involves the solution of the surface problem (4.5) for $\tilde{r}_o$ as well as $\tilde{\theta}_o$. It is necessary therefore to solve the water vapour balance in the sub-cloud layer, and indeed the whole cumulus layer problem before one can determine the surface fluxes. We shall attempt the water vapour balance for the sub-cloud layer in the next section.

$\Delta\theta$ The analogues of 4.3.9 and 4.3.10 are

4.7.3 $$\frac{\Delta p_b}{g} \frac{d}{dt} \Delta\theta = \left(\frac{dZ_b}{dt} - \tilde{W}_b - W_{Db}\right) \left(\frac{\Delta p_b}{g} \Gamma_1 - \frac{1+k}{k} \Delta\theta \tilde{\rho}_b\right)$$

4.7.4 $$\frac{d}{dt} \Delta\theta = \frac{F_{o\theta}}{c_p} \left(\frac{k\Gamma_1}{\bar{\rho}_b \Delta\theta} - \frac{g(1+k)}{\Delta p_b}\right)$$

which if combined reduce again to 4.7.1.

There is again a steady state solution in $\Delta\theta$, if Z_b , $F_{o\theta}$ and Γ_1 are constant

4.7.5 $$\Delta\theta = \frac{k}{k+1}\Gamma_1 \frac{\Delta p_b}{g\bar{\rho}_b} \approx \frac{k}{k+1}\Gamma_1 Z_b$$

This is identical to 4.3.16 for dry convection. Over the ocean, Z_b constant is often a good approximation. Even over land where Z_b has a marked diurnal variation 4.7.5 is a useful first approximation

if $$\frac{d\Delta\theta}{dt} << \frac{d\bar{\tilde{\theta}}}{dt}$$

Substituting 4.7.5, this inequality becomes:

$$\frac{k}{k+1}\Gamma_1 \frac{dZ_b}{dt} << \frac{d\bar{\tilde{\theta}}}{dt}$$

$\underline{W_{Db}}$ If we make the above approximation in 4.6.11, and then substitute for $d\bar{\tilde{\theta}}/dt$ from 4.7.2, or if the value for $\Delta\theta$ given by 4.7.5 is substituted in 4.7.1; we obtain the cloud mass flux in terms of $F_{o\theta}$, Z_b , $\tilde{W}$.

4.7.6 $$-W_{Db} = \frac{g(k+1)F_{o\theta}}{c_p \Gamma_1 \Delta p_b} + \tilde{W}_b - \frac{dZ_b}{dt}$$

This equation can be interpreted differently from 4.7.1. As an approximation to 4.6.11, with $d\Delta\theta/dt = 0$, it says that the transition layer is maintained when the mean potential temperature in the sub-cloud layer $\bar{\tilde{\theta}}$, increases at the same rate as potential temperature at cloud-base, $\tilde{\theta}_b$.

From 4.7.6 it is clear that the large-scale subsidence and rise of cloud base both reduce W_{Db} , the convective mass flux into the cumulus layer, in an exactly similar manner. Thus variation of cloud-base is an important control on the amount of active cloud. The smaller W_{Db} , the smaller the heat transport in the cumulus layer (see 3.10), which in turn reduces the rate of deepening of the cumulus layer (all other factors being equal - see chapter 5). The magnitudes of all terms in 4.7.6 may be comparable e.g. typical diurnal $\frac{dZ_b}{dt} = 15$ mb/hr ($+4$ cm s^{-1}).

If subsidence increases ($\tilde{W}_b$ becomes more negative), then it is clear from 4.7.6 that ($-W_{Db}$) falls to zero, and we revert to the dry model again with no clouds.

In the other limit as ($-\tilde{W}$) $\longrightarrow 0$, $|W_{Db}|$ increases tending to

$$\frac{g(k+1)F_{o\theta}}{c_p \Gamma_1 \Delta p_b} = \frac{1}{\Gamma_1}\frac{d\bar{\tilde{\theta}}}{dt} \qquad \text{if } Z_b \text{ is constant .}$$

Eq. 4.6.10 may perhaps be applicable to a field of cumulonimbus. If $\frac{dZ_b}{dt} << \tilde{W}_b$ which is probable 4.6.11 becomes

4.7.7. $$\frac{d\bar{\tilde{\theta}}}{dt} + \frac{d\Delta\theta}{dt} = -(\tilde{W}_b + W_{Db})\Gamma_1$$

Now $\frac{d\Delta\theta}{dt}$ must be small or zero if the field of convection is to persist, and if $\frac{d\bar{\tilde{\theta}}}{dt}$ is small then $\tilde{W}_b$ and W_{Db} must largely cancel. Evaporation of falling rain might give an additional term in 4.7.7, but one could regard this as local to a cumulonimbus and relevant only to the determination of W_{Db} . 4.7.7. could be used to relate the sub-cloud layer to the cumulonimbus layer, and determine W_{Db} . Hence one can estimate the water vapour flux out of the sub-cloud layer (see 4.8). The estimation of $d\bar{\tilde{\theta}}/dt$ remains a problem.

4.8 II Water Vapour balance in the sub-cloud layer

The extension of 4.4.1 and 4.4.2 for $\overline{\tilde{r}}$ and Δr to include a parameterisation for the cumulus is closely similar to the extension of 4.3.4 and 4.3.5 for $\overline{\theta}$, $\Delta\theta$.

Assuming

$$z_b = z_t$$

we write

4.8.1 $$\frac{F_{br}}{L} = \tilde{\rho}_b \, W_{Db} \, (\Delta r - \delta r)$$

where $$\Delta r = \tilde{r}_b - \overline{\tilde{r}}^b$$
$$\delta r = r(p) - \overline{\tilde{r}}^b$$

δr cannot be neglected in comparison with Δr, and as a first approximation one might write

$$r(p) = \tilde{r}_o$$

by neglecting dilution in the sub-cloud layer. Then

4.8.2 $$\delta r = \tilde{r}_o - \overline{\tilde{r}}^b$$

4.8.3 and $$\frac{F_{br}}{L} = -\tilde{\rho}_b \, W_{Db} (\tilde{r}_o - \tilde{r}_b)$$

The extension of 4.4.1 is

4.8.4 $$\frac{\Delta p_b}{g} \frac{d\overline{\tilde{r}}^b}{dt} = \frac{F_{or}}{L} + \tilde{\rho}_b \Delta r \left(\frac{dz_b}{dt} - \tilde{w}_b - W_{Db} \right) + \tilde{\rho}_b \, \overline{w}_{Db} \, \delta r$$

The second term on the R.H.S. represents the drying of the sub-cloud layer by the incorporation of drier air from above the transition layer. The last term is of comparable magnitude, and parameterises an additional drying of the sub-cloud layer because the air rising to form the clouds has a mixing ratio above that of $\overline{\tilde{r}}^b$. These terms are the feed-back through the water vapour budget on the height of cloud-base. By reducing $\overline{\tilde{r}}^b$ over land, $\tilde{r}_o$ is reduced, and cloud-base rises. This reduces $|W_{Db}|$ (see 4.7.6). Hence in 4.8.4, the last term alone cannot dry out the sub-cloud layer until there are no clouds: this can only happen if Δr is large. Over the sea, where $\tilde{r}_o$ is essentially constant, any fall of $\overline{\tilde{r}}^b$ just raises the surface flux F_{or}, so the ocean may be regarded as a vast reservoir, which supplies the water vapour (and the heat) necessary to constitute the clouds predicted by the equations of 4.7. (Strong subsidence will still remove clouds by lowering

the inversion below the L.C.L. of surface air. The dilution of surface air as it rises will raise its L.C.L. if $\bar{\tilde{r}}^{b}$ is low: an effect we have neglected.)

Δr Equation

From the definition of Δr

4.8.5 $$\frac{d}{dt}(\Delta r) = \frac{d\tilde{r}_b}{dt} - \frac{d\bar{\tilde{r}}^{b}}{dt}$$

However no theory has yet been developed for $\frac{\partial \tilde{r}}{\partial t}$ in the cumulus layer. The convective mass flux model of 3.7 is inadequate, because this model follows convective elements only while their potential temperature θ_c differs from that of the environment θ_e. The air that flows through the bases of the clouds has a higher θ_E than the cumulus layer (which often has nearly constant θ_E). Mixing dilutes the clouds, but the air in them has a higher θ_E than the environment at all levels. Even after the evaporation of all cloud water and descent to potential temperature equilibrium $\theta_c = \theta_e$ the mixing ratio of the air which was recently in a cloud is above that of the environment. Shear in the vertical wind and the circulations of later cumuli will distribute this water vapour through the layer.

A very simple theory for $\frac{\partial \tilde{r}}{\partial t}$ will now be proposed, based on a parameterisation of 3.3.3

3.3.3 $$\tilde{\rho}\frac{\partial \tilde{r}}{\partial t} + \tilde{\rho}\tilde{W}\frac{\partial \tilde{r}}{\partial Z} = -\frac{\partial}{\partial Z}(\tilde{\rho}\,\widetilde{W'(r' + r'_L)})$$

($\tilde{r}_L$ has been neglected)

The water transport by the cumulus clouds will be parameterised

4.8.6 $$\widetilde{W'(r' + r'_L)} = -W_D\left\{(r_c + r_L) - \tilde{r}\right\}$$

where $(r_c + r_L)$ is the total water content of a 'typical' cloud. This is inevitably an oversimplification.

Substituting 4.8.6 in 3.3.3, and neglecting variations of $\tilde{\rho}$

4.8.7 $$\frac{\partial \tilde{r}}{\partial t} = -(\tilde{W} + W_D)\frac{\partial \tilde{r}}{\partial Z} + W_D\frac{\partial}{\partial Z}(r_c + r_L) + (r_c + r_L - \tilde{r})\frac{\partial}{\partial Z}W_D$$

The analogue of 3.4.13 for cloud total water content (water substance is conserved: see 3.2.5) is

4.8.8 $$\frac{\partial}{\partial Z}(r_c + r_L) = -\frac{(r_c + r_L - \tilde{r})}{S}$$

for ascent with mixing. We shall suppose this is valid for $Z_b < Z < Z_1$.

Substituting 4.8.8. in 4.8.7. gives

4.8.9 $$\frac{\partial}{\partial t}\tilde{r} = -(\tilde{W} + W_D)\frac{\partial \tilde{r}}{\partial Z} + \frac{F_{rT}}{\bar{\rho}L}\left(\frac{1}{S} - \frac{1}{W_D}\frac{\partial W_D}{\partial Z}\right)$$

where $-F_{rT}/\bar{\rho}L = W_D[(r_c + r_L) - \tilde{r}]$

F_{rT} is a total water flux (including r_L) and is the analogue of $F_{\theta L}$.

4.8.9. parameterises $\frac{\partial \tilde{r}}{\partial t}$ in terms of

(i) the total environmental vertical velocity ($\tilde{W} + W_D$). For $Z_b < Z < Z_1$ this term generally reduces $\tilde{r}$.

(ii) an input of water vapour into the cumulus layer which is positive if

$$\frac{1}{W_D}\frac{\partial W_D}{\partial Z} < \frac{1}{S}$$

that is, if the ascending mass flux increases less fast than the dilution, mass (and therefore water vapour) is being shed from the clouds.

Now

$$\frac{d}{dt}\tilde{r}_b = \left(\frac{\partial \tilde{r}}{\partial Z}\right)_1 \frac{d}{dt} Z_b + \left(\frac{\partial \tilde{r}}{\partial t}\right)_b$$

Substituting from 4.8.8

4.8.10 $$\frac{d}{dt}\tilde{r}_b = \left(\frac{\partial \tilde{r}}{\partial Z}\right)_1 \left(\frac{d}{dt} Z_b - \tilde{W}_b - W_{Db}\right) + \frac{F_{br}}{\rho L}\left(\frac{1}{S} - \frac{1}{W_{Db}}\frac{\partial}{\partial Z} W_{Db}\right)$$

Substituting 4.8.10 in 4.8.5 gives

4.8.11 $$\frac{d}{dt}(\Delta r) = -\frac{d\bar{\tilde{r}}^b}{dt} + \left(\frac{dZ_b}{dt} - \bar{W}_b - W_{Db}\right)\left(\frac{\partial \tilde{r}}{\partial Z}\right)_1 + \frac{F_{br}}{\rho L}\left(\frac{1}{S} - \frac{1}{W_{Db}}\frac{\partial}{\partial Z} W_{Db}\right)$$

This determines Δr , from $\bar{\tilde{r}}, (\partial \tilde{r}/\partial Z)_1, F_{br}$ — the variables discussed in 4.7 $\frac{dZ_b}{dt}$, $\bar{\tilde{W}}_b$, W_{Db} ; and $\frac{\partial}{\partial Z}(W_{Db})$ which will be determined in chapter 5.

Closure:

The 4 water vapour variables of the sub-cloud layer F_{or}, $\bar{\tilde{r}}$, Δr, δr are determined by integrating 4.5.2, 4.8.2, 4.8.4, 4.8.11 from an initial condition, given $\tilde{r}_o$ (see surface problem 4.5)

$\frac{dZ_b}{dt}$, W_{Db} (see 4.7) , $\bar{\tilde{W}}_b$, $(\tilde{\rho})$

and $(\partial \tilde{r}/\partial Z)_1$, $\partial W_D/\partial Z$, S in the cumulus layer

The hydrostatic relation between $p, Z, \tilde{\rho}$ has been assumed.

As mentioned earlier, the solution for $\tilde{r}_o$ over land additionally involves 4.5.3, 4.5.4 and $F_{o\theta}$. The equations of 4.5, 4.7, and 4.8 must be solved simultaneously.

In this section we find 3 new variables from the cumulus layer are necessary to solve the water vapour balance of the sub-cloud layer namely $(\partial\tilde{r}/\partial Z)_q$; and S, $\frac{\partial W_D}{\partial Z}$ which are needed to determine $(\partial\tilde{r}/\partial t)_b$. These will be discussed in chapter 5, where we shall model the cumulus layer.

4.9 Relation between heights of cloud-base and the transition layer

It was assumed for simplicity in 4.6 that

4.6.4 $$Z_b = Z_t$$

and the transition layer was idealised by letting

$$Z_s \longrightarrow Z_t$$

In 4.6 it was suggested that W_{Db} is controlled by the transition layer $\Delta\theta$. However a relation was deduced for $\Delta\theta$ in a simple case in 4.7

4.7.5 $$\Delta\theta \approx \frac{k}{k+1}\,\Gamma_1\,Z_b$$

and in the same section W_{Db} was determined purely from the budget and structure of the sub-cloud layer without any specific equation relating W_{Db} to $\Delta\theta$. The assumption of 4.6.4 made this possible.

We shall now indicate diagramatically how the transition layer controls W_{Db} so that $Z_t - Z_b$ is small and 4.6.4 nearly satisfied. The validity of the preceding model is not affected.

Z_t was originally defined as the level reached by dry convection from the surface. To distinguish some parcels that regain buoyancy and become clouds, a spectrum of convective elements of different W', θ' is necessary; so a single Z_t is a simplification. It is convenient however to distinguish a transition layer

$$Z_s < Z < Z_t$$

where Z_t is the height at which some median convective element stops if there is no water condensation.

Fig. 4.9.1 shows schematically that, the larger $Z_t - Z_b$, the easier it is for parcels to regain buoyancy. Indeed it can be seen that the population of convective elements reaching Z_s will fall into two classes: those that regain buoyancy before ceasing to rise (which will continue

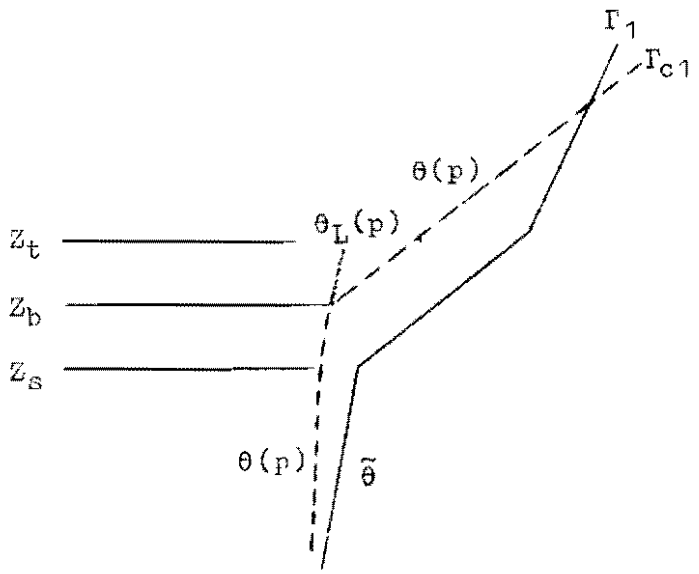

Fig. 4.9.1

upwards since $\Gamma_{c1} > \Gamma_1$), and those that do not. The fraction that regain buoyancy is critically dependent on $Z_t - Z_b$.

A simple numerical estimate will illustrate this. Consider the deceleration of an ascending parcel (vertical velocity W', perturbation potential temperature θ') above Z_t for simplicity, using parcel mechanics (Fig. 4.9.2.).

Fig. 4.9.2

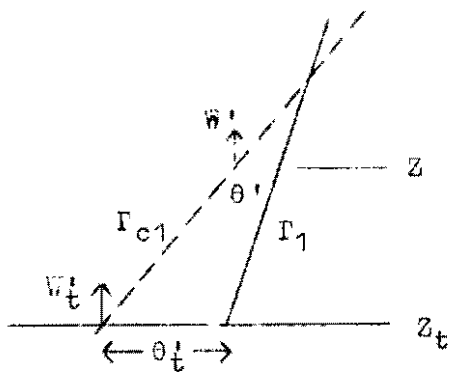

$$W'^2 - W_t'^2 = -\int_{Z_t}^{Z} 2g\frac{\theta'}{\bar{\theta}}\,dZ$$

$$\theta' = \theta_t' - (\Gamma_{c1} - \Gamma_1)(Z - Z_t)$$

For the limiting case in which $\theta' = 0$ when $W' = 0$

$$W_t'^2 = \frac{g\theta_t'^2}{\bar{\theta}(\Gamma_{c1} - \Gamma_1)}$$

For $W_t = 1\ m\ s^{-1}$

$\Gamma_{c1} - \Gamma_1 = 1°C\ km^{-1}$

$\theta_t \approx 0.2°$

A buoyancy deficit greater than this will stop all convective elements with $W_t' \leq 1\ m\ s^{-1}$

Fig. 4.9.1 shows that θ_t' is approximately

$$\theta_s(p) - \bar{\theta}_t + \Gamma_{c1}(Z_t - Z_b)$$

The critical control is $(Z_t - Z_b)$. Γ_{c1}, being a function of Γ_w, does vary with temperature: a typical value in the tropical atmosphere is about $+4°C\ km^{-1}$ (see chapter 6).

In practice there is a size spectrum of convective elements and a more detailed analysis, allowing for example for the variation in Γ_{c1}, with element size, suggests that variations of $\pm 0.2°C$ in θ_t' are sufficient to control W_{Db}. Thus in the tropical atmosphere this can be achieved with variations in $Z_t - Z_b$ of $\pm$ 50 m.

The virtual temperature correction is often important at cloud-base where Δr is negative and $\Delta\theta$ positive. $\Delta\theta_v$ is therefore less than $\Delta\theta$, typically less than one degree. It is likely that $z_t - z_b$ is therefore about 100m in the tropics. There is an indication here that one might find larger values of $z_t - z_b$ at lower temperatures, that is in higher latitudes.

For budget purposes it was assumed that

4.5.3 $$\frac{dz_b}{dt} \approx \frac{dz_t}{dt}$$

This remains a useful approximation. Indeed if the top of the dry layer is taken at z_t in Fig.4.9.1, the budget problem for the dry layer remains unchanged. The heat flux out of the top of the layer

$$0 < z < z_t$$

is now a flux of θ_L, as some condensation has taken place already. Numerically, however, it is irrelevant whether condensation takes place in the cumuli below z_t or not, as the water is advected upwards. This is clear from the dotted path of $\theta_L(p)$ in Fig. 4.9.1. The parameterisation becomes

$$\frac{F_{t\theta L}}{c_p} = -\tilde{\rho}_t \, w_{Dt} \, (\theta_L(p) - \tilde{\theta}_t)$$

$$= \tilde{\rho}_t \, w_{Dt} \, (\Delta\theta - \delta\theta)$$

$$\Delta\theta = \tilde{\theta}_t - \overline{\tilde{\theta}}^t$$

$$\delta\theta = \theta_L(p) - \overline{\tilde{\theta}}^t$$

Numerically this is barely distinguishable from 4.6.6 where we assumed 4.6.4. Indeed we shall continue to use 4.6.4 in later chapters.

The choice of a level to divide dry and cumulus layers is a little arbitrary. z_t seems most suitable because:

(a) the upper bound of a stable transition layer on a sounding can probably be identified, and may theoretically be associated with the limit of essentially dry convection from the ground;

(b) any liquid water condensed in the ascending cumulus clouds between z_b and z_t can be handled by the use of θ_L rather than θ, and plays no part in the heat budget of the dry layer as it is advected into the cumulus layer.

The purpose of this section has been to clarify why it has not been necessary to use a specific dynamical relationship between $\Delta\theta$ and W_{Db}. W_{Db} can be controlled by small variations in $z_t - z_b$, but this does not affect the heat flux $F_{t\theta L}$, or therefore the budget of the layer $0 < z < z_t$. Further any changes in $z_t - z_b$ of about $\pm$ 50m do not significantly affect the equality

$$\frac{dz_t}{dt} = \frac{dz_b}{dt}$$

Thus we may work from this equality and deduce W_{Db} as in 4.7, knowing that only a relatively small change in $z_t - z_b$ controls W_{Db}.

4.10 Summary of Chapter 4

This chapter falls into two parts.

Sections 4.2 to 4.5 establish a simple closed model for the time development of a dry convective boundary layer given an initial stratification, $\tilde{\theta}$, and the surface boundary conditions. This model incorporates a generalisation of a parameterisation proposed by Ball (1960) for the lifting of an inversion by dry convection.

In sections 4.3 to 4.9 this model is extended to describe the sub-cloud layer, by including an additional parameterisation for the sensible heat and water vapour fluxes into the cumulus layer. By demanding that the more stable transition layer at the top of the dry layer always remained at cloud-base height, it was possible to determine the convective mass flux W_{Db} into the cumulus layer. Retrospectively, in 4.9, it was found that only very small variations (about 100m) in the relative height of cloud-base and transition layer are necessary to exert a sensitive control on W_{Db}.

The problem is simplified over the sea, if $\tilde{\theta}_o$, $\tilde{r}_o$ are assumed known. Over land both the sensible heat and water vapour budgets must be solved simultaneously in order to calculate the partition of the incoming

solar radiation into sensible and latent heat fluxes at the surface. Nonetheless given a set of surface observations and a series of soundings in time, it is possible to test the model in many ways. This will be attempted in chapter 6.

The most important conclusion to be drawn from this chapter is that W_{Db}, which is a measure of the intensity of the cumulus convection in this model, is not a simple function of surface heat flux or water vapour flux. Instead we have

4.7.6 $$\left(\frac{dZ_b}{dt} - \widetilde{W}_b - W_{Db}\right) = \frac{g(k+1)F_{o\theta}}{c_p \Gamma_1 \Delta p_b}$$

The sum of three terms on the L.H.S. is essentially a function of surface heat flux. The rise and fall of cloud-base is a function of both the heat and water vapour balances in the sub-cloud layer, and is most marked over land.

We see that rise of cloud-base and subsidence have equivalent effects: they both reduce W_{Db}.

In the next chapter, which is the last of the theoretical development, the time development of the structure of the cumulus layer will be related to the fluxes through cloud-base (W_{Db}, $F_{b\theta}$, F_{br}); $\widetilde{W}$; and the 'free' atmosphere above the convective boundary layer.

Chapter 5 The Cumulus Layer

5.1 Introduction

In this chapter the cumulus model will be closed. The fluxes into the cumulus layer through cloud-base W_{Db}, $F_{b\theta}$, F_{br} were calculated in chapter 4 from a simple model of the sub-cloud layer, assuming certain characteristics of the cumulus layer (the stratification and the water vapour input parameterised in 4.8).

The problem of lapse rate structure in the cumulus layer, first considered in 3.8, will now be examined in more detail. A simple two-layer model will be constructed in 5.2.

This model will be used for the instantaneous distribution of potential temperature in the cumulus layer. When budget equations and the boundary conditions are added, one obtains a closed system of equations for the time development of the cumulus layer (5.3). These quantify the factors controlling the rate of rise of the top of the cumulus layer: principally subsidence, variations in the height of cloud-base, and the surface sensible heat flux.

A similar set of equations is then proposed for the time development of the water vapour distribution (5.4).

As in earlier chapters, vertical shear in the horizontal wind has not been considered, though this may alter the dilution and dissipative parameters used in 5.2 for the ascent and descent of a 'typical' cloud. Radiation too has been neglected, and liquid water is carried with the air in the clouds.

5.2 Lapse Rate Model

A quantitative model of the lapse rate structure of the cumulus layer as a function of time is a very complex problem unless drastic simplifications are made. We shall make the following assumptions:

(a) a two-layer approximation : see Fig. 5.2.1

(b) a single scale of cloud : a "typical" cloud

(c) a simple 1-Γ model for a typical cloud

(d) an instantaneous equilibrium between lapse rate structure, the typical cloud, and $\bar{\Gamma}$ (see Fig. 5.2.1)

Fig. 5.2.1 shows the simple 2-layer structure which will be modelled.

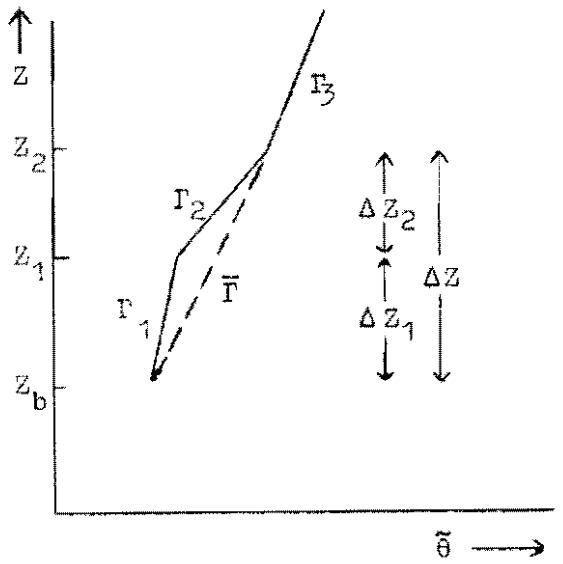

Fig. 5.2.1

$\bar{\Gamma}$ is the mean value of $\partial\tilde{\theta}/\partial z$ from top to bottom of the cumulus layer. By definition

5.2.1 $$\Gamma_1 \Delta z_1 + \Gamma_2 \Delta z_2 = \bar{\Gamma} \Delta z$$

where $\Delta z = \Delta z_1 + \Delta z_2$

The most significant of the above simplifications is (d).

In terms of Fig. 5.2.1, we suppose that an instantaneous equilibrium exists such that Γ_1, Γ_2, Δz_1, Δz_2 are at all times functions of $\bar{\Gamma}$, Δz only, and not of their time derivatives. This hypothesis is likely to be a good approximation even when $\bar{\Gamma}$ and Δz change with time, and gives useful results which can be tested (see chapter 6). In addition to 5.2.1, we require

2 further relations to determine Γ_1 , Γ_2 , $\frac{\Delta z_1}{\Delta z_2}$, supposing we know $\bar{\Gamma}$ and Δz (for which equations are constructed in 5.3).

To obtain these relations, we assume an instantaneous relation between the (characteristic) stratification and the typical individual cloud. The philosophy of the modification of the mean atmosphere by the cumulative life-cycles of many clouds, whose life-cycles in their turn depend on the stratification, was discussed in 3.8. If one considers $\bar{w} = 0$, then the clouds cool the upper part of the layer, that is destabilise the layer, and successive 'typical' clouds become larger and ascend higher. The modification of the stratification and the deepening of the cumulus layer proceed together. The problem becomes tractable if we assume a one-to-one correspondence between the two-layer stratification, the regions of warming and cooling and therefore the ascent and descent of our typical cloud. This was shown schematically in Fig. 3.8.5.

It is then possible to write two further relationships based on a 1-D model for the 'typical' cloud.

(i) A kinetic energy relationship:

If we neglect the small K.E. input and buoyancy deficit at z_b , ascending saturated air gains upward kinetic energy in Δz_1 and overshoots to z_2, before falling back.

(ii) A thermodynamic relationship

is indicated by the path of the typical parcel shown on the θ_L, z diagrams (Fig. 3.8.5, 5.2.2).

Because of the asymmetry between ascent and descent with dilution (see 3.5), saturated cloud air descending from z_2 evaporates all its liquid water and comes to potential temperature equilibrium with the mean atmosphere long before reaching z_b. We shall assume that the air of our typical cloud comes to equilibrium at z_1 , so that the regions of heating and cooling during the life-cycle of the cloud coincide with the two layers of different lapse rate.

As far as the temperature structure of the model is concerned, the cumulus layer is not being modified by mixing of cloud with environment at a different temperature, but as discussed in 3.8 by compensating descent and

ascent in the environment. The modification is considered in 5.3: in this section we determine instantaneous values of Γ_1, Γ_2 in the two layers by relating them to two relations ((i) and (ii) above) for a typical cloud. Since dilution is of great importance in (ii) (and needs to be considered in (i) also), we shall first discuss a relation between dilution scale length S, and the depth of the cumulus layer.

Dilution Scale Length

The scale length S was introduced as a parameterisation for dilution (or entrainment) in 3.4.

3.4.4 $$\frac{1}{M}\frac{dM}{dZ} = \pm \frac{1}{S}$$

3.4.5

for ascent and descent respectively.

S is a parameter about which we know little, although it will be recalled that Simpson and Wiggert (1969) and others have used the similar relationship (see 2.2.1)

5.2.2 $$\frac{1}{M}\frac{dM}{dZ} = \frac{0.2}{a}$$

where a is the radius of a cloud tower. They found good agreement between a 1-D model, and the height reached by individual towers, assuming a to be constant.

In 2.5 we also noted that two models of a convective element predicted

5.2.3 $$\frac{a}{d} \sim 0.5$$

for a dominant cloud size. In both models d is the depth of a layer of conditional instability, which corresponds most closely to ΔZ_1, in our model, the layer over which the cumulus clouds gain upward momentum. With these considerations in mind, S will be parameterised directly in terms of ΔZ_1 and for simplicity is assumed the same for ascent and descent.

5.2.4 $$\frac{1}{S} = \frac{E}{\Delta Z_1}$$

We shall find in chapter 6, that the model predicts lapse rates well with $E = 0.4$, which means that 5.2.4 and 5.2.2 are equivalent if we assume 5.2.3 and $d \sim \Delta Z_1$.

Thermodynamic Relationship

Fig. 5.2.2 shows the ascent and descent of our model cloud, which rises to Z_2, and descends first evaporating its liquid water, and then 'dry' to potential temperature equilibrium with the environment at Z_1, (see also figs. 3.5.1, 3.8.5). The physical consequence implied in this diagram is that the upper layer is cooled, and the lower warmed (see 3.5).

Fig. 5.2.2

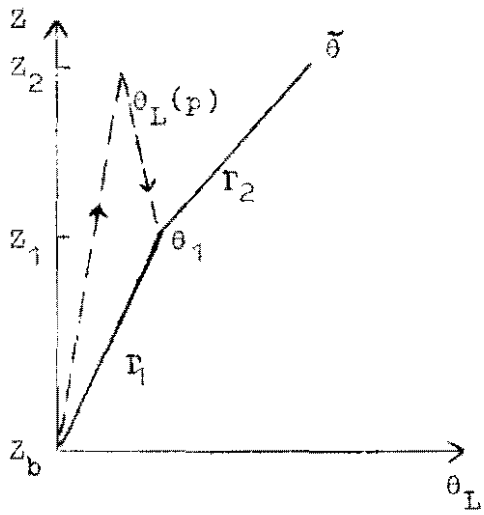

$\tilde{\theta} = \tilde{\theta}_L$

neglecting $\tilde{r}_L$

If we use the dilution relationship 3.4.13, we obtain for the ascent and descent of a parcel by integration:

5.2.5 $$\theta_{Lf}(p) - \theta_{Lb}(p) = \Gamma_1 S\, e^{-(\Delta Z_1 + 2\Delta Z_2)/S} + (\Gamma_2 - \Gamma_1) S\, e^{-2\Delta Z_2/S} - 2\Gamma_2 S\, e^{-\Delta Z_2/S} + \Gamma_1\, \Delta Z_1 + \Gamma_2 S$$

where $\theta_{Lb}(p)$ is the value of θ_L of a 'parcel' ascending through cloud-base.

$\theta_{Lf}(p)$ is the value of θ_L of a 'parcel' descending to Z_1.

The simplification has been made in 5.2.5 (and Fig. 5.2.2) that

5.2.6 $$\theta_{Lb}(p) = \tilde{\theta}_b$$

which is of little numerical importance here.

The condition that air finally descending with the evaporated cloud residue to Z_1, has the potential temperature $\tilde{\theta}_1$, is, using 5.2.6

5.2.7 $$\theta_{Lf}(p) - \theta_{Lb}(p) = \Gamma_1 \Delta Z_1$$

Combining 5.2.5 and 5.2.7, we obtain after a little manipulation

$$\frac{\Gamma_1}{\Gamma_2} = \frac{1 - 2e^{\Delta Z_2/S} + e^{2\Delta Z_2/S}}{1 - e^{-\Delta Z_1/S}}$$

On this model, the ratio of the lapse rates is solely a function of $\Delta Z_1/\Delta Z_2$ and $\Delta Z_1/S = E$.

Expanding in powers of $\Delta Z_1/S, \Delta Z_2/S$, we find that the first two non-zero terms in both numerator and denominator give sufficient accuracy, and after rearrangement, we obtain

$$\frac{\Gamma_1}{\Gamma_2} = \frac{\left(\frac{\Delta Z_1}{S}\right)\left(\frac{\Delta Z_2}{\Delta Z_1}\right)^2\left(1 + \frac{\Delta Z_1}{S}\,\frac{\Delta Z_2}{\Delta Z_1}\right)}{1 - \frac{\Delta Z_1}{2S}}$$

Substituting 5.2.4

5.2.9 $$\frac{\Gamma_1}{\Gamma_2} = \frac{E(\Delta Z_2/\Delta Z_1)^2\left(1 + E(\Delta Z_2/\Delta Z_1)\right)}{1 - E/2}$$

This will be used as a thermodynamic relationship between Γ_1/Γ_2 and $\Delta Z_1/\Delta Z_2$. The dependence on the dilution parameter E is indicated in the following table.

Table 5.2.1

$\frac{\Gamma_1}{\Gamma_2}$	$\Delta Z_1/\Delta Z_2$		
E	0.3	0.4	0.5
1.0	0.75	0.86	1.00
0.5	1.05	1.16	1.35
0.1	2.24	2.44	2.82

← Lower limit on $\Delta Z_1/\Delta Z_2$

There is a lower limit on $\Delta Z_1/\Delta Z_2$ for a given E because $\Gamma_1 < \Gamma_2$.

Eq. 5.2.9 predicts a relationship between Γ_1/Γ_2 and $\Delta Z_1/\Delta Z_2$ which may be tested. Values of Γ_1/Γ_2 of about 0.5 and 0.1 are typical of convection over land and beneath an inversion, respectively.

As dilution of cloud by the environment, parameterised by E, is not well understood, there may be some dependence of E on other variables such as vertical shear in the horizontal wind. Some caution is therefore necessary; in the absence of further theory, one must depend on observations to provide values for E (see chapter 6). However the work of Simpson et al

(1965, 1969) has clearly shown that the range of possible values for the entrainment constant in a 1-D model of an individual cumulus cloud is very limited (see 2.2).

Kinetic Energy relationship

There is a second independent relationship in wet convection between the stratification and the typical cloud path, depending on differences of θ rather than θ_L. The path of cloud potential temperature on ascent is shown schematically in Fig. 5.2.3. The potential temperature difference at cloud-base is neglected (and likewise the upward kinetic energy at cloud-base). An average value of Γ_{c1} in the cumulus layer can be used as a first approximation.

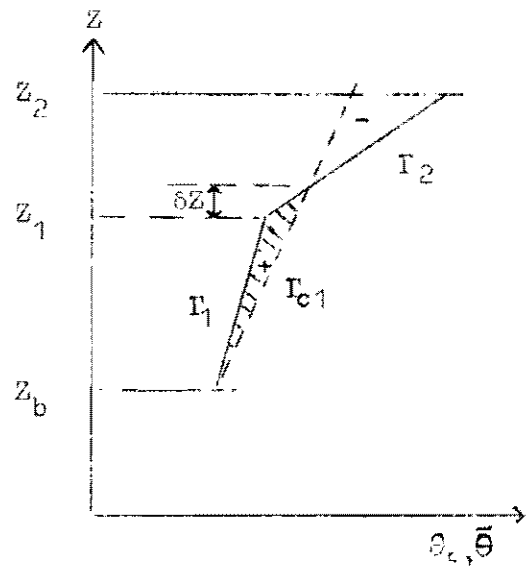

Fig. 5.2.3

The shaded area, equivalent to the positive area on a tephigram between parcel lapse rate and the mean sounding, is well known to be a measure of the maximum available potential energy for an ascending parcel. The simplest treatment of the problem would be to suppose the parcel overshoots to some height (z_2) such that the negative area in Fig. 5.2.3 equals the positive one. Then

5.2.10 $$\tfrac{1}{2}(\Gamma_{c1} - \Gamma_1)\,\Delta z_1(\Delta z_1 + \delta z) = \tfrac{1}{2}(\Gamma_2 - \Gamma_{c1})(\Delta z_2 - \delta z)^2$$

$$\text{where } \delta z = \frac{\Gamma_{c1} - \Gamma_1}{\Gamma_2 - \Gamma_{c1}}\,\Delta z_1$$

However this is likely to be a poor estimate of z_2 for several reasons.

(a) Γ_{c1} , the parcel lapse rate for ascending saturated air was derived by diluting an ascending cloud with its environment (see 3.4). The environment is not ascending with the cloud, but is mixed into it by 'turbulence' of unspecified character, thus sharing the upward momentum of the cloud. This is a process involving a transfer of kinetic energy from the scale of the mean upward motion of the cloud, to a smaller 'turbulent' scale, which continues further dilution. (This is analogous to the collision problem in particle mechanics - see Telford: 1966, 1969).

(b) The kinetic energy of the mean motion generated by horizontal temperature gradients is shared between horizontal and vertical velocity. This reduces the maximum upward mean velocity of a cloud parcel and has been variously parameterised in 1-D models as a drag or virtual mass coefficient (see 2.2).

(c) In flow where shearing is substantial, the convective circulation may become organised so that the kinetic energy of the low level inflow is added to that of the updraft. This occurs in organised cumulonimbus, and may be a feature of ordinary convection, although no relevant observations are known to the author.

In this thesis we shall not consider the effects of vertical shear in the horizontal wind, and will only modify 5.2.10 by introducing a parameter

$$D < 1$$

to give

5.2.11 $$D(\Gamma_{c1} - \Gamma_1)\,\Delta Z_1(\Delta Z_1 + \delta Z) = (\Gamma_2 - \Gamma_{c1})(\Delta Z_2 - \delta Z)^2$$

where $$\delta Z = \frac{\Gamma_{c1} - \Gamma_1}{\Gamma_2 - \Gamma_{c1}}\,\Delta Z_1$$ as before .

An estimate of D will be made from a 1-D model. Eq. 2.2.2 (see Simpson and Wiggert: 1969) becomes in our notation

5.2.12 $$\frac{d}{dZ}\left(\frac{1}{2}W_c^2\right) = \frac{g\emptyset}{1+\gamma} - \frac{W_c^2}{S}$$

This equation can be integrated for the path shown on Fig. 5.2.3 to give D as a function of S, and hence of E (see 5.2.4). D does not depend on the factor (1 + γ), but does depend further on $\Delta Z_1/\Delta Z_2$. The solution for D thus requires further iteration of the set of equations 5.2.1, 5.2.9 and 5.2.11, which is not justified by the approximate nature of 5.2.11. The problem will be simplified by using values of D which are functions of E only, estimated for the case of ΔZ_1 , ΔZ_2 equal.

These values are given in Table 5.2.2.

Table 5.2.2

E	D
0.3	0.6
0.4	0.5
0.5	0.4

These numbers are approximate, and are given to indicate the trend and magnitude. Table 5.2.3 is not very sensitive to alterations in D of $\pm$ 0.1 for the same value of E.

Solution of lapse rate equations

For given values of E, D, $\bar{\Gamma}$ and Γ_{c1} equations 5.2.1, 5.2.9, 5.2.11 have a unique solution for

$$\Gamma_1 , \quad \Gamma_2 , \quad \Delta Z_1/\Delta Z_2$$

for all

$$\bar{\Gamma} > \Gamma_{c1}$$

This solution is independent of ΔZ , which must be found by integrating the time development of the layer (see 5.3). An equation for $\bar{\Gamma}$ will also be given in 5.3, while Γ_{c1} (see 3.4.6) depends significantly on the water vapour content of the cumulus layer (see 5.4). Different average values of Γ_{c1} in layers 1 and 2 are appropriate if the cumulus layer is deeper than one or two km, as Γ_w and the saturation deficit of the environment ($r_s - r_e$) change with height. A single value of Γ_{c1} in the cumulus layer will however be used here.

The form of the solution is that as $\bar{\Gamma}$ increases; Γ_2 increases rapidly, while Γ_1 slowly decreases and $\frac{\Delta z_1}{\Delta z_2}$ increases. This is indicated in table 5.2.3 for constant Γ_{c1}, E, D. The agreement with observation seems encouraging and will be discussed in chapter 6.

Table 5.2.3

E	D	°C km^{-1} Γ_{c1}	$\bar{\Gamma}$	Γ_1	Γ_2	$\frac{\Delta z_1}{\Delta z_2}$
0.4	0.5	4.0	4.5	3.3	5.8	1.1
0.4	0.5	4.0	5.0	2.8	7.9	1.35
0.4	0.5	4.0	6.5	2.0	16.0	2.15

The qualitative interpretation of these solutions are as follows.

We have neglected the negative buoyancy and upward kinetic energy at cloud-base, so it is necessary that

$$\Gamma_1 < \Gamma_{c1}$$

in order that the model cloud gains upward velocity.

If $\bar{\Gamma} < \Gamma_{c1}$ then ascending saturated air can never become negatively buoyant (saturated parcels will ascend into the stratosphere, where $\bar{\Gamma}$ becomes greater than Γ_{c1} again).

If $\bar{\Gamma}$ is large compared with Γ_{c1}, then since

$$\Gamma_1 < \Gamma_{c1}$$

it follows from 5.2.1 that Γ_2 must become large. ($\Delta z_1/\Delta z_2$ cannot become small). The model says that the lower layer z_b to z_1, will destabilise until the model clouds overshoot sufficiently far into the very stable layer $z_1 \rightarrow z_2$ for parcels falling back from z_2 to come to equilibrium at z_1. The last row of numbers given in table 5.2.3 are not inconsistent with convection beneath an inversion, even though radiative cooling has been neglected (see also chapter 6).

Conclusion:

A simple but physically useful model of the lapse rate structure of the cumulus layer has been constructed. The least well defined assumption that has been made is that of instantaneous equilibrium. There will be situations where the nature of the underlying surface changes suddenly, when the assumption of an equilibrium structure will be incorrect. However in general the assumption may be reasonable: only comparison with observation will tell.

However this assumption is fundamental to the approach of the model of the cumulus layer in 5.3, since the heat transports in the cumulus layer by the clouds are specified only in terms of the fluxes through cloud base and the lapse rate structure. No attempt will be made to calculate

$$\widetilde{w'\theta'} \quad , \quad \widetilde{w'r'_L} \qquad \text{etc.}$$

These can be inferred (if required) from changes in $\tilde{\theta}$ deduced from the lapse rate model, which incorporates the mechanics and thermodynamics of a typical cloud.

It should be appreciated that there is no essential difference between maintaining Γ_1 , Γ_2 as the cumulus layer deepens or gets warmer, while keeping $\bar{\Gamma}$ constant; and changing Γ_1 , Γ_2 if $\bar{\Gamma}$ changes in the course of the time development of the layer.

5.3 Time Development of the Cumulus Layer

Part I : Temperature Structure

In this section an important set of equations is constructed to describe the modification of the two-layer cumulus model by the heat transports imposed by a field of non-precipitating cumulus convection. The nature of this modification process; the warming of the lower layer and the cooling of the upper layer, was discussed in detail in chapter 3. The convective mass flux and sensible heat flux into the cumulus layer through cloud base were modelled in chapter 4. The lapse rate model of 5.2 incorporates the θ_L transport, and the mass transport of a typical cloud. These transports by the clouds are made quantitative through the lapse rate model, and the inputs at cloud-base.

As indicated in chapter 1, the use of levels whose heights vary with time as the depth of the dry or cumulus layers alter, complicates the heat budget for a layer, but simplifies the parameterisation of the convective transports. Analogous to the definition of $\overline{\tilde{\theta}}^s$ in 4.3, we define average variables for the layers ΔZ_1 , ΔZ_2

5.3.1
$$\frac{\Delta p_1}{g}\,\overline{\tilde{\theta}}^1 = \int_{Z_b}^{Z_1} \tilde{\theta}\,\tilde{\rho}\,dZ$$

5.3.2
$$\frac{\Delta p_2}{g}\,\overline{\tilde{\theta}}^2 = \int_{Z_1}^{Z_2} \tilde{\theta}\,\tilde{\rho}\,dZ$$

where
$$\Delta p_1 = p_b - p_1$$
$$\Delta p_2 = p_1 - p_2$$

Fig. 5.3.1 serves to define the variables of this section.

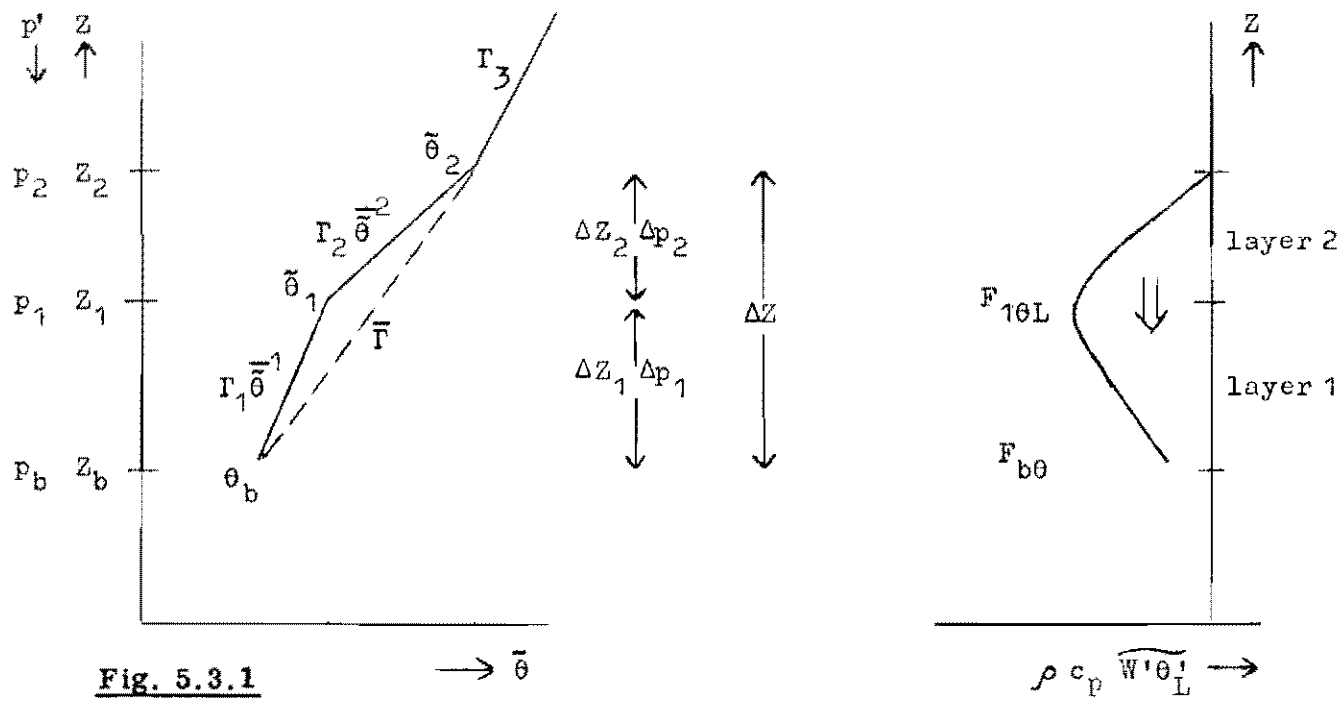

Fig. 5.3.1

The algebraic simplification will be made that $\bar{\tilde{w}}$ is independent of height in the cumulus layer.

Heat Balance:

The heat balance for layer 1 can be written, using 3.10.4, and the definition 5.3.1, as

5.3.3 $$\frac{d}{dt}(\bar{\tilde{\theta}}^1 \Delta p_1) = \frac{g}{c_p}(F_{b\theta} - F_{1\theta L}) - \tilde{\theta}_1 \frac{d}{dt} p_1 + \tilde{\theta}_b \frac{d}{dt} p_b - \bar{\tilde{w}} \Gamma_1 \Delta p_1$$

Similarly for layer 2

5.3.4 $$\frac{d}{dt}(\bar{\tilde{\theta}}^2 \Delta p_2) = \frac{g}{c_p} F_{1\theta L} - \tilde{\theta}_2 \frac{d}{dt} p_2 + \tilde{\theta}_1 \frac{d}{dt} p_1 - \bar{\tilde{w}} \Gamma_2 \Delta p_2$$

since $F_{2\theta L} = 0$

These relations, like many of those in chapter 4, are simpler to handle numerically in pressure co-ordinates. However in the belief that it is easier at first reading to understand the model if the equations are expressed in height co-ordinates, the density variations in the cumulus layer will be neglected from here on. 5.3.3 and 5.3.4 then become, after expanding the L.H.S.

5.3.5 $$\Delta z_1 \frac{d}{dt} \bar{\tilde{\theta}}^1 = \frac{F_{b\theta}}{\rho c_p} - \frac{F_{1\theta L}}{\rho c_p} + (\tilde{\theta}_1 - \bar{\tilde{\theta}}^1)\frac{dz_1}{dt} - (\tilde{\theta}_b - \bar{\tilde{\theta}}^1)\frac{dz_b}{dt} - \bar{\tilde{w}} \Gamma_1 \Delta z_1$$

5.3.6 $$\Delta z_2 \frac{d}{dt} \bar{\tilde{\theta}}^2 = \frac{F_{1\theta L}}{\rho c_p} + (\tilde{\theta}_2 - \bar{\tilde{\theta}}^2)\frac{dz_2}{dt} - (\tilde{\theta}_1 - \bar{\tilde{\theta}}^2)\frac{dz_1}{dt} - \bar{\tilde{w}} \Gamma_2 \Delta z_2$$

where ρ is a mean density.

These are the heat budget equations, and defining relations for the variables $\bar{\tilde{\theta}}^1$, $\bar{\tilde{\theta}}^2$. $F_{b\theta}$ is an input to the problem (4.6.6), but $F_{1\theta L}$ is an unknown. We shall relate $\tilde{\theta}_b$, $\tilde{\theta}_1$, $\bar{\tilde{\theta}}_1$ etc. and their time derivatives to the lapse rate model through the following definitions (only approximate in height co-ordinates)

5.3.7 $$\overline{\tilde{\theta}}^{1} - \tilde{\theta}_b = \tfrac{1}{2}\Gamma_1 \Delta z_1$$

5.3.8 $$\tilde{\theta}_1 - \overline{\tilde{\theta}}^{1} = \tfrac{1}{2}\Gamma_1 \Delta z_1$$

5.3.9 $$\overline{\tilde{\theta}}^{2} - \tilde{\theta}_1 = \tfrac{1}{2}\Gamma_2 \Delta z_2$$

5.3.10 $$\tilde{\theta}_2 - \overline{\tilde{\theta}}^{2} = \tfrac{1}{2}\Gamma_2 \Delta z_2$$

With the further definitions

5.3.11 $$\Delta z_1 = z_1 - z_b$$

5.3.12 $$\Delta z_2 = z_2 - z_1$$

5.3.13 $$\Delta z = \Delta z_1 + \Delta z_2$$

it is possible to relate the budget equations to the lapse rate structure and its changes.

Combining 5.3.5 with definitions 5.3.7, 5.3.8 and 5.3.11, we obtain

5.3.14 $$\frac{F_{b\theta}}{\rho c_p} - \frac{F_{1\theta L}}{\rho c_p} = \Delta z_1 \left[\frac{d\tilde{\theta}_b}{dt} - \Gamma_1 \left(\frac{dz_b}{dt} - \tilde{w} \right) \right] + \frac{1}{2} \Delta z_1^2 \frac{d}{dt}\Gamma_1$$

This equation will be used subsequently to eliminate $F_{1\theta L}$ from 5.3.6 (see 5.3.16). However it is helpful to interpret 5.3.14 first, and relate it to the discussion in earlier chapters. We see that given $\Gamma_1, \frac{d\Gamma_1}{dt}, \Delta z_1$ from the lapse rate model this equation gives $F_{1\theta L}$ since $F_{b\theta}, d\tilde{\theta}_b/dt, dz_b/dt$ were determined by equations for the sub-cloud layer. Indeed if we substitute from 4.6.10

4.6.10 $$\frac{d\tilde{\theta}_b}{dt} = \left(\frac{dz_b}{dt} - \tilde{w}_b - w_{Db} \right) \Gamma_1$$

we can re-express 5.3.14 in terms of the convective mass flux through cloud-base w_{Db}, determined in chapter 4.

5.3.15 $$\frac{F_{b\theta}}{\rho c_p} - \frac{F_{1\theta L}}{\rho c_p} = -\Delta z_1 \left(w_{Db}\Gamma_1 - \frac{1}{2}\Delta z_1 \frac{d}{dt}\Gamma_1 \right)$$

Finally we can recover Eq.3.10.6 by observing that the term $d\Gamma_1/dt$ is associated with a variation of w_D with height. Since

3.7.5 $$\frac{\partial \tilde{\theta}}{\partial t} = -(\tilde{w} + w_D)\Gamma_1$$

differentiating with respect to z, gives

$$\frac{d}{dt}\Gamma_1 = -\Gamma_1 \frac{\partial}{\partial Z} W_D$$

since $\tilde{W}$ has been assumed constant, and Γ_1, is a function of time only. Hence

$$W_D(Z) = W_{Db} - \frac{Z - Z_b}{\Gamma_1} \frac{d}{dt}\Gamma_1$$

So 5.3.15 can be re-written

3.10.6 $$\frac{F_{b\theta}}{\rho c_p} - \frac{F_{1\theta L}}{\rho c_p} = -\int_{Z_b}^{Z_1} W_D(Z)\, \Gamma_1\, dZ$$

We have shown how 5.3.14 can be re-expressed in terms of the mass flux model. However this is not how it will be used in this chapter. The lapse rate model will give $d\Gamma_1/dt$ directly from $d\bar{\Gamma}/dt$ (see Eq.5.3.19), and hence we shall be able to eliminate $F_{1\theta L}$ from 5.3.5 and 5.3.6. It is possible to test whether the value of $d\Gamma_1/dt$ demanded by the assumed instantaneous equilibrium of lapse rate structure gives an unrealistic value of $\partial W_D/\partial Z$. This requires further study of individual cumuli.

Solution for dZ_1/dt

Returning to 5.3.14, we may eliminate $F_{1\theta L}$ from 5.3.6 (the other budget equation), using also the definitions 5.3.9, 5.3.10, 5.3.12 and 5.2.1, to give dZ_1/dt.

5.3.16 $$\frac{dZ_1}{dt} = \frac{\Delta Z}{(\Gamma_2 - \Gamma_1)\Delta Z_2}\left\{\frac{d\bar{\theta}_b}{dt} + \tilde{W}\bar{\Gamma} - \Gamma_1 \frac{dZ_b}{dt}\right\} + \frac{1}{(\Gamma_2 - \Gamma_1)\Delta Z_2}\left\{\frac{\Delta Z_1^2}{2}\frac{d\Gamma_1}{dt} + \frac{\Delta Z_2^2}{2}\frac{d\Gamma_2}{dt} - \frac{F_{b\theta}}{\rho c_p}\right\}$$

This equation looks complicated, but qualitatively it represents the downward heat transfer which cools layer 2 and warms layer 1, lifting the level Z_1 between the two layers. The second set of terms is small under some circumstances; when the lapse rate Γ_1, Γ_2 in the two layers do not change with time, typically we find $F_{b\theta} << F_{1\theta}$.

We note the following

(i) $\frac{d\bar{\theta}_b}{dt}$, $\frac{dZ_b}{dt}$, $F_{b\theta}$ are given by the solution of the sub-cloud layer problem. Given the large scale $\tilde{W}$, $\bar{\Gamma}$ (which determines Γ_1, Γ_2, $\Delta Z_1/\Delta Z_2$: see 5.2) and $d\bar{\Gamma}/dt$ (to determine $d\Gamma_1/dt$, $d\Gamma_2/dt$), we may find dZ_1/dt. The equation for $\bar{\Gamma}$ will follow.

(ii) It is clear that rising cloud-base and subsidence ($\tilde{W}$ negative) both reduce dZ_1/dt. $\frac{d\tilde{\theta}_b}{dt}$ decreases as the depth of the sub-cloud layer increases, being related to $d\overline{\tilde{\theta}}/dt$ and $\frac{d\Delta\theta}{dt}$ (4.6.11).

(iii) 5.3.16 can be re-arranged for comparison with 5.3.14 and with the subsequent discussion made in terms of W_{Db}

5.3.17
$$\left(\frac{dZ_1}{dt} - \tilde{W}\right)(\Gamma_2 - \Gamma_1)\Delta Z_2 = \Delta Z\left\{\frac{d\tilde{\theta}_b}{dt} - \Gamma_1\left(\frac{dZ_b}{dt} - \tilde{W}\right)\right\} + \begin{matrix}\text{smaller}\\ \text{terms}\end{matrix}$$
$$= -\Delta Z\, W_{Db}\,\Gamma_1 + \begin{matrix}\text{smaller}\\ \text{terms}\end{matrix}$$

Mathematically the additional dependence of dZ_1/dt on $\tilde{W}$ as well as on W_{Db} (itself $\tilde{W}$ dependent) is clear. Physically this equation is a statement about the downward transfer of heat. Neglecting $d\Gamma_1/dt$, $d\Gamma_2/dt$, $F_{b\theta}$

$$F_{1\theta L} = \rho c_p W_{Db}\,\Gamma_1\,\Delta Z_1$$

If $\tilde{W} = 0$, we obtain the very simple case shown in Fig. 5.3.2 (see also Fig. 3.10)

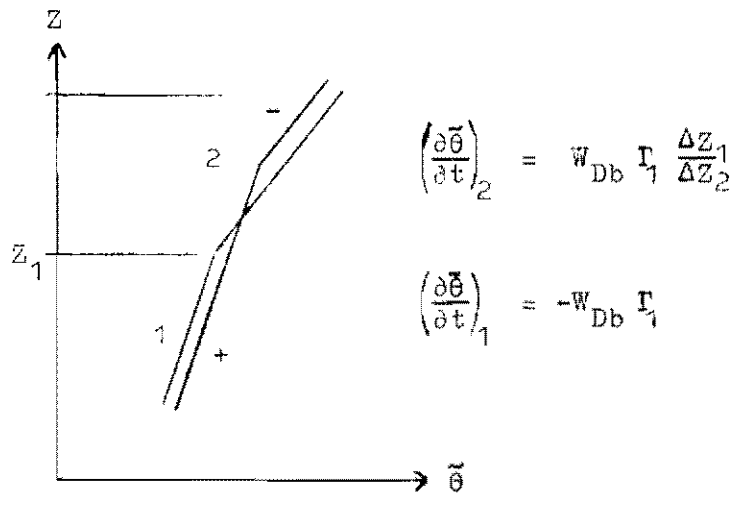

Fig. 5.3.2

For continuity of temperature at Z_1

$$(\Gamma_2 - \Gamma_1)\,\frac{dZ_1}{dt} = \left(\frac{\partial\tilde{\theta}}{\partial t}\right)_1 - \left(\frac{\partial\tilde{\theta}}{\partial t}\right)_2$$

After substituting for $\left(\frac{\partial\tilde{\theta}}{\partial t}\right)_1$, $\left(\frac{\partial\tilde{\theta}}{\partial t}\right)_2$ we recover 5.3.17 for $\tilde{W} = 0$.

Summary of heat budget:

Given $F_{b\theta}$, $d\tilde{\theta}_b/dt$, dZ_b/dt , and $\tilde{W}$

eq. 5.3.14 gives $F_{1\theta L}$

eq. 5.3.16 gives dZ_1/dt

provided the lapse rate model is used to relate $\Gamma_1, \Gamma_2, \frac{\Delta Z_1}{\Delta Z_2}$ to $\bar{\Gamma}$ at an instant in time. An equation for $\bar{\Gamma}$ as a function of time is therefore necessary.

Equation for $d\bar{\Gamma}/dt$

This connects the deepening of the cumulus layer, subsidence, the undisturbed stratification above the cumulus layer and the sub-cloud layer. The boundary condition at the top of the cumulus layer is

5.3.18 $$\frac{d\tilde{\theta}_2}{dt} = \Gamma_3\left(\frac{dZ_2}{dt} - \tilde{W}\right)$$

Whence it follows (from definitions 5.2.1, 5.3.13 and 5.3.7 to 5.3.10) that

5.3.19 $$\frac{d}{dt}(\bar{\Gamma}\,\Delta Z) = \Gamma_3\left(\frac{dZ_2}{dt} - \tilde{W}\right) - \frac{d\tilde{\theta}_b}{dt}$$

(Compare 4.3.7)

The model is now closed.

$\tilde{W}, \Gamma_3$ are assumed known.

dZ_2/dt, $d\Delta Z/dt$ are linked through the lapse rate model to $\bar{\Gamma}$, dZ_1/dt (5.3.16) and dZ_b/dt .

dZ_b/dt, $d\tilde{\theta}_b/dt$ are solutions of the sub-cloud layer problem.

It follows that one can integrate 5.3.19 to give $\bar{\Gamma}$ as a function of time, and hence Γ_1 , Γ_2 $\frac{\Delta Z_1}{\Delta Z_2}$ as functions of time, using the equations of 5.2. Given $\frac{\Delta Z_1}{\Delta Z_2}$, ΔZ is then found by integrating $\frac{dZ_1}{dt}$, and dZ_b/dt to give ΔZ_1 .

It is illuminating to expand 5.3.19

5.3.20 $$\Delta Z\,\frac{d}{dt}\bar{\Gamma} = (\Gamma_3 - \bar{\Gamma})\frac{d}{dt}Z_2 - \frac{d\tilde{\theta}_b}{dt} + \bar{\Gamma}\frac{dZ_b}{dt} - \tilde{W}\Gamma_3 .$$

This is an important equation as the magnitude of $\bar{\Gamma}$ was a sensitive control of Γ_1, Γ_2 in the model of 5.2. Increase of $\bar{\Gamma}$ (for constant Γ_{c1}) increased $(\Gamma_2 - \Gamma_1)$, which reduces dz_1/dt (see 5.3.16).

Interpretation of 5.3.20

(a) $\frac{d\tilde{\theta}_b}{dt}$ given by the sub-cloud layer problem, is related to the warming of the sub-cloud layer (as $\Delta\theta$ is nearly constant). This term reduces $\bar{\Gamma}$ continuously ('destabilising').

(b) $\tilde{w}$ negative (subsidence), increases $\bar{\Gamma}$ ('stabilising').

(c) $\frac{d}{dt}z_b$ positive (rise of cloud-base), increases $\bar{\Gamma}$ ('stabilising').

(d) $\frac{d}{dt}z_2$ positive, increases $\bar{\Gamma}$ if $\Gamma_3 > \bar{\Gamma}$ and vice versa.

The feedback here is complicated, but we see there may be a tendency in diurnal convection for $\bar{\Gamma}$ to increase while cloud-base is rising, and then to decrease in the afternoon as cloud-base stops rising. As $\bar{\Gamma}$ decreases towards Γ_{c1}, the model Γ_2 tends to Γ_1, so that $\frac{dz_1}{dt}$ increases rapidly. However once the cumulus layer becomes deeper than a few km, the clouds will begin to precipitate, and this model will cease to be valid.

There is a steady state solution for $\bar{\Gamma}$ given, for z_b constant, by

5.3.21 $$\frac{d\tilde{\theta}_b}{dt} = (\Gamma_3 - \bar{\Gamma})\frac{d}{dt} z_2 - \tilde{w}\Gamma_3$$

This is a valid solution only if it is attained for a value of $\bar{\Gamma} > \Gamma_{c1}$. It may be relevant to the lifting of the trade inversion, although the radiative fluxes must first be added. Radiative cooling acts in the sense of continuously increasing $\bar{\Gamma}$, by reducing $d\tilde{\theta}_b/dt$ more than $d\tilde{\theta}_2/dt$.

Summary of 5.2 and 5.3

In the cumulus layer 13 undetermined variables have been used.

Γ_1, Γ_2, $\overline{\Gamma}$, ΔZ_1, ΔZ_2, ΔZ, Z_1, Z_2, F_{10L}, $\tilde{\theta}_1$, $\tilde{\theta}_2$, $\overline{\tilde{\theta}}^1$, $\overline{\tilde{\theta}}^2$

There are 13 independent equations and definitions:

5.2.9, 6.2.11	(lapse rate model)
5.3.5, 5.3.6	(heat budget)
5.2.1 and 5.3.7 to 5.3.13	(definitions)
5.3.19	($\overline{\Gamma}$: upper boundary condition)

This set is soluble, giving all variables; in particular

$$\overline{\Gamma}, \Gamma_1, \Gamma_2, Z_1, Z_2$$

as functions of

$$d\theta_b/dt, dZ_b/dt, F_{b\theta}, \tilde{W}, \Gamma_3 \text{ and time.}$$

Equations for the cloud-base variables were discussed in chapter 4; $\tilde{W}$, and Γ_3 in the 'free' atmosphere must be known.

5.4 Time Development of the Cumulus Layer

Part II : Water Vapour Structure

In this section we examine the time development of the water vapour distribution of the cumulus layer. As discussed in 4.8, we require $(\partial\tilde{r}/\partial Z)_1$ in order to complete the water vapour balance of the sub-cloud layer. This in turn is essential over land to find the surface fluxes of sensible heat and water vapour.

The general approach will be closely similar to that of 5.3. We consider a simple two-layer model in which Z_1, Z_2 are now determined (by 5.2 and 5.3), and the unknowns are $(\partial\tilde{r}/\partial Z)_1$, $(\partial\tilde{r}/\partial Z)_2$, $\overline{\tilde{r}}^1$, $\overline{\tilde{r}}^2$ etc. Diagramatically

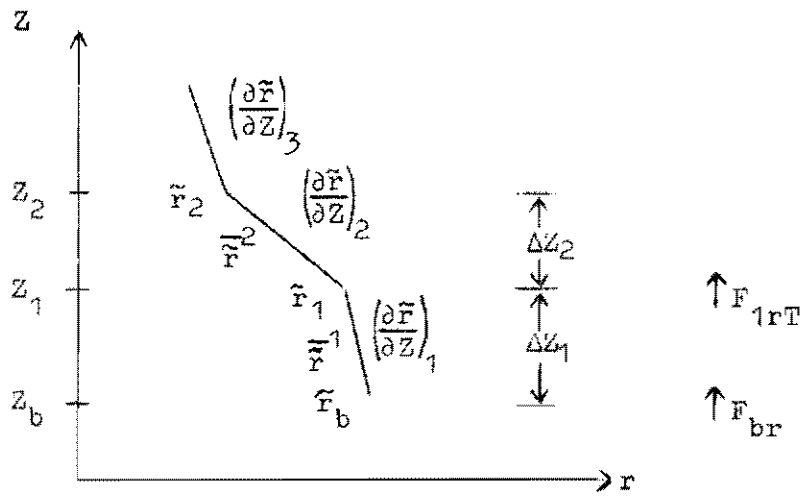

Fig. 5.4.1

For simplicity the variation of air density in the cumulus layer will be neglected, so that the budget equations for r in the two layers (the analogues of 5.3.5 and 5.3.6) are

5.4.1
$$\Delta Z_1 \frac{d}{dt}\overline{\tilde{r}}^1 = \frac{F_{br}}{\rho L} - \frac{F_{1rT}}{\rho L} + (\tilde{r}_1 - \overline{\tilde{r}}^1)\frac{d}{dt}Z_1 - (\tilde{r}_b - \overline{\tilde{r}}^1)\frac{d}{dt}Z_b - \tilde{W}\left(\frac{\partial\tilde{r}}{\partial Z}\right)_1 \Delta Z_1$$

5.4.2
$$\Delta Z_2 \frac{d}{dt}\overline{\tilde{r}}^2 = \frac{F_{1rT}}{L} + (\tilde{r}_2 - \overline{\tilde{r}}^2)\frac{d}{dt}Z_2 - (\tilde{r}_1 - \overline{\tilde{r}}^2)\frac{d}{dt}Z_1 - \tilde{W}\left(\frac{\partial\tilde{r}}{\partial Z}\right)_2 \Delta Z_2$$

where
$$\Delta Z_1\,\overline{\tilde{r}}^1 = \int_{Z_b}^{Z_1} \tilde{r}\, dZ$$

$$\Delta Z_2\,\overline{\tilde{r}}^2 = \int_{Z_1}^{Z_2} \tilde{r}\, dZ$$

$$F_{br}/\rho L = (\widetilde{W'r'})_{Z_b}$$

$$F_{1rT}/\rho L = \left\{W'(r' + r'_L)\right\}_{Z_1}$$

As in 3.3.3, we neglect changes in $\bar{r}_L$ compared with those of $\bar{r}$. An equation for F_{br} has already been derived (4.8.3) but F_{1rT} is an unknown. We shall again relate $\tilde{r}_b$, $\bar{\tilde{r}}^1$ and their time derivatives, to the vertical gradient of $\tilde{r}$ through the definitions

5.4.3 $$\bar{\tilde{r}}^1 - \tilde{r}_b = \tfrac{1}{2}(\partial\tilde{r}/\partial Z)_1 \Delta Z_1$$

5.4.4 $$\tilde{r}_1 - \bar{\tilde{r}}^1 = \tfrac{1}{2}(\partial\tilde{r}/\partial Z)_1 \Delta Z_1$$

5.4.5 $$\bar{\tilde{r}}^2 - \tilde{r}_1 = \tfrac{1}{2}(\partial\tilde{r}/\partial Z)_2 \Delta Z_2$$

5.4.6 $$\tilde{r}_2 - \bar{\tilde{r}}^2 = \tfrac{1}{2}(\partial\tilde{r}/\partial Z)_2 \Delta Z_2$$

The validity of this two-layer model for the water vapour balance will be commented on later.

From section 4.8, we have the pair of relationships (here we have assumed ρ, $\bar{\tilde{W}}$ constant above Z_b)

4.8.3 $$\frac{F_{br}}{\rho L} = -W_{Db}(\bar{r}_o - \tilde{r}_b)$$

4.8.10 $$\frac{d}{dt}\tilde{r}_b = \left(\frac{\partial\tilde{r}}{\partial Z}\right)_1 \left(\frac{d}{dt}Z_b - \bar{\tilde{W}} - W_{Db}\right) + \frac{F_{br}}{\rho L}\left(\frac{1}{S} - \frac{1}{W_{Db}}\frac{\partial}{\partial Z}W_{Db}\right)$$

There is also the upper boundary condition (compare 5.3.18)

5.4.7 $$\frac{d}{dt}\tilde{r}_2 = \left(\frac{\partial\tilde{r}}{\partial Z}\right)_3 \left(\frac{d}{dt}Z_2 - \bar{\tilde{W}}\right)$$

We consider, for the purposes of this section, that we have the 9 undetermined variables

$$F_{br},\ F_{1rT},\ \tilde{r}_b,\ \tilde{r}_1,\ \tilde{r}_2,\ \bar{\tilde{r}}^1,\ \bar{\tilde{r}}^2,\ \left(\frac{\partial\tilde{r}}{\partial Z}\right)_1,\ \left(\frac{\partial\tilde{r}}{\partial Z}\right)_2$$

We suppose the following are known:

r_o (which over land requires simultaneous solution of the sub-cloud layer),

$\bar{\tilde{W}}$, $(\partial\tilde{r}/\partial Z)_3$ from the large-scale data, and

$\frac{d}{dt}Z_b$, W_{Db}, $\frac{\partial}{\partial Z}W_{Db}$, $\frac{d}{dt}Z_1$, $\frac{d}{dt}Z_2$ from 4.7, 5.2 and 5.3.

The set of 9 equations and definitions

5.4.1, 5.4.2	(water vapour budget)
4.8.3, 4.8.10	(lower boundary conditions)
5.4.7	(upper boundary condition)
5.4.3 to 5.4.6	(definitions)

can thus be solved for the 9 undetermined variables, given an initial set of values for $\tilde{r}_b$, $\tilde{r}_1$, $\tilde{r}_2$, $(\partial\tilde{r}/\partial Z)_1$, $(\partial\tilde{r}/\partial Z)_2$. In particular we can find

$$(\partial\tilde{r}/\partial Z)_1 \ , \ (\partial\tilde{r}/\partial Z)_2 \qquad \text{as functions of time.}$$

The procedure is straightforward .

Starting with a set of initial values for $(\partial\tilde{r}/\partial Z)_1$, $(\partial\tilde{r}/\partial Z)_2$, $\tilde{r}_2$, we have $\tilde{r}_b$ and F_{br} (knowing $\tilde{r}_o$, Z_1, Z_2). By combining 5.4.1 to 5.4.6 , we obtain the analogue of 5.3.16 (or 5.3.17).

5.4.8
$$\left(\frac{d}{dt}Z_1 - \tilde{W}\right)\left\{\left(\frac{\partial\tilde{r}}{\partial Z}\right)_2 - \left(\frac{\partial\tilde{r}}{\partial Z}\right)_1\right\}\Delta Z_2 = \Delta Z\left\{\frac{d}{dt}\tilde{r}_b - \left(\frac{\partial\tilde{r}}{\partial Z}\right)_1\left(\frac{d}{dt}Z_b - \tilde{W}\right)\right\} - \frac{F_{br}}{\rho L} + \frac{1}{2}\Delta Z_1^2\frac{d}{dt}\left(\frac{\partial\tilde{r}}{\partial Z}\right)_1 + \frac{1}{2}\Delta Z_2^2\frac{d}{dt}\left(\frac{\partial r}{\partial Z}\right)_2$$

A second equation in the time derivatives of $\left(\frac{\partial\tilde{r}}{\partial Z}\right)_1$, $\left(\frac{\partial\tilde{r}}{\partial Z}\right)_2$ is constructed from 5.4.3 to 5.4.6 and 5.4.7. This is the analogue of 5.3.19

5.4.9
$$\left(\frac{\partial\tilde{r}}{\partial Z}\right)_3\left(\frac{d}{dt}Z_2 - \tilde{W}\right) = \frac{d}{dt}\tilde{r}_b + \frac{d}{dt}\left\{\left(\frac{\partial\tilde{r}}{\partial Z}\right)_1\Delta Z_1 + \left(\frac{\partial\tilde{r}}{\partial Z}\right)_2\Delta Z_2\right\}$$

$d\tilde{r}_b/dt$ can be eliminated from 5.4.8 and 5.4.9 using 4.8.10 and the resulting pair can be solved simultaneously for $\frac{d}{dt}\left(\frac{\partial\tilde{r}}{\partial Z}\right)_1$ $\frac{d}{dt}\left(\frac{\partial\tilde{r}}{\partial Z}\right)_2$. The time development of the water vapour structure of the model is thus uniquely determined. One can integrate forward in time from any given initial state (which may be before the onset of convection).

The weakness of this model lies in the specification of a two layer straight-line approximation to the water vapour distribution, in which $(\partial\tilde{r}/\partial Z)_1$, $(\partial\tilde{r}/\partial Z)_2$ are functions of time only. We need only to specify $\frac{d\tilde{r}_b}{dt}$ to uniquely determine the time development, and implicitly the distribution

of the water vapour input to the cumulus layer. This may well be too restrictive. It may be necessary to specify both the stratification and the input of water vapour in more detail. The model used in 5.2 to obtain a thermodynamic relationship for the rise and fall of a typical cloud could be extended, and its implications for the input of water vapour to the cumulus layer examined.

As we have in this model specified the water vapour input by the cumulus clouds only through eq. 4.8.10, this equation becomes critical, and deserves more rigorous examination both theoretically and observationally. One should consider the input of water vapour to the cumulus layer over the whole life cycle of a cloud.

5.5 Summary

In chapters 3, 4 and 5 a simple closed model of cumulus convection has been developed. The main convective interactions of the non-precipitating boundary layer have been outlined and made quantitative. The effects of radiative transports and vertical shear in the wind have been omitted. Most attention has been paid to the physics and structure of the cumulus layer; the treatment of the dry convective layer has been relatively brief, but can readily be extended.

The main predictions of chapter 5 have been the following:

(1) the dependence of lapse rates Γ_1, Γ_2 in the cumulus layer on $\bar{\Gamma}$ the mean lapse rate from cloud base to the top of the cumulus layer (see 5.2). For example, we noted the development of an inversion for large $\bar{\Gamma}$, and the requirement that $\bar{\Gamma} > \Gamma_{c1}$ during cumulus convection; both from a simple parameterisation of 'entrainment'.

(2) the dependence of $\bar{\Gamma}$ on $d\tilde{\theta}_b/dt, dZ_b/dt$ and $\tilde{W}$ (eq.5.3.20)

(3) the dependence of $\frac{dZ_1}{dt}$ on $d\tilde{\theta}_b/dt, dZ_b/dt$ and $\tilde{W}$ (eq. 5.3.16) (and dZ_2/dt)

(4) the time development of $(\partial\tilde{r}/\partial Z)_1, (\partial\tilde{r}/\partial Z)_2$ (see 5.4). This model for the water vapour structure is considered less satisfactory than that for the temperature structure.

In the next chapter we shall examine some data, principally from a day of convection in the tropics, in the light of this model, and test some of its predictions.

Chapter 6 Observational Evidence

6.1 Introduction

The model proposed in the last three chapters predicts the magnitudes of the transports and the stratification in the convective layer in a wide range of meteorological situations. The available data needs to be re-examined in the light of the relationships and predictions that have been derived, and this is a major task. In this chapter only some limited aspects will be compared with observation. These cannot adequately confirm the theory, but indicate

(i) that the theory gives insight into the stratifications and transports observed in certain situations, bearing in mind the considerable uncertainties in the data;

(ii) what methods might be used to test more thoroughly parts of the theory .

We shall examine principally one day of cumulus convection in the tropics. The temperature stratification will be analysed using the model of 5.2, and W_{Db} will be estimated from the time development of both the sub-cloud layer and the cumulus layer. In 6.3 the case of cumulus convection beneath an inversion will also be considered briefly.

NOTE (2012)

This is a rather cavalier analysis based on a single day of data!

6.2 Analysis of the data

The data used were obtained on 3rd September 1969 at Anaco, Venezuela during Project Vimhex: a joint undertaking between Colorado State University and the Venezuelan Meteorological Service. The following were available

(i) 5 radiosonde ascents at 0730, 1000, 1200, 1400, 1600 (local time)

(ii) hourly screen measurements of T, T_w

(iii) surface radiation data: downward and reflected short wave and net radiation

(iv) time lapse film from 1515 to 1700 (local time). This has not been used quantitatively.

The soundings were plotted at levels up to 100mb (the tropopause was at 125mb), and then adjusted to give a constant mean temperature from the surface to 100mb as follows. The heights of the 100mb surface above a fixed pressure level (989mb) were made equal by adding a constant temperature correction δT to the sounding at all levels (see table 6.2.1).

Table 6.2.1

Local time	Z=0 at 989 mb Z (100 mb)	δZ	$\bar{T}$=260° K δT
0730	16554 m		
1000	(16554) m		
1200	16596 m	+ 42 m	- 0.7° C
1400	16498 m	- 56 m	+ 0.9° C
1600	16554 m		

Comments

(1) The 100mb height given by the sounding at 1000 hours is an extrapolated estimate: the sounding reached only 130mb, but it closely corresponded to the 0730 sounding up to this height.

(2) The above procedure is open to criticism. Its justification is that there is no systematic trend during the day. Further

the sounding at 1400 hrs when uncorrected is wholly cooler, and the sounding at 1200 hrs noticeably warmer, than the soundings at 1000 hrs and 1600 hrs, throughout the depth of the troposphere.

(3) The procedure affects estimates of the heat budget of the convective layer at two-hourly intervals, and of the surface fluxes. We shall find that with these simple corrections, the mean temperature $\overline{\tilde{\theta}}$ of the sub-cloud layer increases uniformly in a plausible manner throughout the day. The surface heat flux estimates are also reasonable.

Smoothing of the data

Some smoothing of the data was first necessary. The procedure used was as follows.

Surface data

From the hourly screen values of temperature and wet bulb temperature were calculated the surface r_o. The screen values of T_o, r_o were plotted against time, together with the radiosonde surface data from a different site about a km away, and then smoothed: see Fig. 6.2.1. The surface radiosonde data, particularly mixing ratio, did not fit the screen data very well, and were mostly ignored. This raises some doubts about the representivity of the surface data, which cannot here be resolved, as data representative of the surrounding countryside (wooded grassland) are not readily available.

Sub-cloud layer

Potential temperature and mixing ratio were plotted against height, and smoothed by drawing a straight line through the points below cloud-base (Figs. 6.2.2 and 6.2.3). There is a certain subjectivity here: $\partial\theta/\partial Z$ was smoothed to the dry adiabatic, or a slightly stable lapse rate, and $\partial r/\partial Z$ was smoothed so that r decreased slowly with height. From this smoothed data $\overline{\tilde{\theta}}$, $\overline{\tilde{r}}$ could be estimated. These values are tabulated as tables 6.5.2 and 6.5.3. In this chapter we shall assume measurements of θ, r are representative of horizontal means $\tilde{\theta}$, $\tilde{r}$.

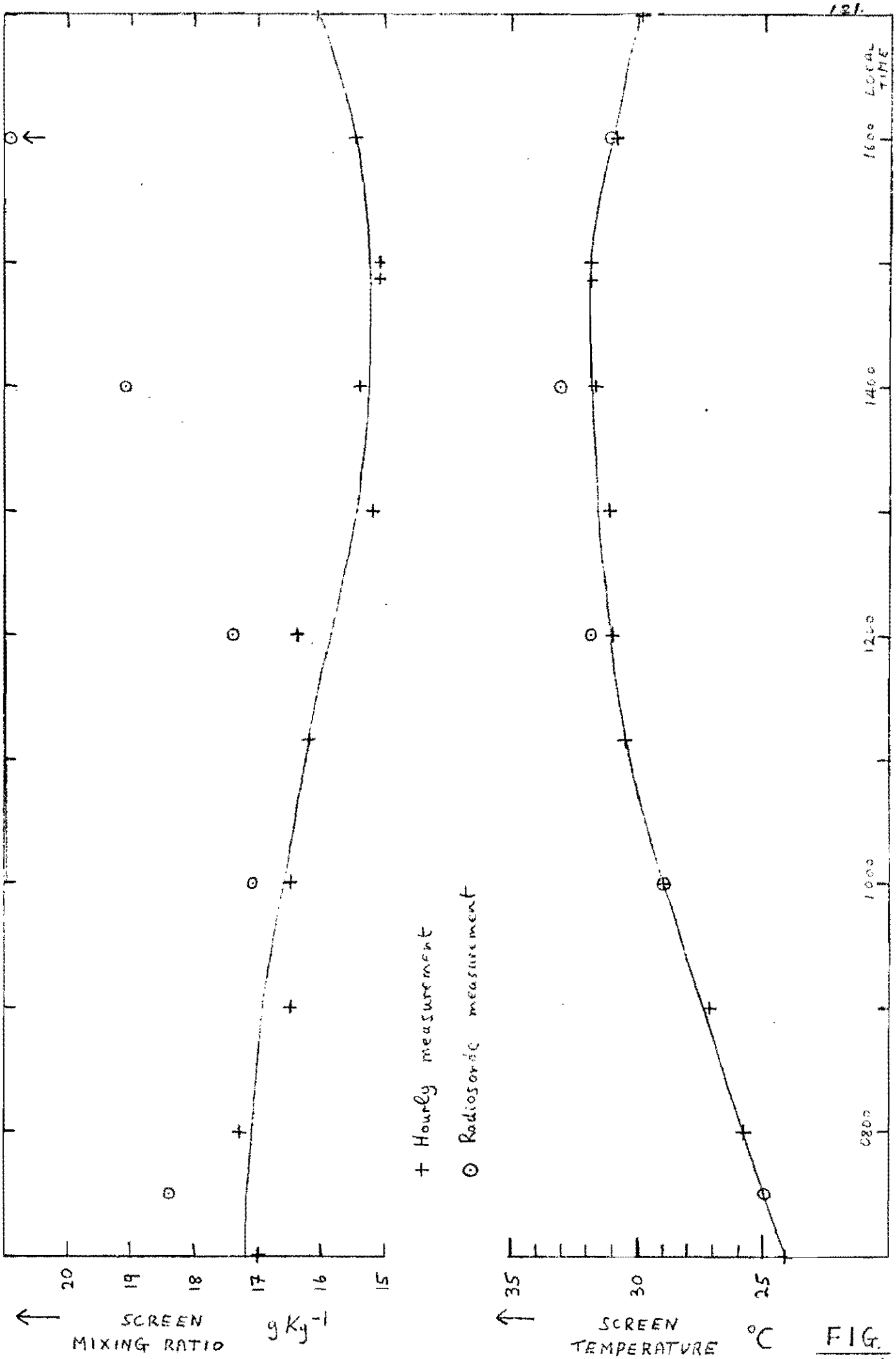
SCREEN MIXING RATIO
g Kg⁻¹
20
19
18
17
16
15
SCREEN TEMPERATURE
°C
35
30
25
0800
1000
1200
1400
1600
LOCAL TIME
+ Hourly measurement
⊙ Radiosonde measurement

FIG. 6.2.1

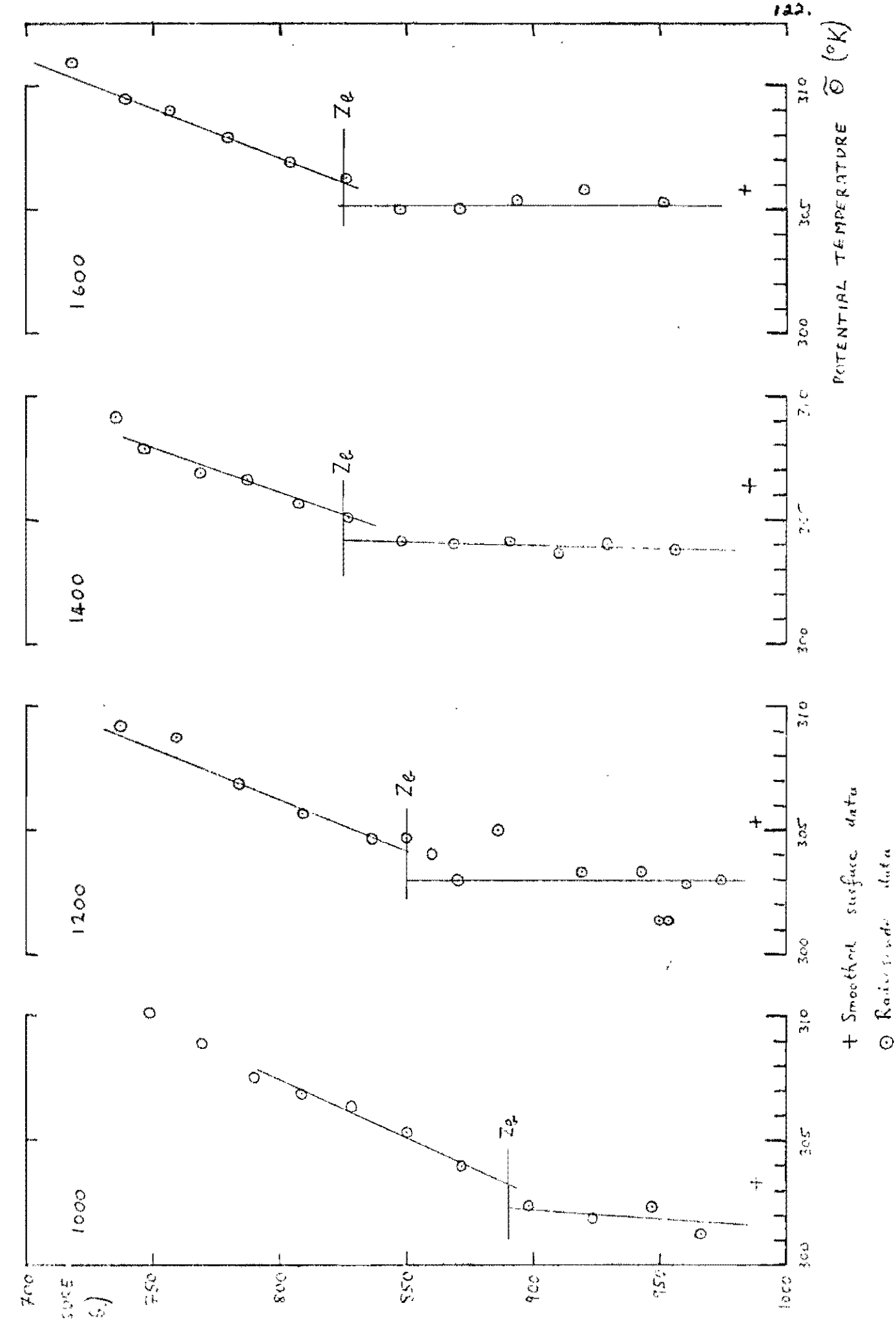
1600
1400
1200
1000
Ze
Ze
Ze
Ze
300
305
310
POTENTIAL TEMPERATURE $\bar{\theta}$ (°K)
700
750
800
850
900
950
1000
PRESSURE (mb)
+ Smoothed surface data
⊙ Radiosonde data

FIG. 6.2.2.

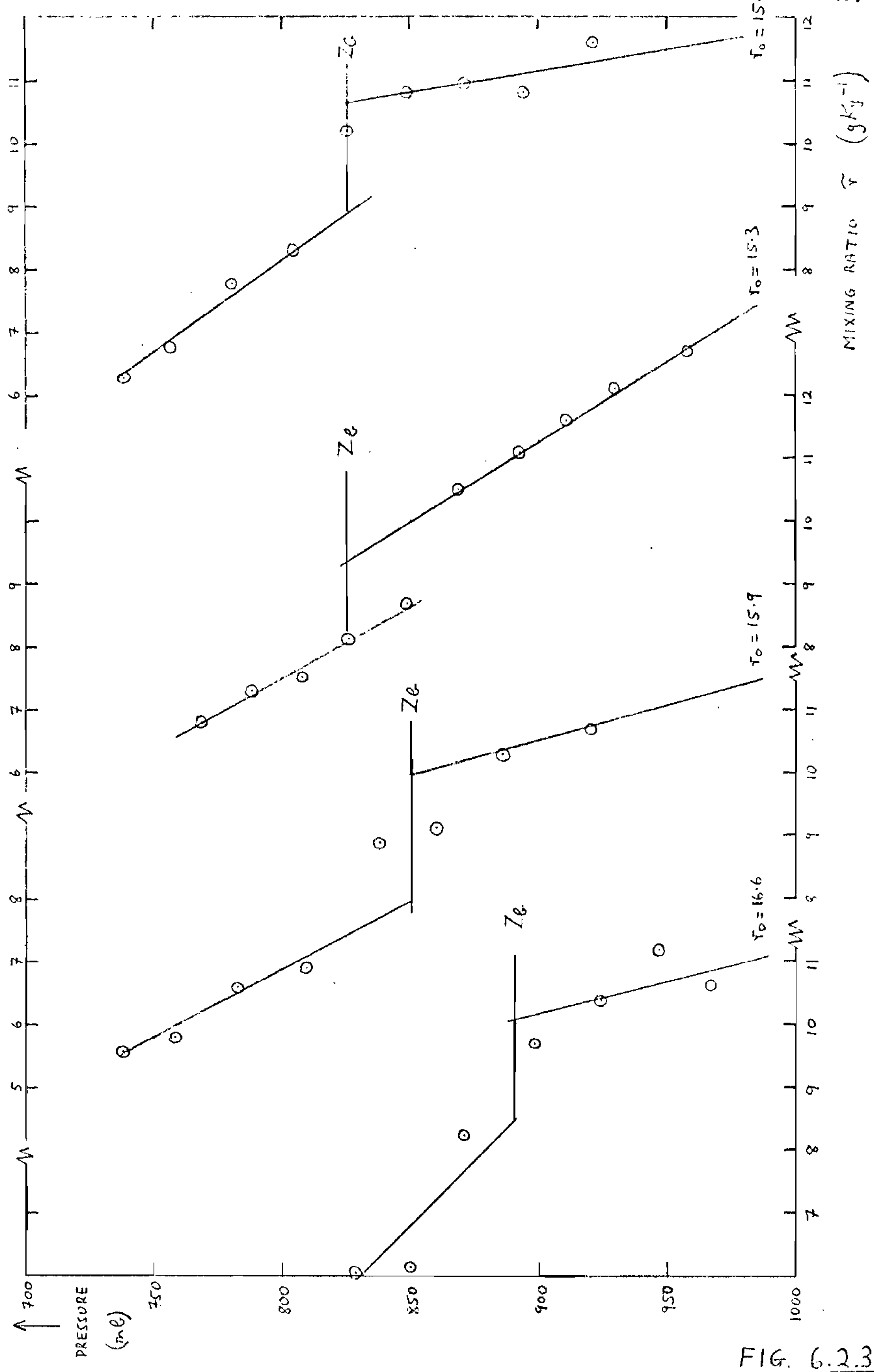
PRESSURE (mb)
700
750
800
850
900
950
1000
MIXING RATIO r (gKg⁻¹)
Ze
r₀ = 15.5
r₀ = 15.3
r₀ = 15.9
r₀ = 16.6

FIG. 6.2.3

Cumulus Layer

By a similar procedure the temperature and mixing ratio in the cumulus layer above cloud-base were smoothed, and the line extended back to cloud-base. Thus values could be obtained for $\tilde{\theta}_b$, $\tilde{r}_b$, and hence $\Delta\theta$, and Δr defined as

$$\Delta\theta = \tilde{\theta}_b - \overline{\tilde{\theta}}$$
$$\Delta r = \tilde{r}_b - \overline{\tilde{r}}$$

(see also tables 6.5.2 and 6.5.3).

Structure of soundings

The soundings are all structurally consistent with the cumulus model of earlier chapters. They show the following features: see Figs. 6.2.2, 6.2.3.

(i) A superadiabatic layer, with a fall of $\tilde{\theta}$ (of about 1 to 2° C) and $\tilde{r}$ (of about 2 to 5 gKg^{-1}) from the surface to the first radiosonde data point (about 20mb) above the surface.

(ii) A dry convective layer, depth about one km, in which $\tilde{\theta}$ was constant, or increased slightly with height (at about 0.5 °C km^{-1} and $\tilde{r}$ fell slowly (about -1.5 $gkg^{-1}km^{-1}$). (Thus $\tilde{\theta}_v$ increased slightly with height at about 0.2 °Ckm^{-1}). This layer extended up to a transition layer (iii).

(iii) A transition layer of depth about 200m, in which there was a marked increase of $\tilde{\theta}$, and fall of $\tilde{r}$. The top of this transition layer was taken as the level of the cloud-base. The lifting condensation level of the air at screen level was typically some 50 to 100m lower. However it should be appreciated that θ_w in the air ascending through cloud-base is a degree or more lower than θ_w at screen level, because of dilution in the sub-cloud layer, and the existence of the superadiabatic layer.

(iv) A cumulus layer, whose depth increased during the day to several km. In the lower part of this layer the lapse rate $\frac{\partial\tilde{\theta}}{\partial Z}$ was about +4° Ckm^{-1} and $\frac{\Gamma}{\Gamma_w}$ was about 0.7, consistant with earlier studies of cumulus convection (Ludlam, 1966). A detailed comparison of the lapse rate structure in the cumulus layer with the model of 5.2 will be given in the next section 6.3.

6.3 Temperature stratification in the cumulus layer

In this section we shall examine the lapse-rate model proposed in 5.2. The agreement with observation is encouraging if we assume $E = 0.4$, $D = 0.5$. In addition to these parameters, the model needs as input ΔZ, $\bar{\Gamma}$ and Γ_{c1}. From these are predicted ΔZ_1, ΔZ_2, Γ_1, Γ_2, and one may then consider how well this model structure agrees with a given sounding.

This will be accomplished subjectively by dividing the given cumulus sounding by eye into two layers, and measuring the average lapse rates. Z_1 estimated in this way essentially corresponds to the minimum in θ_s on the sounding. This proves a satisfactory method as the visual and model two-layer approximations to the sounding agree closely. We shall also plot some actual soundings, and their model equivalent in $\theta_s - p$ co-ordinates (Fig.6.3.1) so that a visual comparison can be made.

Procedure:

An average value for Γ_{c1}, the parcel lapse rate for saturated air ascending with dilution, was estimated for the interval Z_b to Z_1, from eq. 3.4.6.

3.4.6
$$\Gamma_{c1} = \Gamma_w - \frac{L\theta}{c_p T} \frac{(r_s(T_c) - r_e)}{K S}$$

An average value of $r_s(T_c) - r_e$ for this height interval was estimated from the sounding, and similar averages for K, Γ_w were calculated. The mixing scale length S was calculated from 5.2.4.

5.2.4
$$\frac{1}{S} = \frac{E}{\Delta Z_1}$$

Preliminary calculations indicated that $E = 0.4$ gave a good fit to the data, and this value was used (the effect of the variation of E is shown for the Anaco 1200 sounding). The value of ΔZ_1, in 5.2.4 is that determined by the model so that some iteration is necessary to determine self-consistant values for ΔZ_1, S and Γ_{c1} in the model. Only a single value of Γ_{c1} (as mentioned, an average for the layer Z_b to Z_1) was used, but the approximation involved is smaller than the scatter in the data.

Thus, taking $\Delta Z, \bar{\Gamma}, r_s - r_e$ from the sounding, the model has been used to predict $\Delta z_1, \Delta z_2, \Gamma_1$ and Γ_2. A comparison is then made with the sounding.

Anaco Data

For the 0730 sounding, data ~~was~~ were available only at 50mb intervals, and as the convection then occupied only a shallow layer, there was insufficient vertical resolution to test the model. This sounding was not used in this or the subsequent sections 6.4 and 6.5.

Data for the other four soundings is tabulated in table 6.3.1, and the calculated model structure is compared with the two-layer visual approximation to the sounding in table 6.3.2. In Fig. 6.3.1 the actual sounding (black dots) can be compared with the model solution (straight lines). It is important to appreciate that the model solution depends on the choice of $z_b, \theta_b, z_2, \theta_2$ from which z_1, and the lapse rates are predicted. The scatter in the individual points is considerable and in particular we note that the choice of z_2 for the 1600 sounding at the top of a marked stable layer at 550mb is open to doubt. By this time the moist layer extended to 450mb and visual observations showed that a few cumulus clouds reached even higher levels. Indeed, within the next hour a few cumulonimbus had developed. Thus it is probable that by 1600 hrs the 2-layer model of the cumulus layer, with a single size scale of cloud, may have become an inadequate description: some clouds were beginning to precipitate, and were deepening until they were modifying the whole troposphere.

It can also be seen that the 1000 sounding, in which it is difficult to discern any 2-layer structure, does not fit the model. This sounding showed very low values for the mixing ratio in the cumulus layer (much lower than at 0730), which lead to the low value of Γ_{c1} in table 6.3.2, and which must therefore be regarded as suspect. Above 700mb the temperature soundings at 0730 and 1000 hrs agreed very closely, so this level has been taken as z_2.

It is clear from table 6.3.2 and Fig. 6.3.1 that the three soundings, at 1200, 1400 and to a lesser extent at 1600 hrs, fit the model quite well in

Table 6.3.1 Sounding data: Anaco: 3 September 1969

TIME	p_b	p_1	p_2	ΔZ	$\frac{T}{\theta}\bar{\Gamma}$	$\frac{T}{\theta}\bar{\Gamma}_w$	$r_s - r_e$	K	$\frac{L}{c_p}\frac{r_s - r_e}{K}$
1000	890	?	700	2025	+4.6	+5.4	8	3.3	5.8
1200	850	737	640	2370	+4.3	+5.4	6	3.1	4.6
1400	825	640	500	4075	+4.5	+5.2	5	2.8	4.3
1600	825	675	545	3410	+4.6	+5.2	4.5	2.8	3.9
Error	Subjectively assessed				±0.1	±0.1	±1	±0.1	±0.8
Units	mb	mb	mb	m	°C km^{-1}		g Kg^{-1}	-	°C

Table 6.3.2 Model Calculation compared with sounding

	INPUT			MODEL							SOUNDING			
TIME	ΔZ	$\frac{T}{\theta}\bar{\Gamma}$	$\frac{L}{c_p}\frac{r_s - r_e}{K}$	E	D	S	$\frac{T}{\theta}\Gamma_{c1}$	$\frac{T}{\theta}\Gamma_1$	$\frac{T}{\theta}\Gamma_2$	ΔZ_1	ΔZ_2	$\frac{T}{\theta}\Gamma_1$	$\frac{T}{\theta}\Gamma_2$	ΔZ_1	ΔZ_2
1000	2025	4.6	5.8	0.4	0.5	3.0	3.5	2.3	8.1	1215	810	~ 4.6	?	?	
1200	2370	4.3	4.6	0.3	0.6	3.4	4.1	3.9	4.5	1020	1350	3.6	5.2	1200	1170
				0.4	0.5	3.0	3.9	3.4	5.4	1220	1150				
				0.5	0.4	2.8	3.8	3.0	6.0	1360	1010				
1400	4075	4.5	4.3	0.4	0.5	5.8	4.4	4.1	4.9	1950	2125	4.1	5.0	2115	1960
1600	3410	4.6	3.9	0.4	0.5	4.7	4.3	3.8	5.5	1705	1705	3.6	5.6	1680	1730
Error		±0.1	±0.8					±0.2	±0.2	±50	±50	subjective			
Units	m	°C km^{-1}	°C	-	-	km	°C km^{-1}	°C km^{-1}		m	m	°C km^{-1}		m	m

• Sounding point

× Model Z_1

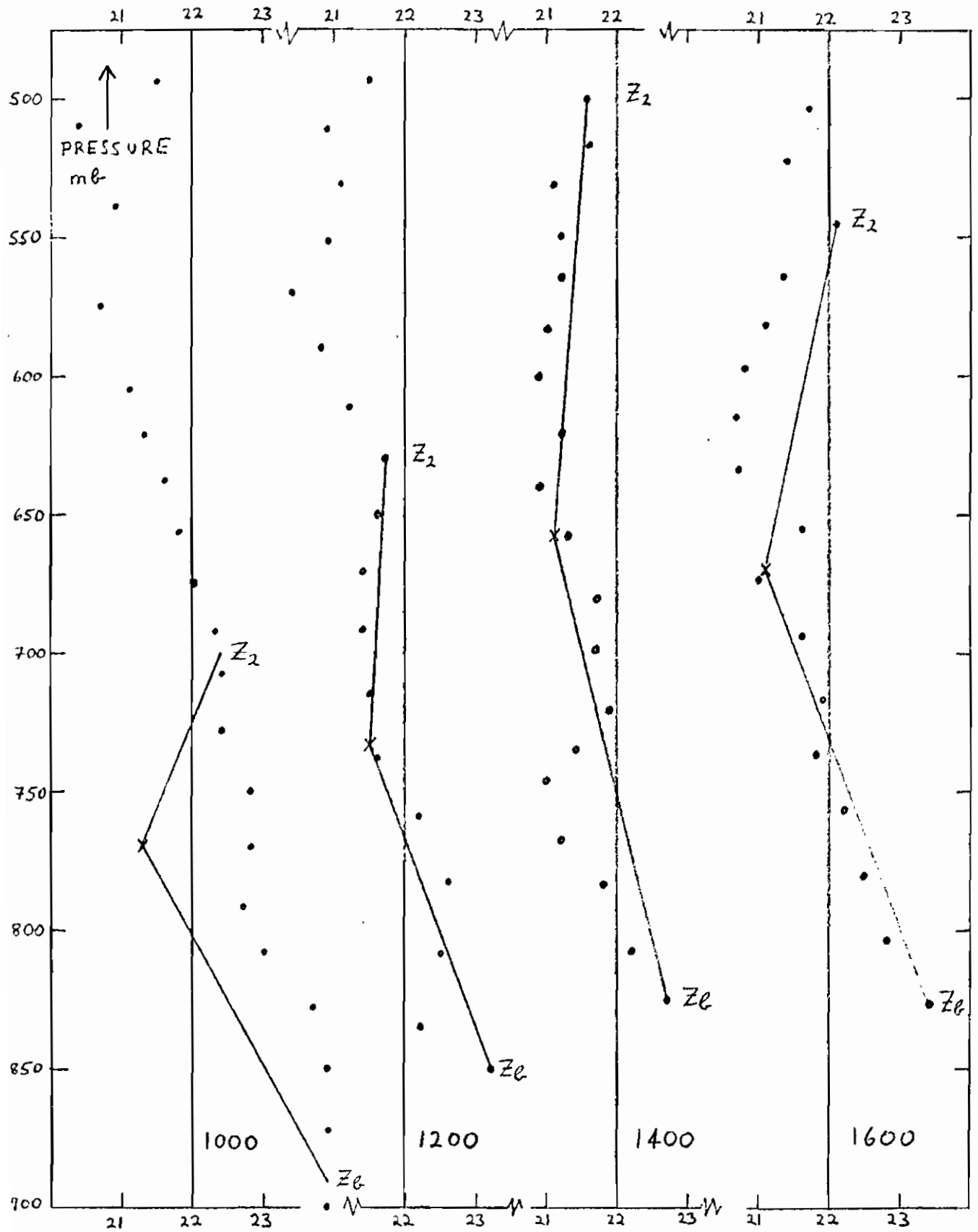

FIG. 6.3.1

$\Gamma_1, \Gamma_2, \Delta z_1$, and Δz_2 . That is, the model could be said to be a good 2-layer representation of these soundings.

Soundings on days of similar convection in the same month at the same site showed similar structure. On all such days

$$\Gamma_{c1} < \bar{\Gamma}$$

when the model gives

$$\Gamma_1 < \Gamma_{c1} < \bar{\Gamma} < \Gamma_2$$

which is typically confirmed by the soundings.

Cumulus Convection beneath an inversion

When $\bar{\Gamma}$ is considerably greater than Γ_{c1} , the model predicts a very stable top to the convective layer (i.e. a large value for Γ_2) and a smaller value for Γ_1, closer to the dry adiabat (see table 5.2.3). There are several considerations in checking this observationally. First there is a tendency towards the formation of layer cloud beneath the stable layer, which can radiatively destabilise the lower part of the cumulus layer, and produce a sharp inversion. This seems a common occurrence over the ocean in mid-latitudes in subsiding air. There is however the further observational problem that it is not always clear from routine soundings and observations whether stratocumulus is present.

In this thesis we have not discussed in detail the balance between subsidence and the surface water vapour flux, which determines whether the cumulus layer tends to saturation, although the model of 5.4 is suited to this purpose. Thus the presence of layer cloud cannot yet be established theoretically. We have also not considered the quantitative effect of layer cloud on the lapse-rate structure. However, despite this uncertainty, two cases will be considered.

Case (a)

Fig. 6.3.2 is a well documented example of a convective stratification, provided by F.H. Ludlam. The stratification near Dunstable, central England, on 15th June 1956 is shown plotted on a tephigram. The dots are individual measurements of temperature and dew-point (converted

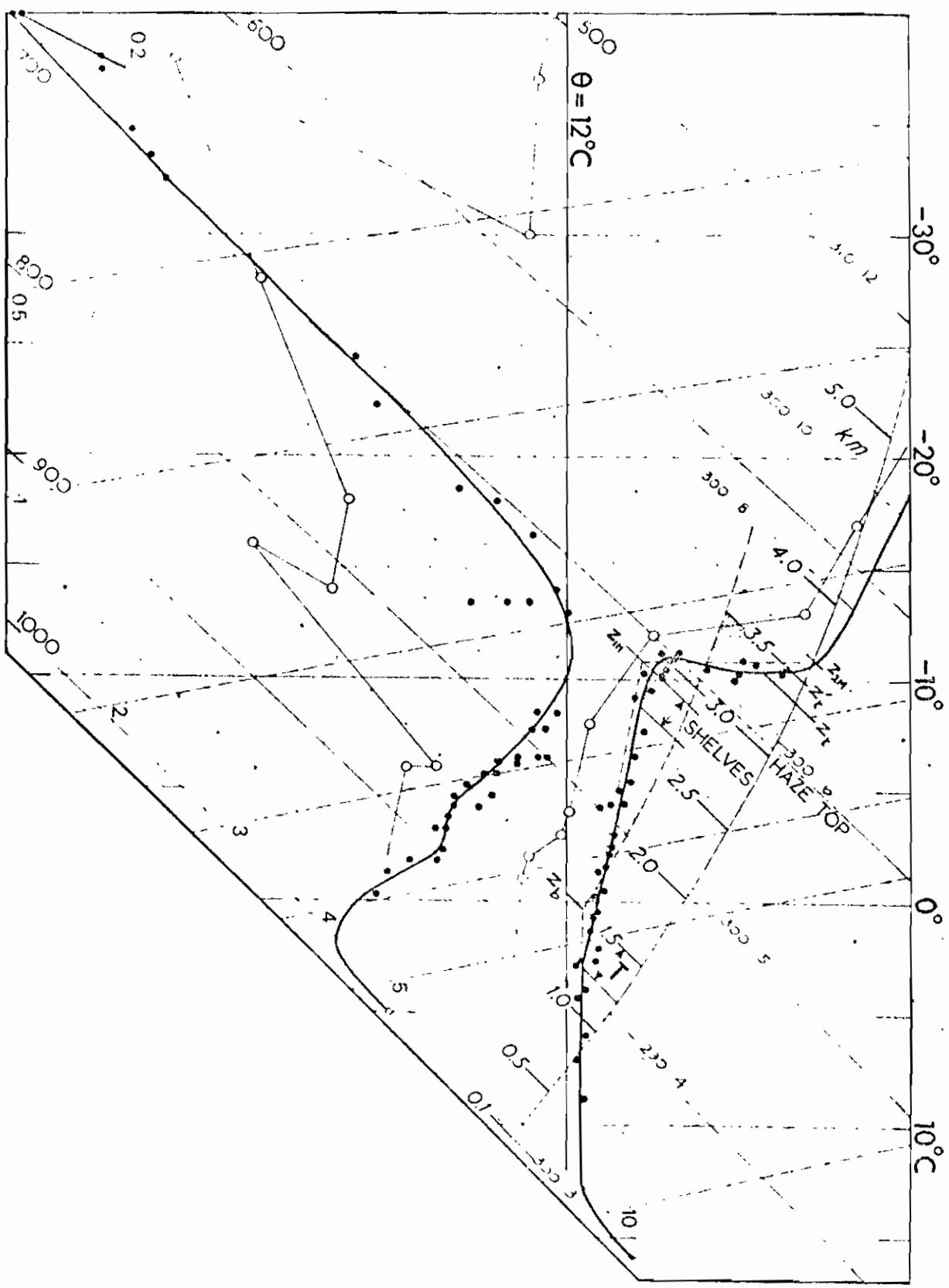
θ = 12°C
500
600
700
800
900
1000
0.2
0.5
1
2
3
4
5
-30°
-20°
-10°
0°
10°C
5.0 km
4.0
3.5
3.0
2.5
2.0
1.5
1.0
0.5
0.1
SHELVES
HAZE TOP

Fig. 6.3.2

from frost-points at temperatures below -10°C) made by an aircraft of the British Meteorological Research Flight during a spiral ascent between 1400 and 1500 GMT. Thick lines have been drawn arbitrarily through these points to represent mean conditions and extended to screen level on the basis of a sounding with a tethered balloon made at 1200 GMT, and to levels above 3.5km on the basis of routine radiosonde ascents made at 1500 GMT. Marks indicate the height of the cumulus bases (Z_b) and peak tops (Z_t as observed from the aircraft, and Z_t' as observed from the ground during a longer period), the transition layer T, the top of the haze in the convection layer, and of the layer occupied by shelf clouds. Winds are entered in degrees and $m\ s^{-1}$.

Thin lines joining significant points marked by open circles are from the sounding made at Liverpool at 0300 GMT which is representative of the stratification in the WNW'ly stream of maritime air from the N.E. Atlantic before it entered England. The convection over the sea had not reached above 1.5km . The stable layer in mid-troposphere on the Liverpool sounding is related to a front.

At 1500 GMT subsidence was not apparent from the large-scale isentropic analysis, but the soundings indicate that $\tilde{W}$ may have been about $-\frac{1}{2}\ cm\ s^{-1}$ in mid-troposphere.

This sounding has then been compared with the model. The kink in the sounding marked Z_{2M} has been arbitrarily taken as the top of the convective layer for the model, and values of Γ_1, Γ_2 ΔZ_1 and ΔZ_2 have been computed as in the previous example from $\bar{\Gamma}, \Delta Z$, and $r_s - r_e$. (Table 6.3.3). This model two-layer approximation to the sounding has been added to fig. 6.3.2 as a pecked line.

The agreement between model and observed temperature stratification is close.

Table 6.3.3

ΔZ m	$T/\theta\ \bar{\Gamma}$ °C km^{-1}	Γ_w °C km^{-1}	$r_s - r_e$ g Kg^{-1}	K	Γ_{c1} °C km^{-1}	Γ_1 °C km^{-1}	Γ_2 °C km^{-1}	ΔZ_1 m	ΔZ_2 m
2130	4.4	3.2	0.9	1.7	2.8	1.5	10	1420	710

Case (b)

To give some indication of the values to be expected in another case of interest, a sample of twelve similar soundings, taken in April and December 1958 in the Pacific trades, were compared with the model. They were chosen for $\bar{\Gamma}$ large, when there was always an inversion. The data had poor resolution in the vertical, as data were tabulated only at a few levels, so the set of values of $\bar{\Gamma}$, ΔZ, $\Delta Z_1/\Delta Z_2$, Γ_1, Γ_2 were simply averaged. The average values are shown in Table 6.3.4. The average values of $\bar{\Gamma}$, ΔZ and $(r_s - r_e)$ were used in the model to deduce values of $\Delta Z_1/\Delta Z_2$, Γ_1, Γ_2 for values of E of 0.4 and 0.5.

Table 6.3.4

	ΔZ m	$\frac{T}{\theta}\bar{\Gamma}$ °C km^{-1}	Γ_w °C km^{-1}	$r_s - r_e$ g Kg^{-1}	K	$\frac{\Delta Z_1}{\Delta Z_2}$	$\frac{T}{\theta}\Gamma_1$ °C km^{-1}	$\frac{T}{\theta}\Gamma_2$ °C km^{-1}
OBSERVED AVERAGE	1420	6.8	5.1	2.3	3	3	2	19
APPROXIMATE RANGE	±500	±1		1 to 3		1.2 to 6	0.2 to 3.6	10 to 40
			E	D	$\frac{T}{\theta}\Gamma_{c1}$ °C km^{-1}			
MODEL	1420	6.8	0.4	0.5	4.3	2.1	2.2	16
			0.5	0.4	4.2	2.6	2.2	19

Much better data is required to test the theory convincingly, but the evidence is not unfavourable. The slightly better fit of the model to the data with E = 0.5 rather than 0.4, implies more 'mixing', which is not impossible as the lapse-rate is rather more unstable in the cumulus layer than in the Anaco data ($\Gamma_{c1} - \Gamma_1$ is here about 2°C km^{-1} : c.f. table 6.3.2). This note of caution is necessary since E is parameterising a complex process about which little is known, and it may prove necessary to tabulate E for a range of conditions.

Radiation plays an important role, even if there is no stratocumulus. Above the stable top to the convection, the air which has subsided from higher levels is typically very dry, so that the moist cumulus layer cools significantly by long wave radiation. This will increase $\overline{\Gamma}$.

However, unless there is layer cloud, this radiative cooling is distributed through the cumulus layer. If the radiative cooling has a longer timescale than the convective modification, it is likely that the lapse rate structure is still controlled by the convection, and a function of $\overline{\Gamma}$.

6.4 Surface Boundary Conditions

This and the succeeding section are concerned with the day of convection in Anaco, Venezuela.

Radiation

Radiation data were available from a standard ventilated net flux radiometer, and upward and downward pointing Eppley pyranometers. The net flux data (N) were tabulated from a paper chart recording for 2 hourly intervals (table 6.4.1).

Various corrections were estimated.

(i) Ground storage (G)

During the night the surface temperature fell about 5°C and the integrated net outgoing flux was about 50 langleys. On this simple basis, the ground storage of radiation was taken as 10 ly per °C rise of surface temperature.

(ii) Radiative exchanges of the layer between the surface and 850mb. Three terms were estimated for the period 1000-1600 hrs.

(a) Line long wave cooling = - 1.8°C day^{-1}
(Elsasser chart)

(b) Solar short wave = + 1.8°C day^{-1}
absorption (Roach, 1961)

(c) Continuum long wave cooling = - 1.1° C day^{-1}
(Estimate based on unpublished calculations by K.J. Bignell).

The sum of these terms is equivalent to only -1.6 ly hr^{-1} for the surface-to-850mb layer, during the period 1000-1600 hrs., and was neglected.

Table 6.4.1 Radiation data

	1000-1200	1200-1400	1400-1600
Net flux N	43	41	26
Ground loss G	10	5	- 5
N - G	33	36	31
Error	± 5	± 5	± 5
Units	ly hr^{-1}		

Bowen Ratio : $F_{o\theta}/F_{or}$

The estimation of the partition of the energy input to the air (N-G) into sensible and latent heat fluxes is a crucial but difficult problem, as mentioned in 4.5 (see eq. 4.5.3).

The ratio of two bulk aerodynamic expressions of the form of 4.5.1 and 4.5.2 will be used here. Finite differences from screen level to the top of the superadiabatic layer (arbitrarily taken at 975 mb) were obtained from the smoothed data shown in Figs. 6.2.2 and 6.2.3. If we assume that the transfer coefficients for heat and water vapour (C_θ, C_r) are equal, we obtain

6.4.1
$$\frac{F_{o\theta}}{F_{or}} = \frac{c_p}{L} \left\{ \frac{\tilde{\theta}_o - \tilde{\theta}(975 \text{ mb})}{\tilde{r}_o - \tilde{r}(975 \text{ mb})} \right\}$$

This procedure is an extension of 4.5.1 and 4.5.2, as we have used smoothed values of temperature and water vapour at a level (just) above the superadiabatic layer rather than the vertically averaged variables $\bar{\tilde{\theta}}$, $\bar{\tilde{r}}$.

The values are given in table 6.4.2.

Table 6.4.2. Bowen Ratio: 3rd September 1969

	1000	1200	1400	1600	Local time
$\theta_o - \theta(975 \text{ mb})$	1.5	2.3	2.5	0.6	°C
$r_o - r(975 \text{ mb})$	5.6	4.5	2.1	3.8	g Kg^{-1}
Bowen ratio	0.11	0.21	(0.50)	0.06	

The high value of the Bowen ratio (B.R.) obtained at 1400 hours needs consideration. $r_o - r$ (975mb) is low, despite uniform trends in r_o and $\bar{\tilde{r}}$, since $\frac{\partial \tilde{r}}{\partial Z}$ in the sub-cloud layer had a steeper slope than the other soundings (fig. 6.2.3). Yet the surface temperature rose only slightly from 1200 to 1400 hours, and the superadiabatic layer was maintained. It is not apparent why there should be such a large change in the B.R. Further a survey of 8 other soundings under similar convective conditions (4 in the

time span 1200 to 1400 hrs) gave values of the B.R. by this method ranging from 0.09 to 0.19. We think it is justifiable therefore to reject the value obtained using the sounding at 1400 hrs on 3 rd September 1969.

However these values of the Bowen ratio will be unrepresentative of an areal average over the surrounding terrain if the surface data is unrepresentative, and need to be checked by other methods, such as the following.

(i) Equation 4.5.4 gives an estimate of F_{or}

4.5.4 $$V_R F_{or} = [r_s(T_o) - r_o]$$

However we lack appropriate values for V_R and our 'surface' data are at screen level, not the level of the vegetation.

(ii) An upper limit for the mean evaporation over the wet season is set by the mean rainfall. This will emerge from the hydrological study which was undertaken at the same time.

(iii) One may return to the bulk aerodynamic formulae and consider

6.4.2 $$\frac{F_{o\theta}}{\rho_o c_p} = C_\theta V_o [\theta_o - \theta(975 \text{ mb})]$$

A wind velocity V_o in the first few hundred metres was known both from the radiosonde and some pilot balloon ascents, and finite differences of θ are given in table 6.4.2.

The coefficient C_θ will vary slowly with gradient Richardson number (Ri). It can be related to a drag coefficient, C_D, for neutral conditions (Ri = 0) by a relation

$$C_\theta = C_D(1 - \epsilon Ri)$$

valid for small negative Ri ($\gtrsim -1.0$) when the numerical coefficient ϵ is thought to have a value of about 0.3, for measurements of gradient Richardson number between screen level and a height of 100m. The observed value of Ri between these levels was about -0.3, so we conclude that

$$C_\theta \sim 1.1 C_D$$

and the variation of C_θ during the day is therefore only about 10%.

Table 6.4.3 Eq. 6.4.2

TIME	1000	1200	1400	1600	
$\theta_o - \theta(975\ mb)$	1.5	2.3	2.5	0.6	°C
V_o	10	8	6	6	$m\ s^{-1}$
$V_o[\theta_o - \theta(975)]$	15	18.4	15	3.6	°C $m\ s^{-1}$
Mean		16.7	16.7	9.3	°C $m\ s^{-1}$
$(N - G)/\rho c_p$		33	36	31	°C $m\ s^{-1}$
Bowen ratio		.16	.21	.14	
$F_{o\theta}/\rho c_p$		4.6	6.3	3.7	°C $m\ s^{-1}$
C_θ		2.7	3.8	4.0	$\times 10^{-3}$

The numerical values of the fluxes $F_{o\theta}$ in ly hr^{-1}, and $F_{o\theta}/\rho c_p$ in °C $m\ s^{-1}$ are by coincidence the same at 303°K and 985 mb.

Table 6.4.4 Surface Fluxes

TIME	N-G	B.R.	$F_{o\theta}$	$F_{o\theta}$	F_{or}	F_{or}
1000 - 1200	33	0.16	4.6	18.5	28.4	47
1200 - 1400	36	0.21	6.3	25	29.7	50
1400 - 1600	31	0.14	3.7	15	27.3	46
Possible Error	±5	?	(±1	±3)	(±4	±6)
Units	ly hr^{-1}		ly hr^{-1}	°C mb hr^{-1}	ly hr^{-1}	g Kg mb hr^{-1}

'Errors' in $F_{o\theta}$, F_{or} do not include (unknown) errors in Bowen ratio.

Values of C_θ, calculated from eq. 6.4.2, are shown in table 6.4.3. They agree well with each other and with typical land values for a drag coefficient. This table gives no indication that the estimates of Bowen ratio are seriously in error.

The values which have therefore been used for the surface fluxes, based on tables 6.4.1 and 6.4.2, are given in table 6.4.4. They cannot be regarded as adequately accurate, and the next section suggests that the sensible heat flux in particular has been underestimated.

6.5 Estimation of W_{Db}

Given the surface fluxes and the sequence of soundings shown in figs. 6.2.2 and 6.2.3, one may attempt a budget analysis of the sub-cloud layer, and also test equations 4.6.10 and 4.8.10 for $d\tilde{\theta}_b/dt$ and $d\tilde{r}_b/dt$. In addition to these four equations containing W_{Db}, a fifth estimate of W_{Db} can be obtained from eq. 5.3.16, which describes the deepening of the cumulus layer.

However one must assume:

(i) that there is no horizontal gradient of $\tilde{\theta}, \tilde{r}$ (therefore no changes due to horizontal advection). The analysis will cast doubt on this assumption, but observations were available only from a single station.

(ii) that the mean vertical motion $\tilde{W}$ may be neglected, when compared with dZ_b/dt. We have no synoptic-scale vertical motion field for the region on this day; we know only that it was neither a day of strong low-level convergence or divergence. In the period 1000 to 1400 hrs $\frac{dZ_b}{dt}$ was about +3cms^{-1}, which is likely to be large compared with $\tilde{W}$, although Z_b became constant later.

The equations of this section are written in terms of Z, but height will be measured in mb, and fluxes in °C mb hr^{-1}, g Kg^{-1} mb hr^{-1} to allow for the variation of air density. The positive direction will still be upwards.

Temperature Structure

The most direct estimate of W_{Db} (the convective mass flux into the cumulus layer) is to be obtained from 4.6.10 (neglecting $\tilde{W}$).

6.5.1 $$\frac{d}{dt}\theta_b = \left(\frac{d}{dt}Z_b - W_{Db}\right)\Gamma_1$$

W_{Db} was found for each 2 hour interval using this equation - see table 6.5.1.

Table 6.5.1 Temperature Structure: $\partial\tilde{\theta}_b/dt$

TIME	θ_b	Z_b	$\frac{d\theta_b}{dt}$	$\frac{dZ_b}{dt}$	Γ_1	$\frac{dZ_b}{dt}\Gamma_1$	$W_{Db}\Gamma_1$	W_{Db}	W_{Db}
1000	303.3	99							
			+0.45	20	2.9	0.48	0.03	+1	+0.25
1200	304.2	139							
			+0.5	11	3.7	0.41	-0.09	-2.4	-0.6
1400	305.2	161							
			+0.5	- 1	3.9	-0.04	-0.54	-13.8	-3.5
1600	306.2	159							
Possible Errors	± 0.2	± 3	±0.15	± 5	±0.4	±0.2	±0.3	± 8	± 2
Units	°K	mb	°C hr^{-1}	mb hr^{-1}	°C/100 mb	°C hr^{-1}	°C hr^{-1}	mb hr^{-1}	cm s^{-1}

Table 6.5.2 Sensible Heat Budget of sub-cloud layer

TIME	$\Delta\theta$	$\bar{\tilde{\theta}}$	$\frac{d\bar{\tilde{\theta}}}{dt}$	Z_b	$\frac{dZ_b}{dt}$	$Z_b\frac{d\bar{\tilde{\theta}}}{dt}$	$\Delta\theta\frac{dZ_b}{dt}$	$\frac{F_{o\theta}}{\rho c_p}$	$\Delta\theta\, W_{Db}$	W_{Db}
1000	1.3	302.0		99						
	1.3		0.5	119	20	60	26	19	-15	-12
1200	1.2	303.0		139						
	1.2		0.5	150	11	75	13	25	-37	-31
1400	1.2	304.0		161						
	1.1		0.6	160	-1	96	-1	15	-82	-75
1600	1.0	305.2		159						
Possible Error	±0.2	±0.2	±0.15	±5	±5	±20	±6	?	±25	±25
Units	°C	°C	°C hr^{-1}	mb	mb hr^{-1}	← °K mb hr^{-1} →				mb hr^{-1}

Table 6.5.1 is encouraging; although it is clear that the possible errors are large, the trend is as anticipated. The convective mass flux into the cumulus layer increases as the day progresses, becoming large when $\frac{dZ_b}{dt}$ becomes small.

This table does not depend on the surface heat flux, but would be affected by change of temperature due to horizontal advection. Further if $\tilde{W} \neq 0$, then the last column represents $(W_{Db} + \tilde{W}_b)$. By definition W_{Db} cannot be positive, but the value of +1 mb hr^{-1} is smaller than the possible error.

Sub-cloud layer sensible heat budget

We may deduce W_{Db} from equation 4.6.8, after substituting 4.6.5. Measuring Z in mb, and neglecting $\tilde{W}$

$$6.5.2 \qquad Z_b \frac{d\bar{\tilde{\theta}}^b}{dt} = \frac{F_{o\theta}}{\rho_o c_p} + \Delta\theta \frac{d}{dt} Z_b - W_{Db} (\Delta\theta - \delta\theta)$$

$\delta\theta$ will also be neglected. The solution is shown in table 6.5.2 .

The errors in table 6.5.2 are very large, but the values for W_{Db} are probably too large negative. 6.5.2 is purely a budget equation, but if we consider 4.7.2 in which the relationship

$$F_{s\theta} = - k F_{o\theta}$$

has also been used, we have some indication that the surface heat flux values may be too low. With the height of cloud-base measured in mb

$$Z_b \frac{d\bar{\tilde{\theta}}}{dt} = (1+k) \frac{F_{o\theta}}{\rho c_p} \qquad k < 1$$

All the values of $Z_b \frac{d\bar{\tilde{\theta}}}{dt}$ in table 6.5.2 are more than twice $F_{o\theta}/\rho c_p$, which suggests $F_{o\theta}$ was higher than estimated in 6.4. This would account for the large negative values of W_{Db}, though there are other possible explanations.

(i) Advection of warmer air. This is possible but should also affect $\tilde{\theta}_b$ in table 3.5.1, as $\Delta\theta$ shows no surprising change.

(ii) The increase of $\overline{\tilde{\theta}}$ from 1400 to 1600 hrs may be an overestimate because of the almost complete disappearance of the superadiabatic layer. There is insufficient vertical resolution in the sounding to resolve this layer but a 2° C potential temperature excess extending over 15mb amounts of 0.2°C over 150 mb.

(iii) An accuracy in $\overline{\tilde{\theta}}$ better than 0.2°C is required to obtain sensible values for W_{Db}. This is beyond the accuracy of these soundings - we have already made rather arbitrary corrections of up to 0.9 °C (table 6.2.1).

Sub-cloud layer water vapour budget

This gives a better estimate of W_{Db} than the sensible heat budget, as the cloud circulations transport a significant amount of water vapour out of the sub-cloud layer. Eq. 4.8.4. becomes, with the neglect of $\overline{\tilde{w}}$ and with z measured in mb,

6.5.3 $$Z_b \frac{d\overline{\tilde{r}}}{dt} = \frac{F_{br}}{\rho_o L} + \Delta r \frac{dZ_b}{dt} - W_{Db}(\Delta r - \delta r)$$

The variable $\delta r = r_c(Z_b) - \overline{\tilde{r}}$ was found from the saturation mixing ratio of air ascending through cloud-base with temperature $\overline{\tilde{\theta}}$. The calculation is shown in table 6.5.3.

The errors in table 6.5.3 are considerable, but W_{Db} is constrained by the large value of $(\delta r - \Delta r).F_{or}$ (like $F_{o\theta}$) appears to be too small, but again, a small advection of moister air (increasing $\overline{\tilde{r}}$ by $1\ g\ Kg^{-1}$ during the period 1000-1600 hrs) would alter the true values of W_{Db} to -1, -6, -12 respectively.

Water vapour structure : $d\tilde{r}_b/dt$

A model was proposed in 4.8 for the modification of the water vapour structure above cloud-base. Eq. 4.8.10, for $\overline{\tilde{w}} = 0$, is

6.5.4 $$\frac{d\tilde{r}_b}{dt} = \left(\frac{dZ_b}{dt} - W_{Db}\right)\left(\frac{\partial \tilde{r}}{\partial Z}\right)_1 + \frac{F_{br}}{\tilde{\rho}_b L}\left(\frac{1}{S} - \frac{1}{W_{Db}}\frac{\partial}{\partial Z} W_{Db}\right)$$

where $\frac{F_{br}}{\rho_b L} = W_{Db}(\Delta r - \delta r)$

Table 6.5.3 Water Vapour Budget of sub-cloud layer

TIME	$r_c(Z_b)$	r_b	$\bar{\bar{r}}$	Δr	$\delta r - \Delta r$	$\frac{d\bar{\bar{r}}}{dt}$	$Z_b\frac{d\bar{\bar{r}}}{dt}$	$\Delta r\frac{dZ_b}{dt}$	$F_{o\theta}$	$W_{Db}(\delta r - \Delta r)$	W_{Db}
1000	15.5	8.5	10.6	-2.1	7.0	+0.1	+12	-48			
				-2.4	6.3	+0.1	+12	-48	47	+13	+2
1200	13.7	8.0	10.8	-2.8	5.7						
				-2.9	5.2	+0.1	+15	-32	50	-3	-1
1400	12.8	8.1	11.0	-2.9	4.7						
				-2.6	4.7	+0.1	+16	+ 3	46	-27	-6
1600	13.6	8.9	11.2	-2.3	4.7						
Possible Error	±0.5	±0.3	±0.2	±0.4	±0.6	±0.3	±45	±10	?	±50	±10
Units	← g Kg^{-1} →					g Kg^{-1} hr^{-1}	← g Kg^{-1} mb hr^{-1} →				mb hr^{-1}

Table 6.5.4 Water Vapour structure: $d\tilde{r}_b/dt$

TIME	r_b	S	$\frac{\delta r-\Delta r}{S}\left(\frac{\partial r}{\partial Z}\right)_1$		$\left(\frac{\partial r}{\partial Z}\right)_1 + \frac{\delta r-\Delta r}{S}$	$\frac{dr_b}{dt}$	$\frac{dZ_b}{dt}\left(\frac{\partial r}{\partial Z}\right)_1$	$\frac{dr_b}{dt} - \frac{dZ_b}{dt}\left(\frac{\partial r}{\partial Z}\right)_1$	W_{Db}
1000	8.5	3.0	2.3	-3.6	-0.7				
				-2.6	-0.5	-0.3	-0.5	+0.2	(+40)
1200	8.0	3.0	1.9	-2.1	-0.2				
				-2.1	-0.8	+0.1	-0.2	+0.3	(+58)
1400	8.1	5.8	0.8	-2.2	-1.4				
				-2.5	-1.6	+0.4	-	+0.4	(+25)
1600	8.9	4.7	1.0	-2.8	-1.8				
Possible Error	±0.3	±1.0	±0.2	±0.5	±0.6	±0.5	(±0.1)	±0.5	(large)
Units	g Kg^{-1}	km 100 mb	← g Kg^{-1}/100 mb →			← g Kg^{-1} hr^{-1} →			mb hr^{-1}

The values in the last column are not meaningful.

This is a difficult equation to test, and we shall find it does not give meaningful values for W_{Db}. First $\partial W_{Db}/dZ$ will be neglected, that is Γ_1 will be assumed constant in the cumulus layer, as it is doubtful if the sequence of soundings can be taken as reliably indicating any trend in Γ_1. It is clear that the clouds can moisten the layer only if

$$\left(\frac{\partial r}{\partial Z}\right)_1 + \frac{\delta r - \Delta r}{S} > 0$$

Table 6.5.4 shows that the quantity is always negative. However the local value of $\tilde{r}$ does increase during the day at the base of the cumulus layer

$$\left(\frac{\partial \tilde{r}}{\partial t}\right)_{Z_b} = \frac{d\tilde{r}_b}{dt} - \frac{dZ_b}{dt}\left(\frac{\partial \tilde{r}}{\partial Z}\right)_1 > 0$$

The model thus cannot be satisfied with W_{Db} negative. The model may be incorrect, or there may be advection of moister air during the day. This was also suggested by table 6.5.3 and again an increase of 1g kg^{-1} during the period of observation would give reasonable values of W_{Db}.

However this is not a good method for estimating W_{Db} for three reasons.

(a) Water vapour fluctuations in the cumulus layer may be comparatively larger than θ fluctuations, and point values of the water vapour structure therefore less representative of an areal mean.

(b) The input of water vapour by the clouds may be poorly modelled in 6.5.4; and the problem of estimating $\partial W_{Db}/\partial Z$ remains.

(c) Even if the model is valid, the coefficient of W_{Db} can be seen from table 6.5.3 to be small, so that its sign is uncertain.

Deepening of the Cumulus layer

W_{Db} can also be estimated from eq. 5.3.16 in terms of the rate of rise of Z_1. We saw in 6.3 that the lapse rate model gave quite a good fit to the structure of individual soundings. However it is unlikely that the sequence of soundings can be taken as representative of any trend in Γ_1. Nonetheless if one assumes reasonable values of Γ_1, Γ_2 (independent of time), one can readily deduce values of W_{Db} consistent with the observed rise of Z_1. Eq. 5.3.16 simplifies, with the neglect of $\tilde{W}$, and lapse rate changes with time, to

$$(\Gamma_2 - \Gamma_1)\Delta Z_2 \frac{dZ_1}{dt} = - \Delta Z\, \Gamma_1 W_{Db} - \frac{F_{b\theta}}{\rho c_p}$$

6.5.5 $$\therefore \quad (\Gamma_2 - \Gamma_1)\Delta Z_2 \frac{dZ_1}{dt} = - W_{Db}[\Gamma_1 \Delta Z + (\Delta\theta - \delta\theta)]$$

using 4.6.6 .

We shall construct a table for this equation by assuming $(\Gamma_1, \Gamma_2) = (3.4, 5.4)^\circ$ C km^{-1} and $\Delta Z_1/\Delta Z_2 = 1$, corresponding to the 1200 hrs sounding. $\delta\theta$ will be neglected.

Values of W_{Db} for the first two time periods are shown in table 6.5.5. As mentioned earlier, the top of the sounding at 1600 hrs was taken at 550mb where there was a well defined stable layer. However this height, and correspondingly Z_1, were lower than at 1400 hrs. Visual observations showed that a few cumulus clouds reached well above 450mb, which was the top of a moist layer on the sounding. Indeed within an hour a few cumulonimbus had developed. Thus it is clear that, although the 1600 sounding suggests that a significant number of clouds reached only 550mb, a few rose 150mb higher. The sounding may have been unrepresentative, or it may be that one cannot assume a single size scale of cloud once the largest clouds become more than several km deep.

The values of W_{Db} in table 6.5.5 are consistent with the best of the earlier estimates.

Conclusion

In this section (6.5), W_{Db} , the convective mass flux into the cumulus layer, has been found from 4 different estimates. The possible errors involved both in the data, and in the assumptions made, are considerable, and consequently the values obtained for W_{Db} are inaccurate. Nonetheless they do indicate well the order of magnitude of W_{Db}, and suggest the trend during the day. We have thus a reasonable estimate of the magnitude of the convective transports.

Table 6.5.6 summarises the values that have been obtained for W_{Db}, and suggests what may be regarded as likely values. These are all a few cm s^{-1}.

Table 6.5.5 Deepening of the Cumulus Layer

TIME	p_1	$\frac{dZ_1}{dt}$	ΔZ	ΔZ_2	Γ_1	Γ_2	$(\Gamma_2-\Gamma_1)\Delta Z_2\frac{dZ_1}{dt}$	$\Gamma_1\Delta Z$	$\Delta\theta + \delta\theta$	W_D
1000	790		2000	1000						
		22	2200	1100	3.4	5.4	48	7.5	1.2	-6
1200	737		2400	1200						
		36	3200	1600	3.4	5.4	115	10.9	1.2	-10
1400	640		4000	2000						
1600	(675)									
Possible Error	±15	±10	±200	±100	±0.3	±0.6	±20	±1	±0.2	±5
Units	mb	mb hr^{-1}	m	m	°C km^{-1}		°C mb hr^{-1}	°C	°C	mb hr^{-1}

Table 6.5.6 Values for W_{Db}

TABLE	6.5.1	6.5.2	6.5.3	6.5.5	LIKELY VALUE FOR	
TIME	$\frac{d\tilde{\theta}_b}{dt}$	$\overline{\tilde{\theta}}$	$\overline{\tilde{r}}$	$\frac{dZ_1}{dt}$	W_{Db}	
1000 - 1200	+1	-12	+2	-8	-5	-1.25
1200 - 1400	-2	-31	-1	-12	-10	-2.5
1400 - 1600	-14	(-75)	-6	-	-15	-3.75
Possible Error	±8	±25	±10	±5	±4	±1
Units	← mb hr^{-1} →				mb hr^{-1}	cm s^{-1}

It follows that with typical cloud vertical velocities of about $2\ m\ s^{-1}$ the areal cover of active cloud in the cumulus layer at an instant in time is small: only 1 to 2% . This value is to be expected to be less than the total areal coverage of cloud which is typically visible from above or below the cumulus layer, for two reasons.

(i) Appropriately averaged over the entire life cycle of a cloud (as in the definition of W_D - see 3.7) W_c is likely to be less than $1\ m\ s^{-1}$, so that a corresponding value of α (see eq. 3.7.2), which includes clouds at all stages of growth and decay, would be about 5%.

(ii) There may be also many little clouds occupying only the first hundred metres above cloud-base, essentially marking the tops of dry convective updrafts in the sub-cloud layer.

Chapter 7 Summary

This thesis has examined some aspects of cumulus convection and developed models for the non-precipitating boundary layer. These have far-reaching implications and indicate a number of avenues for future work.

The convective heat transports (chapter 3) have been discussed from two viewpoints: first in terms of a mass transport model (3.7), a concept which has been used previously by various authors (see 3.9); and secondly in terms of a hitherto unused conservative variable θ_L - a 'liquid water potential temperature.' The use of this variable θ_L simplifies the understanding of the thermodynamics and heat transport of cumulus convection, and indicates certain close similarities between dry and wet convection. Dilution of convective elements has been shown to be related to the irreversible nature of the convective circulations, and to necessitate an upward transport of liquid water, and a downward total heat transport in the cumulus layer. Thus cumulus convection is a destabilising process. In the upper part of the dry convective layer there is a similar downward (sensible) heat transport.

A model of the dry layer (chapter 4) carries forward the work of Ball (1960), and predicts the time development of this layer in the presence of a large-scale vertical velocity, $\tilde{w}$. Derived equations for the strength ($\Delta\theta$) and rate of lifting of an inversion need to be tested. This model was then extended to the sub-cloud layer in order to link the cumulus convection to the surface fluxes of sensible heat and water vapour, and to $\tilde{w}$. The many interactions within the problem are summarised most briefly in the approximate equation 4.7.6.

4.7.6. $$\left(\frac{dZ_b}{dt} - \tilde{w}_b - W_{Db}\right) = \frac{g(k+1)F_{o\theta}}{c_p \Gamma_1 \Delta p_b}$$

The suppression of convection by large scale subsidence ($\tilde{w}$ negative) has long been known observationally. We see that 4.7.6 predicts that $(-W_{Db})$ is similarly reduced by rise of cloud-base, a hitherto unrecognized influence which needs experimental verification. The data examined in chapter 6 indicate the increasing trend of $(-W_{Db})$ as dZ_b/dt decreases, but the possible errors are large. The dependence of the cumulus convection on the

warming of the sub-cloud layer and therefore the surface sensible heat flux (the R.H.S. of 4.7.6) is to be expected. The surface water vapour flux is involved in the intricate water vapour balance of the sub-cloud layer which 'feeds back' on W_{Db} through dZ_b/dt.

There is a need also for a lapse rate model for the sub-cloud layer, which will predict the temperature stratification, and the depth of the transition layer.

The lapse rate model proposed in 5.2 may prove very useful as a simple quantitative model of the vertical temperature distribution of a convective layer. It carries forward the idea of a characteristic stratification (Ludlam, 1966). With the budget equations and boundary conditions developed in 5.3, we have predicted both the stratification and the time development of the cumulus layer, as a function of $\tilde{W}$, the surface fluxes and the stratification above the convective layer. The comparison in chapter 6 of the lapse-rate model and the time-development model with data is considered encouraging, and suggests that further observational comparison would prove fruitful.

On the theoretical side, the water vapour transport needs to be considered more closely and radiative transfers need to be included in the model. It would also be useful to consider deep convection, particularly the heat and water vapour balance of the sub-cloud layer when there is low level convergence, in the light of this model. A study of vertical momentum transport by cumulus is necessary as well, and this requires a more detailed dynamical model of a cumulus cloud than has been used here; one in which shear is considered.

In conclusion it is thought that the work described in this thesis gives further insight into the role of cumulus convection in the atmosphere.

REFERENCES

Asai T.	1967	On the characteristics of cellular cumulus convection. J. Meteor. Soc. Japan 45, p.251.
	1968	Cellular cumulus convection in a moist atmosphere heated below. J. Meteor. Soc. Japan 46, p.301.
Ball F.K.	1956	Energy changes involved in disturbing a dry atmosphere. Quart. J.R.Met.Soc. 82, p.15.
	1960	Control of inversion height by surface heating. Quart. J.R.Met.Soc. 86, p.483.
Fraser, A.B.	1968	The White Box: the mean mechanics of the cumulus cycle. Quart.J.R.Met.Soc.94, p.71
Grant, D.R.	1965	Some aspects of convection as measured from aircraft. Quart. J.R.Met.Soc. 91, p.268
Haman K.	1969	On the influence of convective clouds on the large scale stratification. Tellus 21, p.40.
Hess S.L.	1959	Introduction to Theoretical Meteorology.
Kuo H.L.	1965	Cellular convection in a conditionally unstable atmosphere. Tellus 17, p.413
Levine J.	1959	Spherical vortex theory of bubble-like motion in cumulus clouds. J. Meteor. 16, p.653
Ludlam F.H.	1966	Cumulus and cumulonimbus convection. Tellus 18, p.687
Pearce R.P.	1968	Parameterisation of convective heat and momentum transports suggested by analysis of Caribbean data. Proc. Symp. Num. Wea. Pred. (Tokyo) 1968 I, p.75.
Plank V.G.	1967	The size distribution of cumulus clouds in representative Florida populations. J.Appl.Meteor. 8, p.46.
Roach W.T.	1961	The absorption of solar radiation by water vapour and carbon dioxide in a cloudless atmosphere. Quart.J.R.Met.Soc.87, p.364
Simpson J. et al	1965	Experimental Cumulus Dynamics. Reviews of Geophysics 3, p.387

Simpson J. and Wiggert V.	1969	Models of precipitating cumulus towers. Mon. Wea. Rev. 97, p.471.
Stommel H.	1947	Entrainment of air into a cumulus cloud. J. Meteor. 4, p.91
Telford J.W. and Warner J.	1962	On the Measurement from an aircraft of buoyancy and vertical air velocity in cloud. J. Atmos. Sci. 19, p.415
Telford J.W.	1966	The Convective Mechanism in clear air. J. Atmos. Sci. 23, p.652
	1969	Reply (to B.R. Morton) J. Atmos. Sci. 25 , p.138
Warner J. and Telford J.W.	1967	Convection below cloud-base. J. Atmos. Sci. 24, p.374.